# THE DISCOVERY OF NOVEL ENZYMATIC ACTIVITIES AND ACTIVATION MECHANISM OF SIRT7

A Dissertation

Presented to the Faculty of the Graduate School

of Cornell University

In Partial Fulfillment of the Requirements for the Degree of

Doctor of Philosophy

by

Zhen Tong

August 2016

# THE DISCOVERY OF NOVEL ENZYMATIC ACTIVITIES AND ACTIVATION MECHANISM OF SIRT7

Zhen Tong, Ph. D.

Cornell University 2016

Mammalian SIRT7 is a member of the sirtuin family of nicotinamide adenine dinucleotide (NAD)-dependent protein lysine deacylases that regulate multiple important biological processes including genome stability, metabolic pathways, stress responses, and tumorigenesis. SIRT7 has been shown to be important for ribosome biogenesis and transcriptional regulation. *Sirt7* knockout mice exhibit complications associated with fatty liver and increased aging in hematopoietic stem cells. However, the molecular basis for its biological function remains unclear, to a large extent due to the lack of efficient enzymatic activity *in vitro*.

I started my work on the expression and purification of active human SIRT7 from *E.coli*. First I found that SIRT7 can be activated by double-stranded DNA to hydrolyze acetyl group from lysine residues *in vitro* on histone peptides and histone proteins in the context of chromatin. Later I showed that RNA can increase the catalytic efficiency of SIRT7 even better and SIRT7 can remove long chain fatty acyl groups more efficiently than removing acetyl groups. Truncation and systematic mutagenesis studies revealed residues at both the amino and carboxyl termini of SIRT7 that are involved in RNA-binding and important for activity. RNA immunoprecipitation-sequencing (RIP-seq)

identified ribosomal RNA (rRNA) as the predominant RNA binding partners of SIRT7. The associated RNA was able to effectively activate the deacetylase and defatty-acylase activities of SIRT7. We also provided preliminary results showing that *Sirt7* knockdown slightly increased global lysine fatty-acylation level. These findings provide important insights into the biological functions of SIRT7, as well as an improved platform to develop SIRT7 modulators.

# BIOGRAPHICAL SKETCH

Zhen Tong was born in Wuhu, Anhui, China in 1988. She received her Bachelor degree from Department of Chemistry, Tsinghua University in 2010, majoring in Chemical Biology. She joined the BMCB program (Biochemistry, Molecular and Cellular Biology) at Cornell University in 2010 and started working in Dr. Hening Lin's group in 2011. Her first-year graduate study was kindly supported by Cornell Presidential Fellowship. Her thesis entitled "The discovery of novel enzymatic activities and activation mechanism of SIRT7" was supported and supervised by Dr. Hening Lin.

# ACKNOWLEDGMENTS

My entire work was made possible under the supervision of Dr. Hening Lin. I sincerely appreciate his support in every facet. His guidance on experimental design, data analysis, troubleshooting, manuscript and presentation preparation has been invaluable resource to me. I also want to express my appreciation to my committee members, Prof. John T. Lis and Prof. Dan Luo for their constructive suggestions and assistance.

Dr. Xiaoyang Su helped me greatly when I started working in this lab. I learned lots of fundamental techniques and critical thinking mode from him. Dr. Sushabhan Sadhukhan offered kind assistance for synthesizing various acyl peptides for *in vitro* HPLC activity assay. David D. Kim made significant contribution to the purification of SIRT7 WT and mutants proteins. All the Lin lab members contribute to a friendly, open and collaborative working environment that I truly enjoyed and felt well belonged throughout my graduate study at Cornell.

My research has been greatly facilitated by our collaborators. Dr. Quan Hao and Dr. Yi Wang helped me by optimizing the purification procedures of human SIRT7 to achieve the active enzyme. Dr. John T. Lis, Dr. Abdullah Ozer and Dr. John M. Pagano provided enormous support in RNA-related techniques and troubleshooting. Special thanks to Dr. Carol Bayles at Cornell imaging facility and Dr. Jennifer K. Grenier at Cornell RNA sequencing core for their valuable insights.

Finally, I would like to thank my family and friends for their constant support. No matter what happened, they are always with me. Without their caring and support, I could not have made it through this long but meaningful Ph.D. journey.

TABLE OF CONTENTS

LIST OF FIGURES

LIST OF TABLES

# CHAPTER 1

## An Overview of Sirtuins

### *Discoveries of Sirtuins*

Yeast silencing information regulator 2 (SIR2) protein, as the founding member of sirtuin family, was first discovered from a screen for modulators of yeast life span[1]. SIR2 was later found to be required for the extension of yeast life span by calorie restriction[2]. These discoveries launched a new field in biology: the study of SIR2 and its homologs in mammals, named as sirtuins.

Sirtuins are evolutionarily conserved in all domains of life. Based on similarity of primary sequences, sirtuins from different species are classified into four classes, class I-IV[3]. Mammalian genome encodes seven sirtuins (SIRT1-7). SIRT1-3 belong to class I, SIRT4 belongs to class II, SIRT5 is in class III, while both SIRT6 and SIRT7 are in class IV.

Sirtuins are distributed in different subcellular locations, including the nucleus (SIRT1, SIRT6, and SIRT7), cytosol (SIRT2), and mitochondria (SIRT3-5). Although in some studies, SIRT1 has been found to be present at cytosol, and SIRT2 has been reported to associate with nuclear proteins[4, 5].

### *Biological functions of Sirtuins*

Sirtuins were initially implicated in silencing gene transcription and aging process by deacetylating histone substrates[6]. In mammals, apart from histones, sirtuins target a diverse set of substrates. By modifying histones, transcription factors, and

epigenetic enzymes, sirtuins play important roles in chromatin biology[7, 8]. Sirtuins also regulate cellular metabolism (e.g. glucose homeostasis, lipid metabolism and insulin secretion) via removing acetyl groups from metabolic enzymes in the mitochondria and cytosol[8]. Because of the central roles sirtuins have in many important biological processes, it is not surprising that they have become the promising targets for treatment of a variety of human diseases such as aging, cancer, cardiovascular disease, inflammation and neurodegenerative disease.

***Catalytic mechanism of Sirtuins***

Sirtuins were discovered as NAD-dependent protein lysine deacetylases yielding three products: deacetylated lysine, nicotinamide, and 2'-O-acetyl-ADP-ribose (OAADPr)[9]. The catalytic mechanism of sirtuin enzymes is illustrated in Figure 1.1. The α-1'-O-alkylimidate intermediate formed upon the displacement of nicotinamide by the attack of the acetyl oxygen. Intramolecular attack by the 2'-OH followed by hydrolysis gives 2'- OAADPr, which can isomerize to 3'- OAADPr non-enzymatically[10].

Biochemical studies revealed that the enzyme binds the acetyl lysine substrate prior to NAD. Nicotinamide is the first product released after cleavage from NAD, followed by deacetylated lysine and OAADPr[11]. The use of NAD as a co-substrate distinguishes sirtuins from other classes of protein deacetylases, and more importantly, allows sirtuins to sense cellular metabolic status for timely regulation.

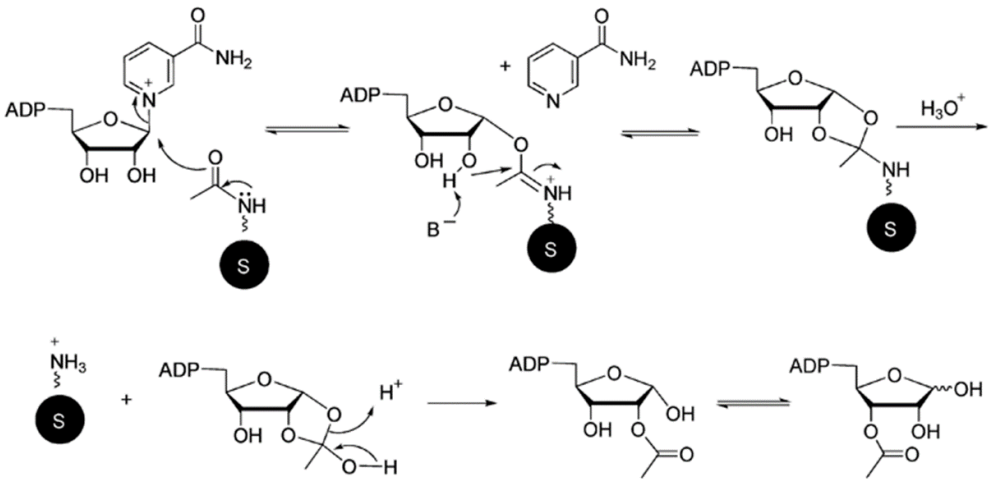

**Figure 1.1** Mechanism of sirtuin-catalyzed NAD-dependent deacetylation

***Overall structure of Sirtuins***

Primary sequence alignment of sirtuins indicates a highly conserved catalytic core domain with variable amino (N-) and carboxyl (C-) terminal segments. The overall structures of the core domains of sirtuins are highly similar, displaying a large Rossman fold domain for NAD binding and a more variant small domain that consists of a zinc-binding ribbon module and a helical module (Figure 1.2). The small domain is tethered to the Rossman fold through four linking loops that form a cleft. The acetyl lysine and NAD insert into the cleft where catalysis occurs.

Up to date, only yeast sirtuin, Hst2 structure has been resolved as a full-length protein that contains flexible N- and C-terminal regions[12]. Interestingly, N- and C-terminal extensions of yHst2 interact respectively with NAD and acetyl lysine binding sites to auto-inhibit the enzyme by formation of a homotrimer[12]. Recently, it was demonstrated that N- and C-terminal domains of mammalian SIRT1 can trans-activate deacetylation activity of endogenous SIRT1[13, 14], suggesting a unique autoregulation

mechanism through its highly variable N- and C-termini.

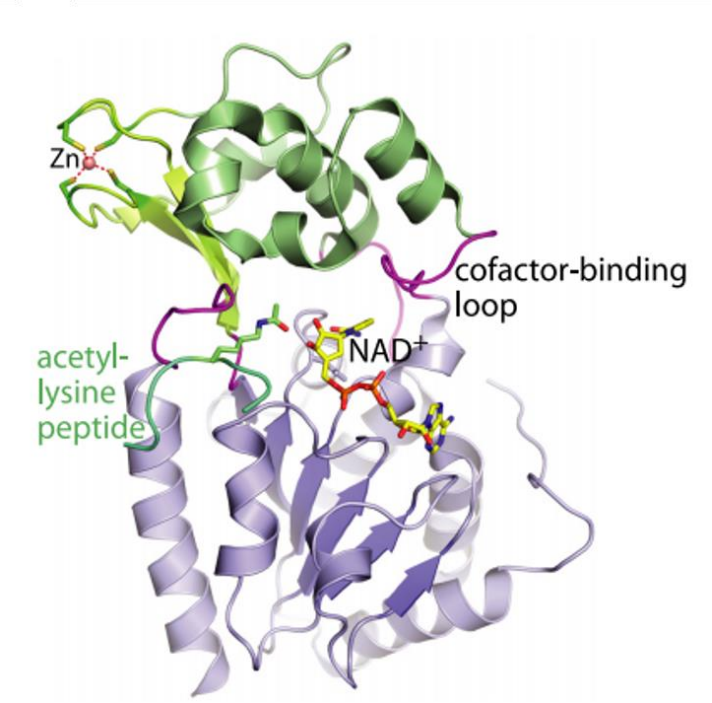


**Figure 1.2** Overall sirtuin structure represented by yeast sirtuin, Hst2. Full-length Hst2 is shown in complex with acetyl lysine and carba-NAD substrates indicated in stick (PDB 1SZC)[15]. The small globular domain is shown in green, the large domain is shown in purple, and the four linking loops in magenta.

***Novel enzymatic activities of Sirtuins***

Among the seven mammalian sirtuins, only the class I members (SIRT1-3) display robust deacetylase activities in vitro, whereas the other four sirtuins (SIRT4-7) only exhibit very weak or non-detectable deacetylase activities in vitro[16, 17]. It has been proposed that some of sirtuins may function as ADP-ribosyltransferases[16, 18], however, despite of the very weak activity in vitro, its physiological significance is still controversial [10, 19]. It was recently demonstrated that mammalian SIRT5, one of the four sirtuins with weak deacetylase activities, functions to remove negatively charged acyl

groups including succinyl and malonyl from protein lysine residues[20, 21] (Figure 1.3). Protein lysine succinylation and malonylation were not previously known as common protein post-translational modifications (PTMs). Subsequent proteomics studies from independent research groups have identified thousands of proteins that are succinylated[22, 23], indicating that this is an abundant and important PTM since many substrate proteins of SIRT5 are metabolic enzymes of which activities are regulated by dynamic succinylation/malonylation level. Indeed, SIRT5 has also been recently shown to hydrolyze glutaryl group from protein lysines[21].

SIRT6, which also displays weak and sequence-specific deacetylase activity on peptide substrates in vitro[24-26], was demonstrated to prefer hydrolyzing long chain fatty acyl groups, such as myristoyl and palmitoyl, from protein lysine residues (Figure 1.3) [27]. This activity is similar to the previously reported activity for the Plasmodium falciparum SIR2 protein, PfSIR2A[28]. One physiological substrate identified for the defatty-acylation activity of SIRT6 is tumor necrosis factor α (TNFα), which is known to be myristoylated on K19 and K20[29]. SIRT6 was shown to promote TNFα secretion by defatty-acylating its K19 and K20 residues. Although SIRT6 exhibits poor deacetylase activity in vitro on the peptide substrates alone, recent studies suggested that histone substrates packaged as nucleosomes[30] or free fatty acids[31] could activate the deacetylase activity of SIRT6. These findings provide possible explanation for SIRT6 to function as a metabolic sensor with multiple switchable enzymatic activities in different subcellular contexts. Interestingly, it was shown that SIRT1-3 can also remove long chain fatty-acyl groups in vitro[31] although the physiological relevance remains to be further studied.

The diverse activities of SIRT1-3 (class I, primarily deacetylation but can also remove long chain fatty acyl groups), SIRT5 (class III, desuccinylation, demalonylation and deglutarylation), and SIRT6 (class IV, more efficient as a defatty-acylase but can also remove the acetyl group) strongly suggest that sirtuins from different classes may exhibit different specificity for acyl lysine substrates.

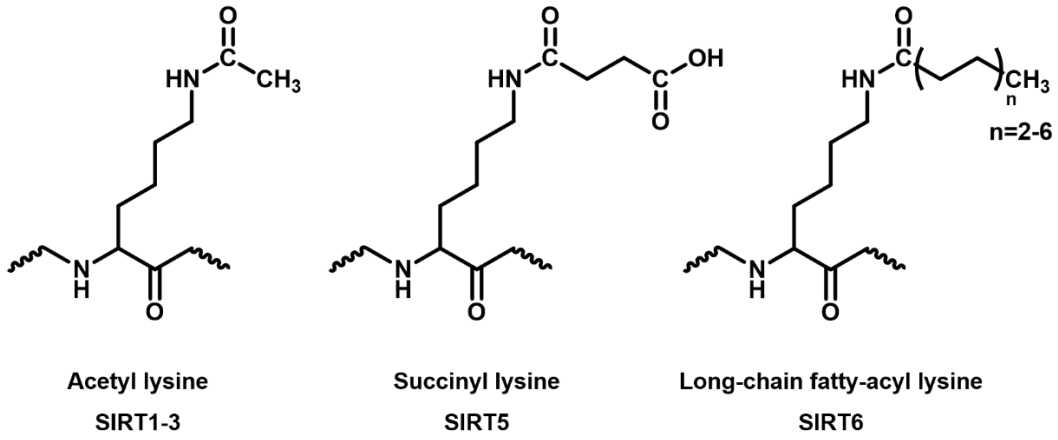


**Figure 1.3** Preferences of lysine acyl modifications by different mammalian sirtuin enzymes.

## An Overview of SIRT7

### *Introduction*

Among the seven mammalian sirtuins, SIRT1-7, with diverse biological functions, enzymatic activities and physiological substrates, SIRT7 is poorly understood. Although both SIRT6 and SIRT7 belong to the class IV sirtuin, they only share ~40% primary sequence similarity with SIRT6 belonging to class IVa, and SIRT7 assigned to class IVb[3]. SIRT7 is mainly localized in the nucleus, specifically concentrated in the nucleolus[17, 32]. Meanwhile, a significant portion of SIRT7 has been reported to localize in the cytosol[33]. Our growing understanding of SIRT7 has implicated its important roles in gene transcription, hepatic lipid metabolism and cancer[34].

### *SIRT7 & Transcription*

Due to its primary localization in the nucleolus under normal conditions, SIRT7 was first reported to be an activator of RNA polymerase I (Pol I) transcription[32]. SIRT7 associates with actively transcribed rDNA genes where it interacts with RNA Pol I and histones. Recently, the mechanism underlying the effect was found to be SIRT7-mediated deacetylation of the PAF53 subunit of RNA Pol I[35]. Deacetylation of PAF53 results in its increased association with RNA Pol I and thus elevated rDNA transcription.

SIRT7 exhibits almost non-detectable deacetylation activity in vitro, and because of this, it was not until 2012 that the first deacetylation substrate of SIRT7 was identified. Chua and co-workers discovered that SIRT7 specifically deacetylates H3K18 by screening a library of acetyl lysine peptide derived from histone sequences[36]. In this

study, SIRT7 was found to be recruited to gene promoters by interacting with ELK4 transcription factor. By selectively deacetylating H3K18 at these promoter regions, SIRT7 inhibits the transcription of a series of tumor suppressive genes, thus contributing to the maintenance of oncogenic transformation. Another major category of SIRT7 targeting genes consists of ribosomal protein genes, which are transcriptional targets of the oncoprotein MYC[37]. MYC recruits SIRT7 to target gene promoters to suppress the expression of ribosomal proteins by deacetylation of H3K18. Intriguingly, it was shown that SIRT7 attenuates ER (endoplasmic reticulum) stress by opposing MYC-dependent expression of ribosomal proteins. The model proposed is that by transiently reducing protein synthesis rates during ER stress, SIRT7 helps to relieve the unfolded protein stress (UPR) in the ER.

Besides, SIRT7 has been reported to play an important role in regulating mitochondrial homeostasis. Sirt7 deficiency in mice induces multiple mitochondrial dysfunction including increased blood lactate levels, cardiac dysfunction and hepatic microvesicular steatosis[38]. These effects of SIRT7 on mitochondrial homeostasis were attributed to its deacetylation of a transcription factor GABPβ1, consequently facilitating GABPα/GABPβ complex formation and activating transcription of nuclear-encoded mitochondrial genes.

***SIRT7 & hepatic lipid metabolism***

Interestingly, three recent studies independently linked non-alcoholic fatty liver formation with SIRT7's biological functions, however, with different effects observed. Two groups reported that Sirt7-deficient mice developed chronic hepatosteatosis during

aging process[37, 38]. Two distinct mechanisms have been proposed to explain this phenotype. Shin et al. stated that SIRT7 helped to alleviate ER stress and to prevent the development of fatty liver disease. In addition, Ryu et al. ascribed the liver disorder in aged Sirt7-deficient mice to the consequences of mitochondrial dysfunction. On the other hand, Yoshizawa et al. reported that Sirt7 knock-out mice were resistant to high-fat diet-induced fatty liver, obesity and glucose intolerance[39]. The mechanism proposed was that binding of SIRT7 to the DDB1-CUL4-associated factor (DCAF1)/damage-specific DNA binding protein 1 (DDB1)/cullin 4B (CUL4B) E3 ubiquitin ligase complex inhibited the degradation of TR4, a nuclear receptor involved in lipid metabolism.

***SIRT7 & cancer***

Elevated SIRT7 expression has been observed in multiple human cancer tissues including prostate, hepatocellular, breast, thyroid, gastric and other carcinomas[40-43]. Two principal biological processes regulated by SIRT7 account for its potential oncogenic character. First, SIRT7 is a lysine deacetylase that specifically removes a histone mark, H3K18 Ac (acetylated H3K18), depletion of which is correlated with highly malignant cancers and poor patient prognosis[36]. In this context, via deacetylation of H3K18 Ac at promoter regions of tumor-suppressive genes such as COPS and NME1, SIRT7 contributes to the maintenance of oncogenic transformation[36]. Second, SIRT7 is enriched in nucleoli, subnuclear sites of ribosome biogenesis that is accelerated in aggressive tumors. Several studies have proved that SIRT7 activates rRNA transcription and ribosome machinery assembly. In SIRT7-depleted cancer cells, rRNA synthesis rate

was reduced and thus led to decreased cell viability and proliferation[32]. SIRT7's interaction with nucleolus-localized chromatin remodeling complexes (e.g. B-WICH and NoRC) might also affect rDNA transcription[44]. Moreover, SIRT7 has been shown to directly promote protein translation and regulate Pol III-mediated transcription of transfer RNA (tRNA) by interacting with mTOR and the TFIIIC2 transcription factor[45]. Altogether, by coordinating rRNA synthesis, Pol III-dependent synthesis of tRNA and ribosome assembly process, SIRT7 serves as a central regulator of cell growth and proliferation, which are two prime factors for tumorigenesis.

With all that said, the impact of SIRT7 on spontaneous tumor development remains unclear. SIRT7 has been reported to interact with MYC and repress transcription of oncogenic MYC-dependent genes by deacetylating H3K18 Ac. It is possible that SIRT7 might even have a tumor suppressive role in the initiation of cancer in early stages.

**Dissertation Statement**

My graduate work focuses on exploring novel enzymatic activitiy and biological function of SIRT7. In chapter 2, I describe the discovery that SIRT7 can be activated by double-stranded DNA to hydrolyze the acetyl group from lysine residues in vitro on histone peptides and histone proteins in the context of chromatin. Chapter 3 describes the discovery that RNA could further activate SIRT7's enzymatic activity. Upon RNA activation, SIRT7 exhibited preference for removing long-chain fatty-acyl groups from lysine residues. Truncation and systematic mutagenesis studies revealed key residues at both the amino and carboxyl termini of SIRT7 that are involved in RNA-binding and

important for the activity. RNA immunoprecipitation-sequencing (RIP-seq) identified ribosomal RNA (rRNA) as the predominant RNA binding partners of SIRT7. The associated RNA was able to effectively activate the deacetylase and defatty-acylase activities of SIRT7. In the chapter 4, I report that the defatty-acylase activity of SIRT7 is likely to be physiologically relevant. Global lysine fatty-acylation level slightly increased upon Sirt7 knockdown. Stable isotope labeling by amino acids in cell culture (SILAC) profile of lysine fatty-acylation proteome identified a list of putative physiological substrates of which lysine fatty acylation level was regulated by SIRT7.

**References**


1. Kaeberlein, M., McVey, M., and Guarente, L. (1999) The SIR2/3/4 complex and SIR2 alone promote longevity in Saccharomyces cerevisiae by two different mechanisms, Genes Dev 13, 2570-2580.
2. Lin, S. J., Defossez, P. A., and Guarente, L. (2000) Requirement of NAD and SIR2 for life-span extension by calorie restriction in Saccharomyces cerevisiae, Science 289, 2126-2128.
3. Frye, R. A. (2000) Phylogenetic classification of prokaryotic and eukaryotic Sir2-like proteins, Biochem Biophys Res Commun 273, 793-798.
4. Sauve, A. A., Wolberger, C., Schramm, V. L., and Boeke, J. D. (2006) The biochemistry of sirtuins, Annu Rev Biochem 75, 435-465.
5. Haigis, M. C., and Sinclair, D. A. (2010) Mammalian sirtuins: biological insights and disease relevance, Annu Rev Pathol 5, 253-295.

6. Imai, S., Armstrong, C. M., Kaeberlein, M., and Guarente, L. (2000) Transcriptional silencing and longevity protein Sir2 is an NAD-dependent histone deacetylase, Nature 403, 795-800.

7. Feldman, J. L., Dittenhafer-Reed, K. E., and Denu, J. M. (2012) Sirtuin catalysis and regulation, J Biol Chem 287, 42419-42427.

8. Sebastian, C., Satterstrom, F. K., Haigis, M. C., and Mostoslavsky, R. (2012) From sirtuin biology to human diseases: an update, J Biol Chem 287, 42444-42452.

9. Jackson, M. D., and Denu, J. M. (2002) Structural identification of 2'- and 3'-O-acetyl-ADP-ribose as novel metabolites derived from the Sir2 family of beta -NAD+-dependent histone/protein deacetylases, J Biol Chem 277, 18535-18544.

10. Du, J., Jiang, H., and Lin, H. (2009) Investigating the ADP-ribosyltransferase activity of sirtuins with NAD analogues and 32P-NAD, Biochemistry 48, 2878-2890.

11. Borra, M. T., Langer, M. R., Slama, J. T., and Denu, J. M. (2004) Substrate specificity and kinetic mechanism of the Sir2 family of NAD+-dependent histone/protein deacetylases, Biochemistry 43, 9877-9887.

12. Zhao, K., Chai, X., Clements, A., and Marmorstein, R. (2003) Structure and autoregulation of the yeast Hst2 homolog of Sir2, Nat Struct Biol 10, 864-871.

13. Ghisays, F., Brace, C. S., Yackly, S. M., Kwon, H. J., Mills, K. F., Kashentseva, E., Dmitriev, I. P., Curiel, D. T., Imai, S. I., and Ellenberger, T. (2015) The N-Terminal Domain of SIRT1 Is a Positive Regulator of Endogenous SIRT1-Dependent Deacetylation and Transcriptional Outputs, Cell Rep.

14. Pan, M., Yuan, H., Brent, M., Ding, E. C., and Marmorstein, R. (2012) SIRT1 contains N- and C-terminal regions that potentiate deacetylase activity, J Biol Chem 287, 2468-2476.

15. Yuan, H., and Marmorstein, R. (2012) Structural basis for sirtuin activity and inhibition, J Biol Chem 287, 42428-42435.

16. Liszt, G., Ford, E., Kurtev, M., and Guarente, L. (2005) Mouse Sir2 homolog SIRT6 is a nuclear ADP-ribosyltransferase, J Biol Chem 280, 21313-21320.

17. Michishita, E., Park, J. Y., Burneskis, J. M., Barrett, J. C., and Horikawa, I. (2005) Evolutionarily conserved and nonconserved cellular localizations and functions of human SIRT proteins, Mol. Biol Cell 16, 4623-4635.

18. Haigis, M. C., Mostoslavsky, R., Haigis, K. M., Fahie, K., Christodoulou, D. C., Murphy, A. J., Valenzuela, D. M., Yancopoulos, G. D., Karow, M., Blander, G., Wolberger, C., Prolla, T. A., Weindruch, R., Alt, F. W., and Guarente, L. (2006) SIRT4 inhibits glutamate dehydrogenase and opposes the effects of calorie restriction in pancreatic beta cells, Cell 126, 941-954.

19. Kowieski, T. M., Lee, S., and Denu, J. M. (2008) Acetylation-dependent ADP-ribosylation by Trypanosoma brucei Sir2, J Biol Chem 283, 5317-5326.

20. Du, J., Zhou, Y., Su, X., Yu, J. J., Khan, S., Jiang, H., Kim, J., Woo, J., Kim, J. H., Choi, B. H., He, B., Chen, W., Zhang, S., Cerione, R. A., Auwerx, J., Hao, Q., and Lin, H. (2011) Sirt5 is a NAD-dependent protein lysine demalonylase and desuccinylase, Science 334, 806-809.

21. Tan, M., Peng, C., Anderson, K. A., Chhoy, P., Xie, Z., Dai, L., Park, J., Chen, Y., Huang, H., Zhang, Y., Ro, J., Wagner, G. R., Green, M. F., Madsen, A. S.,

Schmiesing, J., Peterson, B. S., Xu, G., Ilkayeva, O. R., Muehlbauer, M. J., Braulke, T., Muhlhausen, C., Backos, D. S., Olsen, C. A., McGuire, P. J., Pletcher, S. D., Lombard, D. B., Hirschey, M. D., and Zhao, Y. (2014) Lysine glutarylation is a protein posttranslational modification regulated by SIRT5, Cell Metab 19, 605-617.

22. Park, J., Chen, Y., Tishkoff, D. X., Peng, C., Tan, M., Dai, L., Xie, Z., Zhang, Y., Zwaans, B. M., Skinner, M. E., Lombard, D. B., and Zhao, Y. (2013) SIRT5-mediated lysine desuccinylation impacts diverse metabolic pathways, Mol Cell 50, 919-930.

23. Rardin, M. J., He, W., Nishida, Y., Newman, J. C., Carrico, C., Danielson, S. R., Guo, A., Gut, P., Sahu, A. K., Li, B., Uppala, R., Fitch, M., Riiff, T., Zhu, L., Zhou, J., Mulhern, D., Stevens, R. D., Ilkayeva, O. R., Newgard, C. B., Jacobson, M. P., Hellerstein, M., Goetzman, E. S., Gibson, B. W., and Verdin, E. (2013) SIRT5 regulates the mitochondrial lysine succinylome and metabolic networks, Cell Metab 18, 920-933.

24. Michishita, E., McCord, R. A., Berber, E., Kioi, M., Padilla-Nash, H., Damian, M., Cheung, P., Kusumoto, R., Kawahara, T. L., Barrett, J. C., Chang, H. Y., Bohr, V. A., Ried, T., Gozani, O., and Chua, K. F. (2008) SIRT6 is a histone H3 lysine 9 deacetylase that modulates telomeric chromatin, Nature 452, 492-496.

25. Michishita, E., McCord, R. A., Boxer, L. D., Barber, M. F., Hong, T., Gozani, O., and Chua, K. F. (2009) Cell cycle-dependent deacetylation of telomeric histone H3 lysine K56 by human SIRT6, Cell cycle 8, 2664-2666.

26. Yang, B., Zwaans, B. M., Eckersdorff, M., and Lombard, D. B. (2009) The sirtuin SIRT6 deacetylates H3 K56Ac in vivo to promote genomic stability, Cell cycle 8, 2662-2663.

27. Jiang, H., Khan, S., Wang, Y., Charron, G., He, B., Sebastian, C., Du, J., Kim, R., Ge, E., Mostoslavsky, R., Hang, H. C., Hao, Q., and Lin, H. (2013) SIRT6 regulates TNF-alpha secretion through hydrolysis of long-chain fatty acyl lysine, Nature 496, 110-113.

28. Zhu, A. Y., Zhou, Y., Khan, S., Deitsch, K. W., Hao, Q., and Lin, H. (2012) Plasmodium falciparum Sir2A preferentially hydrolyzes medium and long chain fatty acyl lysine, ACS Chem Biol 7, 155-159.

29. Stevenson, F. T., Bursten, S. L., Locksley, R. M., and Lovett, D. H. (1992) Myristyl acylation of the tumor necrosis factor alpha precursor on specific lysine residues, J Exp Med 176, 1053-1062.

30. Gil, R., Barth, S., Kanfi, Y., and Cohen, H. Y. (2013) SIRT6 exhibits nucleosome-dependent deacetylase activity, Nucleic Acids Res 41, 8537-8545.

31. Feldman, J. L., Baeza, J., and Denu, J. M. (2013) Activation of the protein deacetylase SIRT6 by long-chain fatty acids and widespread deacylation by mammalian sirtuins, J Biol Chem 288, 31350-31356.

32. Ford, E., Voit, R., Liszt, G., Magin, C., Grummt, I., and Guarente, L. (2006) Mammalian Sir2 homolog SIRT7 is an activator of RNA polymerase I transcription, Genes Dev 20, 1075-1080.

33. Kiran, S., Chatterjee, N., Singh, S., Kaul, S. C., Wadhwa, R., and Ramakrishna, G. (2013) Intracellular distribution of human SIRT7 and mapping of the nuclear/nucleolar localization signal, FEBS J 280, 3451-3466.

34. Paredes, S., Villanova, L., and Chua, K. F. (2014) Molecular pathways: emerging roles of mammalian Sirtuin SIRT7 in cancer, Clin Cancer Res : an official journal of the American Association for Cancer Research 20, 1741-1746.

35. Chen, S., Seiler, J., Santiago-Reichelt, M., Felbel, K., Grummt, I., and Voit, R. (2013) Repression of RNA polymerase I upon stress is caused by inhibition of RNA-dependent deacetylation of PAF53 by SIRT7, Mol Cell 52, 303-313.

36. Barber, M. F., Michishita-Kioi, E., Xi, Y., Tasselli, L., Kioi, M., Moqtaderi, Z., Tennen, R. I., Paredes, S., Young, N. L., Chen, K., Struhl, K., Garcia, B. A., Gozani, O., Li, W., and Chua, K. F. (2012) SIRT7 links H3K18 deacetylation to maintenance of oncogenic transformation, Nature 487, 114-118.

37. Shin, J., He, M., Liu, Y., Paredes, S., Villanova, L., Brown, K., Qiu, X., Nabavi, N., Mohrin, M., Wojnoonski, K., Li, P., Cheng, H. L., Murphy, A. J., Valenzuela, D. M., Luo, H., Kapahi, P., Krauss, R., Mostoslavsky, R., Yancopoulos, G. D., Alt, F. W., Chua, K. F., and Chen, D. (2013) SIRT7 represses Myc activity to suppress ER stress and prevent fatty liver disease, Cell Rep 5, 654-665.

38. Ryu, D., Jo, Y. S., Lo Sasso, G., Stein, S., Zhang, H., Perino, A., Lee, J. U., Zeviani, M., Romand, R., Hottiger, M. O., Schoonjans, K., and Auwerx, J. (2014) A SIRT7-dependent acetylation switch of GABPbeta1 controls mitochondrial function, Cell Metab 20, 856-869.

39. Yoshizawa, T., Karim, M. F., Sato, Y., Senokuchi, T., Miyata, K., Fukuda, T., Go, C., Tasaki, M., Uchimura, K., Kadomatsu, T., Tian, Z., Smolka, C., Sawa, T., Takeya, M., Tomizawa, K., Ando, Y., Araki, E., Akaike, T., Braun, T., Oike, Y., Bober, E., and Yamagata, K. (2014) SIRT7 controls hepatic lipid metabolism by regulating the ubiquitin-proteasome pathway, Cell Metab19, 712-721.

40. Frye, R. (2002) "SIRT8" expressed in thyroid cancer is actually SIRT7, Br J Cancer 87, 1479.

41. Kim, J. K., Noh, J. H., Jung, K. H., Eun, J. W., Bae, H. J., Kim, M. G., Chang, Y. G., Shen, Q., Park, W. S., Lee, J. Y., Borlak, J., and Nam, S. W. (2013) Sirtuin7 oncogenic potential in human hepatocellular carcinoma and its regulation by the tumor suppressors MiR-125a-5p and MiR-125b, Hepatology 57, 1055-1067.

42. Malik, S., Villanova, L., Tanaka, S., Aonuma, M., Roy, N., Berber, E., Pollack, J. R., Michishita-Kioi, E., and Chua, K. F. (2015) SIRT7 inactivation reverses metastatic phenotypes in epithelial and mesenchymal tumors, Sci Rep 5, 9841.

43. Zhang, S., Chen, P., Huang, Z., Hu, X., Chen, M., Hu, S., Hu, Y., and Cai, T. (2015) Sirt7 promotes gastric cancer growth and inhibits apoptosis by epigenetically inhibiting miR-34a, Sci Rep 5, 9787.

44. Tsai, Y. C., Greco, T. M., Boonmee, A., Miteva, Y., and Cristea, I. M. (2012) Functional proteomics establishes the interaction of SIRT7 with chromatin remodeling complexes and expands its role in regulation of RNA polymerase I transcription, Mol Cell Proteomics 11, M111 015156.

45. Tsai, Y. C., Greco, T. M., and Cristea, I. M. (2014) Sirtuin 7 plays a role in ribosome biogenesis and protein synthesis, Mol Cell Proteomics 13, 73-83.

# CHAPTER 2

## SIRT7 is Activated by DNA and Deacetylates Histone H3 in the Chromatin Context

**Publication**: Tong, Z., Wang, Y., Zhang, X., Kim, D. D., Sadhukhan, S., Hao, Q., and Lin, H. (2016) SIRT7 Is Activated by DNA and Deacetylates Histone H3 in the Chromatin Context, ACS chemical biology 11, 742-747.

**Author Contributions**: ZT and HL designed the experiment and drafted the manuscript. ZT performed in vitro activity assay, kinetics study and truncation analysis of SIRT7. ZT and XZ carried out in vitro activity assay of SIRT7 on chromatin substrates. YW, DDK, and QH expressed and purified active SIRT7 protein. SS synthesized H3 acyl peptides.

**Abstract**

Mammalian sirtuins (SIRT1-7) are members of a highly conserved family of nicotinamide adenine dinucleotide ($NAD^+$)-dependent protein deacetylases that regulate many biological processes including metabolism, genome stability, and transcription. Among the seven human sirtuins, SIRT7 is the least understood, to a large extent due to the lack of enzymatic activity in vitro. Here we reported that SIRT7 can be activated by DNA to hydrolyze acetyl group from lysine residues in vitro on histone peptides and histones in the chromatin context. Both N- and C- termini of SIRT7 are important for the DNA-activated deacetylase activity. The regulatory mechanism of SIRT7 is different from that of SIRT6, which also showed increased activity on chromatin substrates, but the deacetylase activity of SIRT6 on peptide substrate cannot be activated by DNA. This finding provides an improved enzymatic activity assay of SIRT7 that will promote the development of SIRT7 modulators. Further investigation into the activation mechanism of SIRT7 by DNA could provide new insights into its biological function and help development of sirtuin activators.

**Introduction**

The silent information regulator-2 (Sir2) family of proteins, or sirtuins, are evolutionarily conserved $NAD^+$-dependent protein lysine deacetylases[1-3]. Mammals encode seven sirtuins (SIRT1-SIRT7)[4], which govern important biological processes including transcriptional regulation, genome stability, stress response, metabolism, and aging[5, 6]. The seven mammalian sirtuins have different subcellular localizations, with SIRT1, SIRT6, and SIRT7 being mainly nuclear, SIRT2 being predominantly cytosolic,

and SIRT3-5 being mainly mitochondrial[7]. Among the seven human sirtuins, the molecular function of SIRT7 is the least understood. SIRT7 is enriched in nucleoli where it activates rRNA gene transcription by interacting with Pol I and upstream binding transcription factor (UBF)[8, 9]. In response to metabolic stress, SIRT7 is released from nucleoli leading to hyperacetylation of PAF53, a subunit of Pol I complex, and decreased Pol I transcription[10]. SIRT7 also regulates Pol II-mediated mRNA synthesis. It can be recruited by specific transcription factors (ELK4[11] and Myc[12]) to deacetylate H3K18 acetyl modification specifically and thus suppress downstream gene transcription. SIRT7 has also been reported to regulate transcription of mitochondrial biogenesis genes by directly deacetylating and activating a transcription factor GABPβ1[13]. SIRT7 is also involved in attenuating stress-activated protein kinase (SAPK) and p53-mediated stress responses[14, 15] and regulating Pol III-mediated tRNA transcription and ribosomal biogenesis[16], but the exact molecular mechanism remains unknown.

## Results and Discussion

### SIRT7 deacetylase activity is significantly enhanced by DNA.

Despite all the reports that connect SIRT7's deacetylase activity to its biological functions, the in vitro deacetylase activity of SIRT7 in many cases cannot be detected. For example, no appreciable amount of deacetylation product was observed by high pressure liquid chromatography (HPLC)-based assays using peptide substrates[17]. This was also observed in our laboratory (Figure 1A-B). Inspired by the fact that SIRT7 is localized mainly in the nucleus and involved in regulating transcription and protein

synthesis[11, 16], we postulated that DNA might affect its enzymatic activity, similar to SIRT6 that displays a nucleosome-dependent deacetylase activity[18].

SIRT7 was expressed in E. coli and affinity purified to near homogeneity. An HPLC assay was used to monitor the activity of SIRT7 on H3K9 and H3K18 acetyl (H3K9 Ac and H3K18 Ac) peptides in the absence or presence of double-stranded DNA (dsDNA, salmon sperm DNA sheared to an average size less than 2000bp). In the absence of dsDNA, no deacetylation was observed on either peptide substrate. Strikingly, in the presence of dsDNA, SIRT7 displayed deacetylase activity on both H3K9 Ac and H3K18 Ac peptides (Figure 2.1A-B). SIRT7 activity increased as the mass ration of DNA to SIRT7 was increased and the activity almost reached a plateau when the ratio reaches 1:1 (Figure 2.2). In later studies, we generally used 3:1 DNA to SIRT7 mass ratio to make sure SIRT7 was saturated by DNA. Interestingly, all the other sirtuin proteins (except for SIRT4, which we could not acquire the recombinant protein from E. coli) could not be activated by dsDNA (Figure 2.1C). Even SIRT6, which is closest to SIRT7 and was shown to have a nucleosome-dependent deacetylation activity, could not be activated by dsDNA on peptide substrates. Thus, among all the human sirtuins, the activation of the deacetylase activity on peptide substrates by DNA is a unique property of SIRT7.

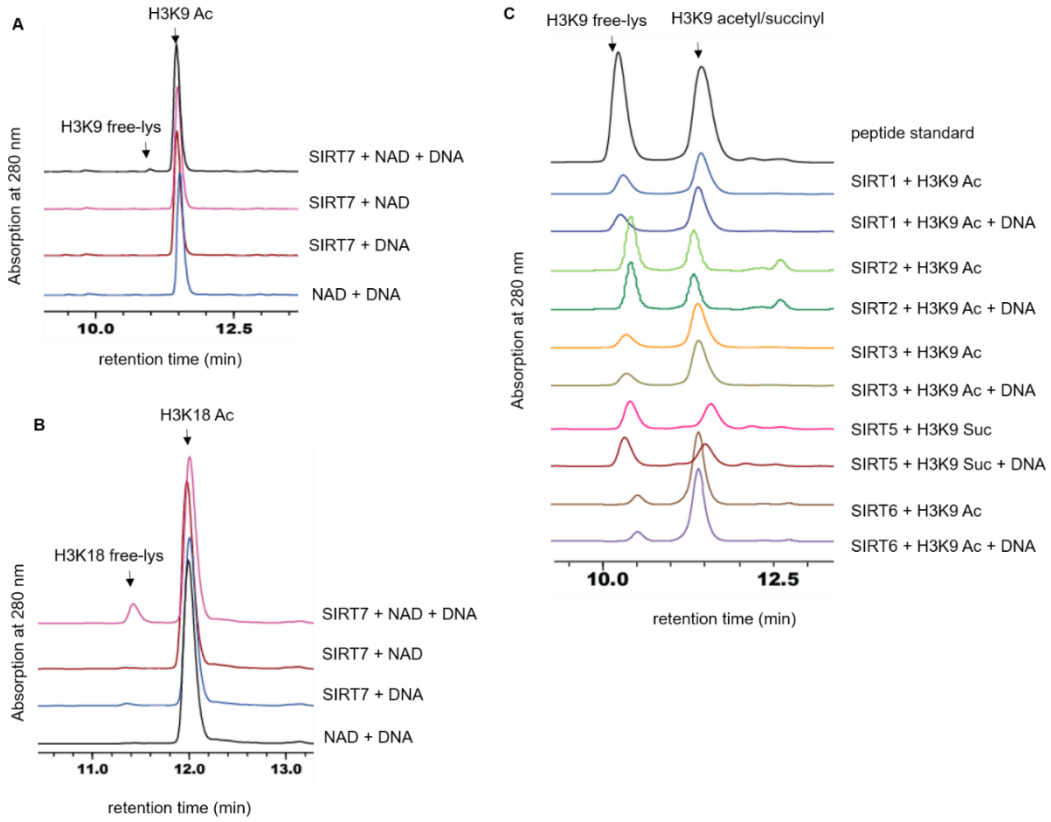


**Figure 2.1** SIRT7 deacetylase activity is significantly enhanced by DNA. (A) Overlaid HPLC traces showing SIRT7-catalyzed hydrolysis of H3K9 acetyl peptide with DNA. (B) HPLC traces showing SIRT7-catalyzed hydrolysis of H3K18 acetyl peptide with DNA. (C) Overlaid HPLC traces showing that other sirtuin proteins cannot be activated by DNA.

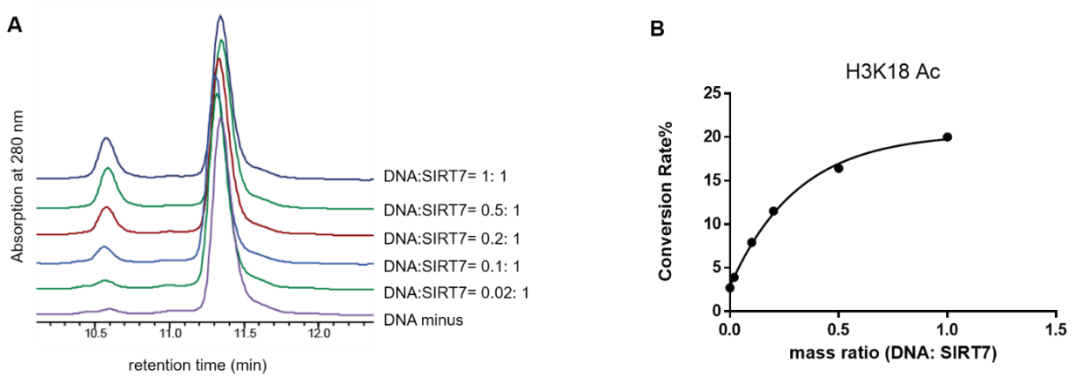


**Figure 2.2** The activity of SIRT7 with different amount of dsDNA. (A) Overlaid HPLC traces showing SIRT7-catalyzed hydrolysis of H3K18 acetyl peptide with different mass ratio of DNA to SIRT7. (B) The conversation rates for the reactions shown in A were plotted against the DNA to SIRT7 mass ratios.

We further determined the turnover number ($k_{cat}$) and Michaelis constant ($K_m$) of SIRT7 in the presence of dsDNA (Table 2.1). Again, without dsDNA we could not detect the activity and thus could not determine the kinetic constants. Consistent with the reported activity screen[11], H3K18 Ac peptide turned out to be a significantly better (16-fold) substrate of SIRT7 compared to H3K9 Ac peptide. For H3K18 Ac, SIRT7 displayed a $k_{cat}$ value of 0.16 $min^{-1}$ and a $K_m$ value of 167 μM ($k_{cat}/K_m$ 16 $M^{-1}s^{-1}$). In contrast, for H3K9 Ac, we could not saturate SIRT7 and thus could only obtain the $k_{cat}/K_m$ value, which was 1.0 $M^{-1}s^{-1}$. This is the first time that we could reliably detect the enzymatic activity of SIRT7 in vitro.

**Table 2.1** Catalytic efficiencies of SIRT7 full-length (FL) and truncations on acetyl peptides

| Acetyl peptide | $k_{cat}$ ($s^{-1}$) | $K_m$ (μM) | $k_{cat}/K_m$ ($M^{-1}s^{-1}$) |
|---|---|---|---|
| H3K9 Ac, FL | NA[c] | NA | NA |
| H3K9 Ac, FL + ds DNA[a] | ND[b] | ND | 1.0 |
| H3K18 Ac, FL | NA | NA | NA |
| H3K18 Ac, FL + ds DNA | $2.7 \times 10^{-3} \pm 3.7 \times 10^{-4}$ | 167 ± 43 | 16 |
| H3K18 Ac, ΔN + ds DNA | ND | ND | ~2.0 |
| H3K18 Ac, ΔC + ds DNA | NA | NA | NA |
| H3K18 Ac, core + ds DNA | NA | NA | NA |

[a]ds DNA: SIRT7=3:1 (mass ratio)

[b]ND: $k_{cat}$ *and* $K_m$ cannot be determined because V~[S] is linear, thus only $k_{cat}/K_m$ value can be determined

[c]NA: product formation cannot be detected

FL: 1-400; ΔN: 56-400; ΔC: 1-364; core: 56-364

We next investigated whether SIRT7 could be activated by DNA on histone protein substrates. We incubated calf thymus histones with recombinant SIRT7 in the presence/absence of dsDNA. The H3K18 Ac level was then blotted using an H3K18Ac-specific antibody. SIRT7 exhibited no deacetylase activity on purified histone proteins. Unexpectedly, addition of exogenous DNA did not significantly decrease the H3K18 Ac level (Figure 2.3A).

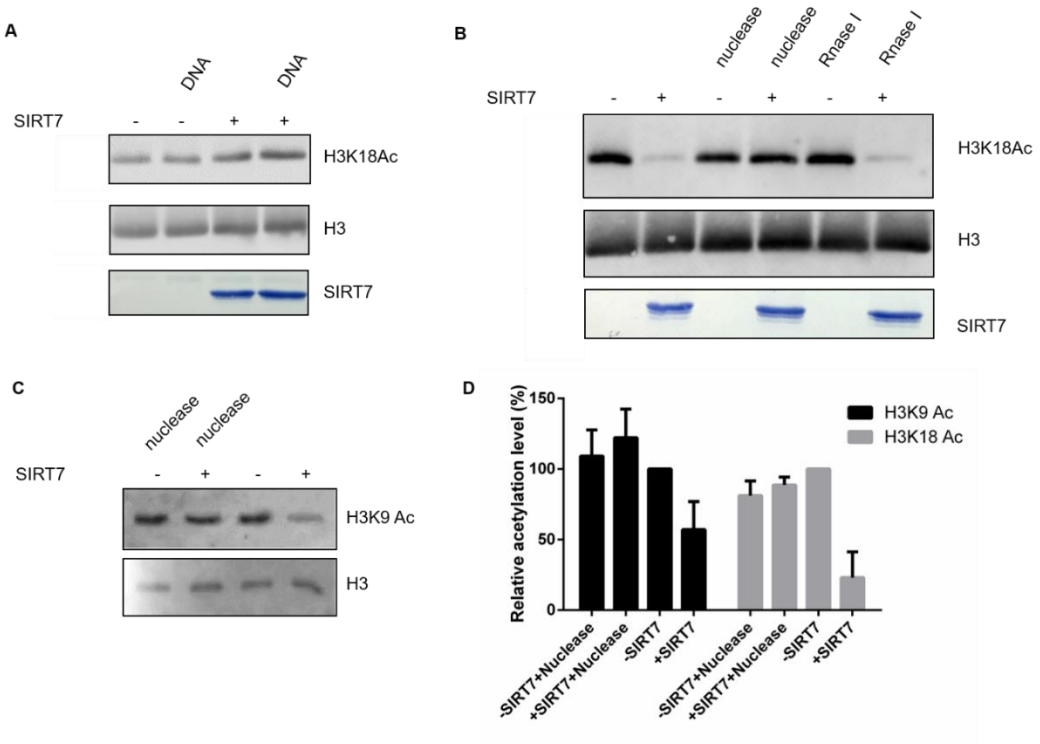


**Figure 2.3** SIRT7 is activated by genomic DNA on chromatin substrates. (A) SIRT7 cannot be activated by exogenous DNA on histone proteins. (B) SIRT7 can deacetylate H3K18 in the chromatin context. (C) Genomic DNA is required for SIRT7 to remove H3K9 Ac from chromatin substrate. (D) Quantification of western blot results shown in (B & C). The levels of H3K9 Ac and H3K18 Ac were normalized by the amount of histone H3 proteins. The relative acetylation level was calculated by setting the negative control (SIRT7 minus reaction) level to 100%.

Nucleosomes consist of a segment of DNA wrapped around a histone octamer. Therefore, we speculated that chromatin compositional DNA may activate SIRT7 to remove histone acetylation. We first extracted chromatin fraction from HEK 293T cells as reported[19]. Using the chromatin substrates, SIRT7 displayed robust $NAD^+$-dependent H3K18 Ac deacetylase activity. Furthermore, nuclease cocktail treatment completely

abolished the deacetylase activity on H3K18Ac while RNase treatment did not, suggesting that chromatin DNA is required for SIRT7's activity on H3K18 (Figure 2.3B). We also tested SIRT7's activity on H3K9 Ac with and without nuclease treatment (Figure 2.3C) and quantified the acetylation level (Figure 2.3D). Interestingly, in the context of chromatin, SIRT7 was able to remove acetyl group from H3K9 residue. We further performed a time-course analysis of SIRT7 on H3K18 Ac in the context of chromatin (Figure 2.4). SIRT7 was able to hydrolyze ~50% of H3K18 Ac within 90 minutes.

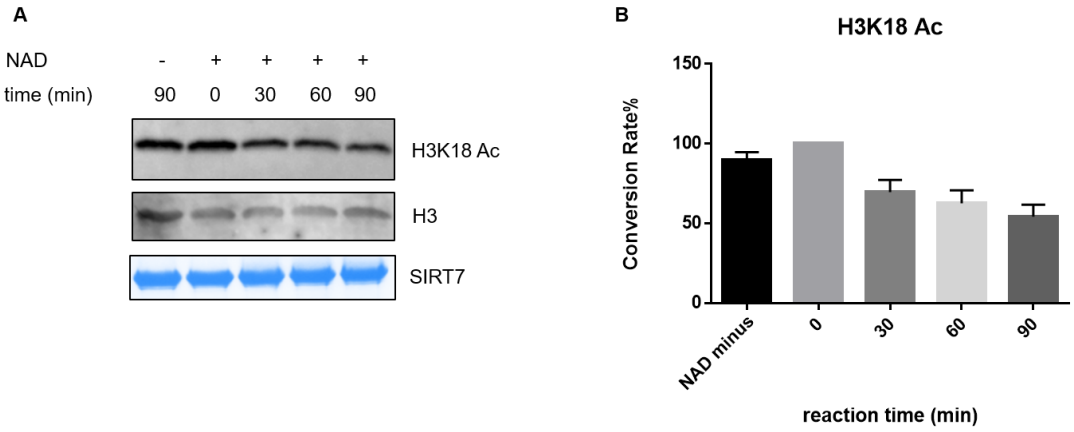


**Figure 2.4** Time course analysis of SIRT7 deacetylase activity on H3K18 Ac on chromatin substrates. (A) Western blot showing SIRT7 H3K18 Ac deacetylase activity in a time-dependent manner. (B) Quantification of western blot results shown in (A). The levels of H3K18 Ac were normalized by the amount of histone H3 proteins. The relative acetylation level was calculated by setting starting reaction (0 min) level to 100%.

We next investigated which domain(s) of SIRT7 is responsible for its activation by DNA. Sirtuin proteins contain a conserved central catalytic core flanked by highly variable N- and C-terminal extensions[20]. Seven human sirtuins are categorized into

four subclasses, where SIRT6 and SIRT7 belong to subclass IV [4]. Bioinformatics prediction of DNA-binding sites of SIRT7 suggested that the N- and C-termini that are rich in Arg and Lys residues could potentially play an important role in binding to negatively charged DNA (Figure 2.5 and 2.6)[21]. Thus, we hypothesized that the N- and C- termini of SIRT7 could be essential for its activation by DNA.


**Figure 2.5** Alignment of protein sequences of different human sirtuins. Black arrows mark the start and end of the core domain of SIRT7.

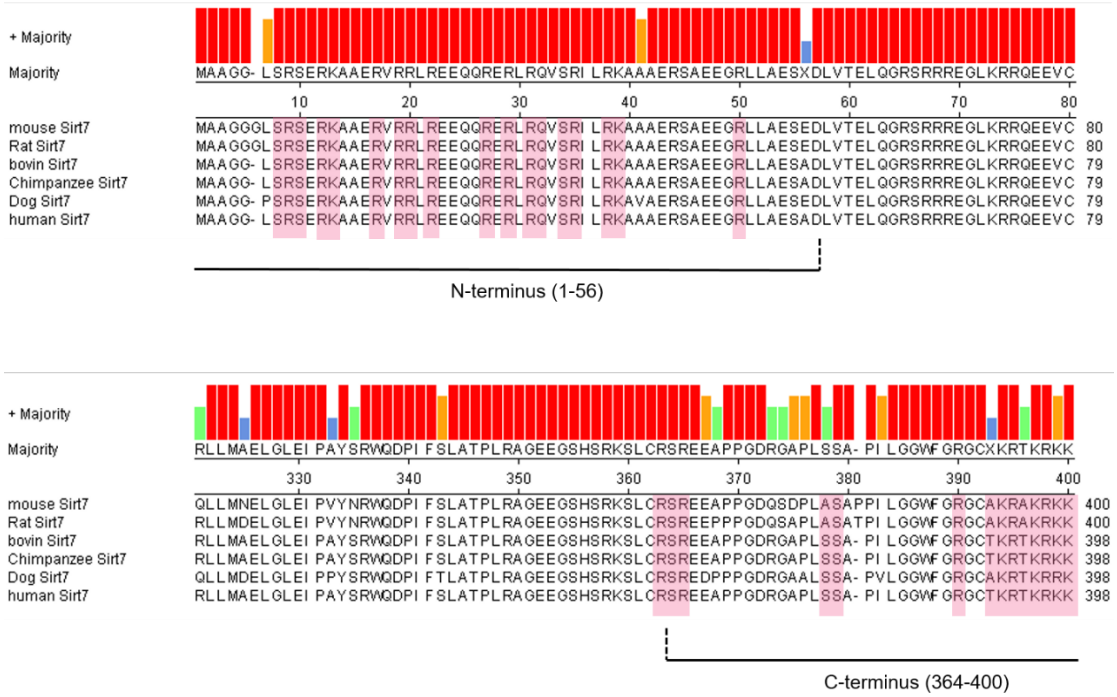


**Figure 2.6** Summary of predicted DNA-binding residues at the N- and C-termini of SIRT7. Bioinformatics software BindN (http://bioinfo.ggc.org/bindn/) was used to predict DNA-binding residues which are highlighted in pink. Most of these residues are conserved among different species.

We obtained full length (FL, residue 1-400) and several truncated SIRT7 lacking either the N- or C-terminal extension: the N-terminal deletion (ΔN, residue 56-400), the C-terminal deletion (ΔC, residue 1-364), and the core domain (56-364) (Figure 2.7A-B). Using the H3K18 Ac peptide, we conducted activity assays for these four proteins. With dsDNA as the in vitro activator, we found SIRT7 ΔC and the core domain did not exhibit detectable enzymatic activity within the detection limit of the HPLC-based assay (Figure 2.7C). SIRT7 ΔN was only slightly activated by DNA. Kinetics studies indicated that the catalytic efficiency of SIRT7 ΔN ($k_{cat}/K_m$ ~2.0 $M^{-1}s^{-1}$) was only 1/8 of FL SIRT7 ($k_{cat}/K_m$ ~16.0 $M^{-1}s^{-1}$) in the presence of dsDNA (Table 2.1).

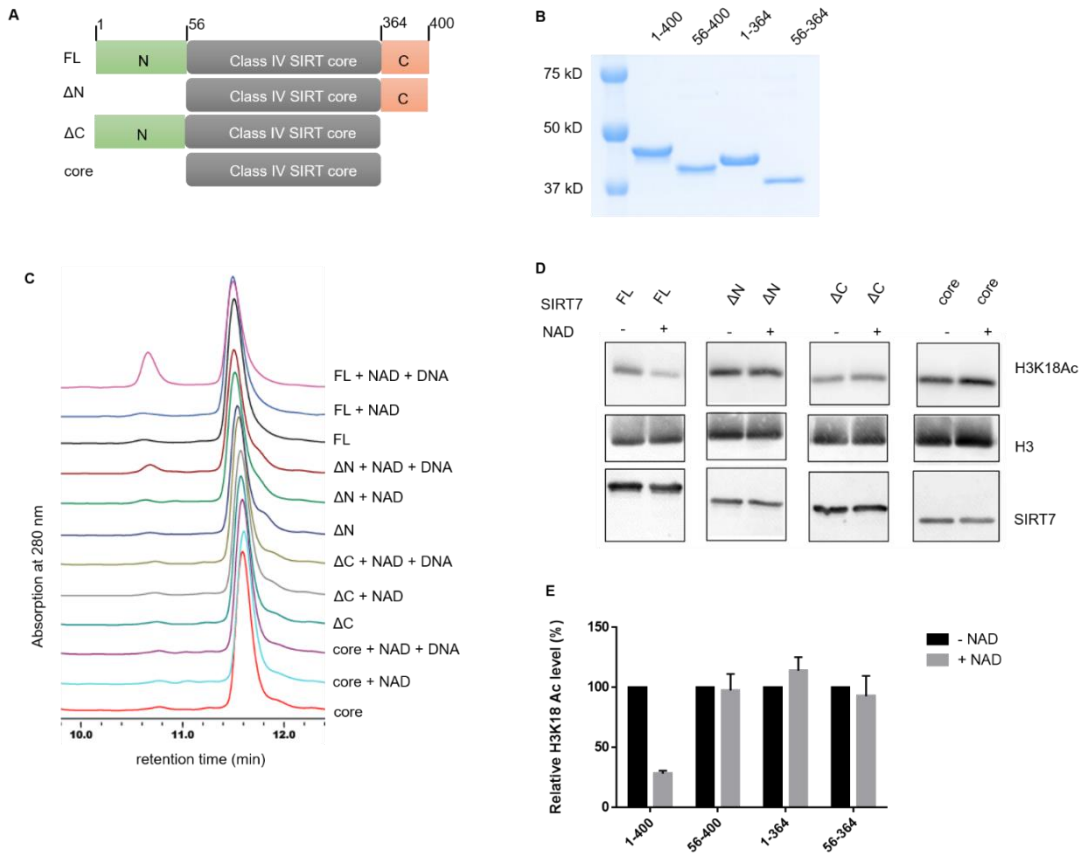


**Figure 2.7** Both the N- and C- termini of SIRT7 are important for its activation by DNA. (A) Scheme showing the full length (FL, residue 1-400), N-terminal deletion (ΔN, residue 56-400), C-terminal deletion (ΔC, residue 1-364), and core domain (56-364) of SIRT7. (B) Coomassie blue-stained gel showing the purity of SIRT7 deletion mutants. (C) HPLC traces showing the activity of different SIRT7 deletion mutants with and without dsDNA on H3K18 Ac peptide. (D) The deacetylase activities of SIRT7 FL and deletion mutants on H3K18 Ac on chromatin substrates. Reactions without NAD were used as negative controls. (E) Quantification of the Western blot results in (D). The H3K18 Ac level in each reaction was normalized by the amount of histone H3 protein. The relative H3K18 Ac level was calculated by setting the level of negative control to 100%.

We further examined whether SIRT7 truncations could deacetylate H3K18 Ac on

chromatin substrates. As shown in Figure 2.7D and quantified in Figure 2.7E, only full length Sirt7 was able to efficiently deacetylate H3K18 Ac group while ΔN, ΔC and core domain exhibited no activity, consistent with the results obtained using the peptide substrate.

In summary, our enzymology data demonstrated that SIRT7 has extremely low basal deacetylase activity on histone peptides, but the activity can be significantly increased by dsDNA. When working on physiologically relevant histone protein substrates, exogenous DNA did not activate SIRT7's deacetylase activity, but the chromatin compositional DNA activated SIRT7 to deacetylate H3K18 Ac. Moreover, studies with SIRT7 truncations implicated that both N- and C- termini are important for its dsDNA-activated deacetylase activity. Interestingly, the N- and C-terminal domains of SIRT7 have been previously implicated in mediating nuclear and nucleolar localization[22] and interaction with Myb-binding protein 1a[23], a SIRT7 inhibitor. Thus, it appears that the N- and C-terminal domains of SIRT7 play multiple roles in regulating SIRT7 physiological function. Our work demonstrates for the first time that SIRT7 enzymatic activity could be regulated by DNA molecules and identified regions of SIRT7 that are important for the activation. SIRT7 has been widely known as a transcription regulator[11-13]. The results presented here suggest that DNA binding and activation could serve as a molecular switch that turns on SIRT7 when it approaches histone substrates on chromatin.

SIRT7 is known to be important for regulating fatty liver formation[12, 13, 24] and tumorigenesis[11, 25-29]. Thus, small molecule inhibitors of SIRT7 will be useful probes to further explore the biological function and therapeutic potential of SIRT7. However, so

far no potent SIRT7 inhibitors have been reported. This is mainly due to lack of a reliable in vitro assay to detect SIRT7 activity. Our finding that DNA can significantly activate SIRT7 will fill in this gap and promote the development of SIRT7 inhibitors. Although controversial, sirtuin activators have been reported to provide health benefits[30-34]. Interestingly, the activation of SIRT1 by small molecules also involves its N-terminal domain[35], similar to the activation of SIRT7 by DNA. Further investigation into the mechanism by which SIRT7 is activated by DNA may provide insights that may help the development of novel sirtuin activators.

**Materials and Methods**

**SIRT7 purification**. The open reading frames of full length human SIRT7 (1-400), ΔN (56-400), ΔC (1-364), and the core domain (56-364) were inserted into the pET28a vector. The plasmid was transformed into E. coli Arctic Express (DE3) cells. Cells were cultured at 37°C in LB broth medium (BD biosciences catalog# 240220). Isopropyl-β-D-1-thiogalactopyranoside (IPTG) was added to a final concentration of 0.2 mM when $OD_{600}$ was between 1-1.5, and the culture was grown for 48 hours at 10 °C. Cells were harvested and then re-suspended in lysis buffer (50 mM $K_2HPO_4$ pH 7.20, 500 mM NaCl, 5% glycerol). The cells were lysed using a cell disrupter. The lysate was centrifuged at 20,000 rpm for 30 min at 4 °C. The supernatant was loaded onto a nickel column (HisTrap HP, GE healthcare life sciences) pre-equilibrated with a buffer containing 50 mM $K_2HPO_4$ (pH 7.20), 500 mM NaCl and 5% glycerol. SIRT7 was eluted with a linear gradient of imidazole (0 to 500 mM) in the buffer. The desired fractions were pooled, concentrated and buffer exchanged

against the cation exchange buffer (80 mM NaCl, 50 mM $K_2HPO_4$ pH 7.20, 5% glycerol). The protein was further loaded onto a cation exchange column (HiTrap SP HP, GE healthcare life sciences) and eluted with a linear gradient of NaCl (80 mM to 1 M) in the buffer containing 50 mM $K_2HPO_4$ (pH 7.20) and 5% glycerol. Fractions were assayed for purity on SDS-PAGE and concentrated, snap frozen and stored at -80 °C.

**Synthesis of acetyl peptides**. Acetyl peptides corresponding to residues 4-13 and 12-24 of Histone H3 ($NH_2$-KQTARKacSTGGWW-COOH and $NH_2$-GGKAPRKacQLATKAWW-COOH) were synthesized by standard solid phase peptide synthesis as described below. Two Trp residues were added to the C-terminus of the peptides to facilitate the detection of peptides by monitoring ultra-violet (UV) light absorption specifically at 280 nm.

Peptides were synthesized by Fmoc SPPS on an automated peptide synthesizer (Focus XC from aapptec) using standard protocols. 500 mg of Wang resin (100-200 mesh, 1% DVB, 1.2 meq/g) was swollen in 10 mL DCM for 6 h. The first amino acid was coupled onto the resin for 3 h in DMF, with a 4-fold excess of amino acid, 4-fold excess of HBTU, and 10-fold excess of DIEA followed by addition of 0.1 equivalent of DMAP in 0.2 ml of DCM. The resin was then treated with $Ac_2O$/pyridine (1:9 v/v) for 10 min to cap any remaining reactive functionalities on the resin. The coupling of the rest amino acids was carried out following standard protocols using 4-fold excess of amino acid, 4-fold excess of HBTU, and 10-fold excess of DIEA. Acetyl modification on lysine residues was introduced through the use of Fmoc-Lys(acetyl)-OH. The peptides were cleaved from the resin using a cocktail of trifluoroacetic acid,

triisopropylsilane, water, ethanedithiol, thioanisole, and phenol (81.5:1:5:2.5:5:5 by vollume) for 2 h. The crude peptides were purified by preparative HPLC. The identities of the peptides were confirmed using LC-MS (LCQ Fleet, Thermo Scientific).

The purified free-lysine and acetyl H3K9 and H3K18 peptides were dissolved in water. The concentrations of peptides were determined at 280 nm using extinctions coefficient of the two Trp residues attached at the C-terminus of the peptides.

**HPLC Assay and kinetics.** Activity of SIRT7 was detected using HPLC. The reactions contained 50 mM Tris (pH 8.0), 150 mM NaCl, 1 mM DTT, 2 mM $NAD^+$, 50 μM H3K9 Ac or H3K18 Ac peptides, and 2 μM SIRT7. Reactions were incubated at 37 °C for 1 h. Salmon sperm DNA mixture (10 mg/ml) was used as the in vitro activator. Mass ratio of DNA to SIRT7 was maintained at 3:1 in the assays unless specified otherwise. The reactions were quenched with 1 volume of 10% (v/v) TFA and spun down for 10 min at 18,000 g to remove proteins. The supernatants were then analyzed by HPLC using a reverse phase analytical column (Kinetex XB-C18 100A, 75 mm × 4.60 mm, 2.6 μm, Phenomenex). The product and substrate peaks were quantified using the absorption peak areas at 280 nm from the two Trp residues added at C-terminus of the peptide substrates.

For kinetics, 2 mM NAD, 50 mM Tris (pH 8.0), 1 mM DTT, 2 μM SIRT7 (full-length) or 8 μM SIRT7 (ΔN, 56-400) was used. Peptide concentration used for H3K18 Ac and H3K9 Ac were 10, 30, 50, 100, 150, 250 and 500 μM with an incubation time of 45 minutes. The quenched reactions were then analyzed by HPLC. The product and substrate peaks were quantified as described above and converted to initial rates, which

were then plotted against the peptide concentrations and fitted to the Michaelis-Menten equation using the Graphpad Prism 6 program.

**Histone deacetylation assay.** Calf thymus histones were obtained from Roche. In vitro deacetylation reactions were performed with 10 μg of SIRT7 and 1 μg of calf thymus histone in deacetylation buffer (50 mM Tris, pH 8.0, 150 mM NaCl, 2 mM $NAD^+$, 1 mM DTT), with or without 30 μg of salmon sperm DNA. The reactions were incubated at 37℃for 2h. The reactions were quenched by adding 3X Laemmli buffers and boiling for 15 minutes at 95℃. The acetylation level of histones was assessed by Western blot using H3K9 Ac (Abcam cat# ab4441)- and H3K18 Ac (Abcam cat # ab1191) -specific antibodies. To more quantitatively determine H3K18 Ac level using Western blot, we used a fluorophore-conjugated secondary antibody (Goat anti-rabbit Dylight 488, thermofisher cat # 35552). Signal intensity of all Western blot bands was quantified using ImageJ.

For the chromatin deacetylation assay, we extracted chromatin fraction from 293T cells as previously described[12]. 293T cells were treated with 2 μM histone deacetylases inhibitor, trichostatin A (TSA) for 2h before harvest. 10 μM SIRT7 protein was incubated with ~1 μM chromatin substrate in deacetylation buffer (50 mM Tris, pH 8.0, 150 mM NaCl, 2 mM $NAD^+$, 1 mM DTT). To remove DNA or RNA, 2 μL nuclease cocktail (Thermo Fisher cat. # 88702) or 4 μL Rnase I (Ambion cat. # AM 2294) was added to 30 μL of reaction mixture and incubated at 37℃for 2h. The acetylation levels of H3K18 Ac and H3K9 Ac were determined as described above.

**Cell culture.** Human 293T cell lines were acquired from the American Type

Culture Collection (ATCC). Cells were cultured in Dulbecco's Modified Eagle Medium (DMEM) complete medium containing glucose and L-glutamine (Invitrogen) supplemented with 10% heat-inactivated fetal bovine serum (Invitrogen).

**References**


1. Imai, S.-i., and Guarente, L. (2010) Ten years of NAD-dependent SIR2 family deacetylases: implications for metabolic diseases, Trends Pharmacol. Sci. 31, 212-220.
2. Imai, S.-i., Armstrong, C. M., Kaeberlein, M., and Guarente, L. (2000) Transcriptional silencing and longevity protein Sir2 is an NAD-dependent histone deacetylase, Nature 403, 795-800.
3. Tanner, K. G., Landry, J., Sternglanz, R., and Denu, J. M. (2000) Silent information regulator 2 family of NAD- dependent histone/protein deacetylases generates a unique product, 1-O-acetyl-ADP-ribose, Proc. Natl. Acad. Sci. U. S. A. 97, 14178-14182.
4. Frye, R. A. (2000) Phylogenetic classification of prokaryotic and eukaryotic Sir2-like proteins, Biochem. Biophys. Res. Commun. 273, 793-798.
5. Houtkooper, R. H., Pirinen, E., and Auwerx, J. (2012) Sirtuins as regulators of metabolism and healthspan, Nat. Rev. Mol. Cell Biol. 13, 225-238.
6. Haigis, M. C., and Sinclair, D. A. (2010) Mammalian Sirtuins: Biological Insights and Disease Relevance, Annu. Rev. Pathol. 5, 253-295.

7. Michishita, E., Park, J. Y., Burneskis, J. M., Barrett, J. C., and Horikawa, I. (2005) Evolutionarily conserved and nonconserved cellular localizations and functions of human SIRT proteins, Mol. Biol. Cell 16, 4623-4635.

8. Ford, E., Voit, R., Liszt, G., Magin, C., Grummt, I., and Guarente, L. (2006) Mammalian Sir2 homolog SIRT7 is an activator of RNA polymerase I transcription, Genes Dev. 20, 1075-1080.

9. Tsai, Y. C., Greco, T. M., Boonmee, A., Miteva, Y., and Cristea, I. M. (2012) Functional proteomics establishes the interaction of SIRT7 with chromatin remodeling complexes and expands its role in regulation of RNA polymerase I transcription, Mol. Cell. Proteomics 11, 60-76.

10. Chen, S., Seiler, J., Santiago-Reichelt, M., Felbel, K., Grummt, I., and Voit, R. (2013) Repression of RNA polymerase I upon stress is caused by inhibition of RNA-dependent deacetylation of PAF53 by SIRT7, Mol. Cell. 52, 303-313.

11. Barber, M. F., Michishita-Kioi, E., Xi, Y., Tasselli, L., Kioi, M., Moqtaderi, Z., Tennen, R. I., Paredes, S., Young, N. L., Chen, K., Struhl, K., Garcia, B. A., Gozani, O., Li, W., and Chua, K. F. (2012) SIRT7 links H3K18 deacetylation to maintenance of oncogenic transformation, Nature 487, 114-118.

12. Shin, J., He, M., Liu, Y., Paredes, S., Villanova, L., Brown, K., Qiu, X., Nabavi, N., Mohrin, M., Wojnoonski, K., Li, P., Cheng, H. L., Murphy, A. J., Valenzuela, D. M., Luo, H., Kapahi, P., Krauss, R., Mostoslavsky, R., Yancopoulos, G. D., Alt, F. W., Chua, K. F., and Chen, D. (2013) SIRT7 represses Myc activity to suppress ER stress and prevent fatty liver disease, Cell Rep. 5, 654-665.

13. Ryu, D., Jo, Y. S., Lo Sasso, G., Stein, S., Zhang, H., Perino, A., Lee, J. U., Zeviani, M., Romand, R., Hottiger, M. O., Schoonjans, K., and Auwerx, J. (2014) A SIRT7-dependent acetylation switch of GABPbeta1 controls mitochondrial function, Cell Metab 20, 856-869.

14. Vakhrusheva, O., Smolka, C., Gajawada, P., Kostin, S., Boettger, T., Kubin, T., Braun, T., and Bober, E. (2008) Sirt7 increases stress resistance of cardiomyocytes and prevents apoptosis and inflammatory cardiomyopathy in mice, Circ. Res. 102, 703-710.

15. Kiran, S., Oddi, V., and Ramakrishna, G. (2015) Sirtuin 7 promotes cellular survival following genomic stress by attenuation of DNA damage, SAPK activation and p53 response, Experimental cell research 331, 123-141.

16. Tsai, Y. C., Greco, T. M., and Cristea, I. M. (2014) Sirtuin 7 plays a role in ribosome biogenesis and protein synthesis, Mol. Cell. Proteomics 13, 73-83.

17. Feldman, J. L., Baeza, J., and Denu, J. M. (2013) Activation of the protein deacetylase SIRT6 by long-chain fatty acids and widespread deacylation by mammalian sirtuins, J. Biol. Chem. 288, 31350-31356.

18. Gil, R., Barth, S., Kanfi, Y., and Cohen, H. Y. (2013) SIRT6 exhibits nucleosome-dependent deacetylase activity, Nucleic Acids Res.

19. Mendez, J., and Stillman, B. (2000) Chromatin association of human origin recognition complex, cdc6, and minichromosome maintenance proteins during the cell cycle: assembly of prereplication complexes in late mitosis, Mol. Cell. Biol. 20, 8602-8612.

20. Sauve, A. A., Wolberger, C., Schramm, V. L., and Boeke, J. D. (2006) The biochemistry of sirtuins, Annu. Rev. Biochem. 75, 435-465.

21. Wang, L., and Brown, S. J. (2006) BindN: a web-based tool for efficient prediction of DNA and RNA binding sites in amino acid sequences, Nucleic Acids Res. 34, W243-248.

22. Kiran, S., Chatterjee, N., Singh, S., Kaul, S. C., Wadhwa, R., and Ramakrishna, G. (2013) Intracellular distribution of human SIRT7 and mapping of the nuclear/nucleolar localization signal, FEBS J. 280, 3451-3466.

23. Karim, M. F., Yoshizawa, T., Sato, Y., Sawa, T., Tomizawa, K., Akaike, T., and Yamagata, K. (2013) Inhibition of H3K18 deacetylation of Sirt7 by Myb-binding protein 1a (Mybbp1a), Biochem. Biophys. Res. Commun. 441, 157-163.

24. Yoshizawa, T., Karim, M. F., Sato, Y., Senokuchi, T., Miyata, K., Fukuda, T., Go, C., Tasaki, M., Uchimura, K., Kadomatsu, T., Tian, Z., Smolka, C., Sawa, T., Takeya, M., Tomizawa, K., Ando, Y., Araki, E., Akaike, T., Braun, T., Oike, Y., Bober, E., and Yamagata, K. (2014) SIRT7 controls hepatic lipid metabolism by regulating the ubiquitin-proteasome pathway, Cell Metab. 19, 712-721.

25. Malik, S., Villanova, L., Tanaka, S., Aonuma, M., Roy, N., Berber, E., Pollack, J. R., Michishita-Kioi, E., and Chua, K. F. (2015) SIRT7 inactivation reverses metastatic phenotypes in epithelial and mesenchymal tumors, Sci. Rep. 5, 9841.

26. Zhang, S., Chen, P., Huang, Z., Hu, X., Chen, M., Hu, S., Hu, Y., and Cai, T. (2015) Sirt7 promotes gastric cancer growth and inhibits apoptosis by epigenetically inhibiting miR-34a, Sci. Rep. 5, 9787.

27. Kim, J. K., Noh, J. H., Jung, K. H., Eun, J. W., Bae, H. J., Kim, M. G., Chang, Y. G., Shen, Q., Park, W. S., Lee, J. Y., Borlak, J., and Nam, S. W. (2013) Sirtuin7 oncogenic potential in human hepatocellular carcinoma and its regulation by the tumor suppressors MiR-125a-5p and MiR-125b, Hepatology 57, 1055-1067.

28. Wang, H. L., Lu, R. Q., Xie, S. H., Zheng, H., Wen, X. M., Gao, X., and Guo, L. (2015) SIRT7 Exhibits Oncogenic Potential in Human Ovarian Cancer Cells, Asian Pac. J. Cancer Prev. 16, 3573-3577.

29. Yu, H., Ye, W., Wu, J., Meng, X., Liu, R. Y., Ying, X., Zhou, Y., Wang, H., Pan, C., and Huang, W. (2014) Overexpression of sirt7 exhibits oncogenic property and serves as a prognostic factor in colorectal cancer, Clin. Cancer Res. 20, 3434-3445.

30. Milne, J. C., Lambert, P. D., Schenk, S., Carney, D. P., Smith, J. J., Gagne, D. J., Jin, L., Boss, O., Perni, R. B., Vu, C. B., Bemis, J. E., Xie, R., Disch, J. S., Ng, P. Y., Nunes, J. J., Lynch, A. V., Yang, H., Galonek, H., Israelian, K., Choy, W., Iffland, A., Lavu, S., Medvedik, O., Sinclair, D. A., Olefsky, J. M., Jirousek, M. R., Elliott, P. J., and Westphal, C. H. (2007) Small molecule activators of SIRT1 as therapeutics for the treatment of type 2 diabetes, Nature 450, 712-716.

31. Baur, J. A., Pearson, K. J., Price, N. L., Jamieson, H. A., Lerin, C., Kalra, A., Prabhu, V. V., Allard, J. S., Lopez-Lluch, G., Lewis, K., Pistell, P. J., Poosala, S., Becker, K. G., Boss, O., Gwinn, D., Wang, M., Ramaswamy, S., Fishbein, K. W., Spencer, R. G., Lakatta, E. G., Le Couteur, D., Shaw, R. J., Navas, P., Puigserver, P., Ingram, D. K., de Cabo, R., and Sinclair, D. A. (2006)

Resveratrol improves health and survival of mice on a high-calorie diet, Nature 444, 337-342.

32. Borra, M. T., Smith, B. C., and Denu, J. M. (2005) Mechanism of Human SIRT1 Activation by Resveratrol, J. Biol. Chem. 280, 17187-17195.

33. Pacholec, M., Bleasdale, J. E., Chrunyk, B., Cunningham, D., Flynn, D., Garofalo, R. S., Griffith, D., Griffor, M., Loulakis, P., Pabst, B., Qiu, X., Stockman, B., Thanabal, V., Varghese, A., Ward, J., Withka, J., and Ahn, K. (2010) SRT1720, SRT2183, SRT1460, and resveratrol are not direct activators of SIRT1, J. Biol. Chem. 285, 8340-8351.

34. Sinclair, D. A., and Guarente, L. (2014) Small-molecule allosteric activators of sirtuins, Annu. Rev. Pharmacol. Toxicol. 54, 363-380.

35. Dai, H., Case, A. W., Riera, T. V., Considine, T., Lee, J. E., Hamuro, Y., Zhao, H., Jiang, Y., Sweitzer, S. M., Pietrak, B., Schwartz, B., Blum, C. A., Disch, J. S., Caldwell, R., Szczepankiewicz, B., Oalmann, C., Yee Ng, P., White, B. H., Casaubon, R., Narayan, R., Koppetsch, K., Bourbonais, F., Wu, B., Wang, J., Qian, D., Jiang, F., Mao, C., Wang, M., Hu, E., Wu, J. C., Perni, R. B., Vlasuk, G. P., and Ellis, J. L. (2015) Crystallographic structure of a small molecule SIRT1 activator-enzyme complex, Nat. Commun. 6, 7645.

# CHAPTER 3

## SIRT7 is an RNA-Activated Protein Lysine Deacylase


### Abstract

Mammalian SIRT7 is a member of the sirtuin family of nicotinamide adenine dinucleotide (NAD)-dependent protein lysine deacylases that regulate multiple biological processes including genome stability, metabolic pathways, stress responses, and tumorigenesis. SIRT7 has been shown to be important for ribosome biogenesis and transcriptional regulation. SIRT7 knockout mice exhibit complications associated with fatty liver and increased aging in hematopoietic stem cells. However, the molecular basis for its biological function remains unclear, in part due to the lack of efficient enzymatic activity in vitro. Previously we have demonstrated that double-stranded DNA could activate SIRT7's deacetylase activity in vitro, allowing it to deacetylate H3K18 in the context of chromatin. Here we show that RNA can increase the catalytic efficiency of SIRT7 even better and that SIRT7 can remove long chain fatty acyl groups more efficiently than removing acetyl groups. Truncation and mutagenesis studies revealed residues at both the amino and carboxyl termini of SIRT7 that are involved in RNA-binding and important for activity. RNA immunoprecipitation-sequencing (RIP-seq) identified ribosomal RNA (rRNA) as the predominant RNA binding partners of SIRT7. The associated RNA was able to effectively activate the deacetylase and defatty-acylase activities of SIRT7. These findings provide important insights into the biological functions of SIRT7, as well as an improved platform to develop SIRT7 modulators.

## Introduction

Silent information regulator-2 (Sir2) proteins, or sirtuins, are a family of evolutionarily conserved enzymes exhibiting unique nicotinamide adenine dinucleotide (NAD)-dependent protein lysine deacetylase activities[1-3]. Mammals encode seven sirtuins (SIRT1-SIRT7)[4], which regulate many important biological processes including genome stability, stress response, metabolism, and aging[5, 6]. The seven human sirtuins display widespread subcellular localizations, with SIRT1, SIRT6, and SIRT7 being predominantly nuclear, SIRT2 being primarily cytosolic, and SIRT3-5 being mainly mitochondrial[7]. Despite the fact that all sirtuins possess a conserved catalytic core domain, emerging evidence demonstrates that sirtuins exhibit varying catalytic activities towards different acyl lysine modifications. SIRT1-3 display robust deacetylase activities, whereas SIRT4-7 have only weak deacetylase activities in vitro. SIRT5 and SIRT6, two of the four sirtuins with weak deacetylase activities, preferentially hydrolyze succinyl/malonyl/glutaryl[8, 9] and long-chain fatty acyl lysine[10], respectively. These studies demonstrate that sirtuins are able to hydrolyze a variety of lysine acyl modifications and regulate a broad range of cellular events.

Among the seven human sirtuins, the function of SIRT7 is still not well understood. SIRT7 is enriched in nucleoli where it activates rRNA gene transcription by interacting with RNA polymerase I (Pol I) and the upstream binding transcription factor (UBF)[11, 12]. In response to metabolic stress, SIRT7 is released from nucleoli leading to hyperacetylation of PAF53 (a subunit of Pol I transcription complex) and decreased Pol I transcription[13]. SIRT7 also suppresses Pol II-mediated mRNA transcription by deacetylating histone H3 Lys18 (H3K18)[14]. Moreover, SIRT7 regulates

transcription of nucleus-encoded mitochondrial biogenesis genes by deacetylating and activating a transcription factor GABPβ1[15]. Interestingly, three recent studies link SIRT7 to the regulation of liver function in mouse, although different effects of SIRT7 on fatty liver formation are reported[15-17].

So far, all the biological functions of SIRT7 have been attributed to its deacetylase activity. However, the in vitro deacetylase activity of SIRT7 in many cases cannot be detected. We have previously shown that double-stranded DNA (dsDNA) can significantly improve SIRT7's deacetylase activity and allows it to deacetylate H3K18 in the context of chromatin[18]. However, the in vitro activity on peptide substrates is still rather weak compared to other sirtuins with efficient deacetylase activities. Here we report that RNA can increase the catalytic efficiency of SIRT7 even better. Furthermore, upon RNA activation, SIRT7 can remove long chain fatty acyl groups more efficiently than removing acetyl groups. Both ribosomal RNA (rRNA) and transfer RNA (tRNA) are potent activators of SIRT7 in vitro. The predominant endogenous RNA binding partners of SIRT7 are rRNA, which can efficiently activate SIRT7 in vitro. Mutagenesis study identified key residues at the N- and C- termini of SIRT7 that are important for the interaction with RNA and enzymatic activity. We believe these results will help to better understand the biological functions of SIRT7 and to develop small molecule modulators of SIRT7.

## Results and Discussion

### SIRT7 deacetylase activity is dramatically enhanced by RNA

We have recently reported that SIRT7 can be activated by dsDNA[18], which

explains its role as a H3K18 deacetylase in regulating transcription. SIRT7 is also involved in regulating rRNA gene transcription, ribosome biogenesis, and protein synthesis[11, 19, 20], which are also thought to be mediated by its deacetylase activity. It is not clear how SIRT7's catalytic activity would be stimulated when functioning to regulate ribosome biogenesis and protein synthesis. We wondered whether RNA species could also activate SIRT7. To test this hypothesis, we used an HPLC assay to monitor the deacetylase activity of SIRT7 on H3K9 and H3K18 acetyl (H3K9 Ac and H3K18 Ac) peptides in the presence of different nucleic acids (dsDNA, rRNA, and tRNA at the mass ratio of nucleic acid to SIRT7 maintained at 3:1). In the absence of nucleic acid, no product was formed. In the presence of either DNA or RNA, the deacetylated H3K18 peptide was detected (Figure 3.1A & 3.1B). Interestingly, among all the nucleic acids we tested in vitro, tRNA turned out to be the most potent activator of SIRT7. None of the other sirtuin proteins (except for SIRT4 which we cannot obtain the recombinant protein from E.coli) can be activated by RNA (Figure 3.1C). Therefore, among all the seven human sirtuins, SIRT7 is unique in that its enzymatic activity could be activated by both DNA and RNA on peptide substrates.

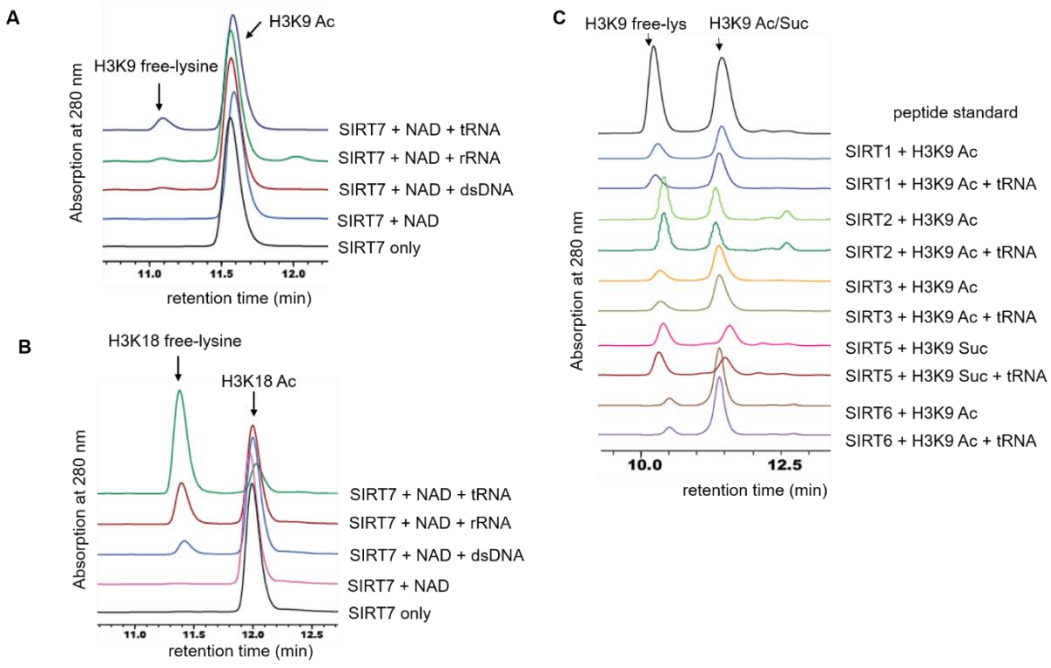


**Figure 3.1** SIRT7 deacetylase activity is dramatically increased by RNA. (A) Overlaid HPLC traces showing SIRT7-catalyzed hydrolysis of H3K9 acetyl (Ac) peptide with different nucleic acids. (B) HPLC traces showing SIRT7-catalyzed hydrolysis of H3K18 acetyl (Ac) peptide with nucleic acids. (C) Overlaid HPLC traces showing that other sirtuin proteins cannot be activated by tRNA.

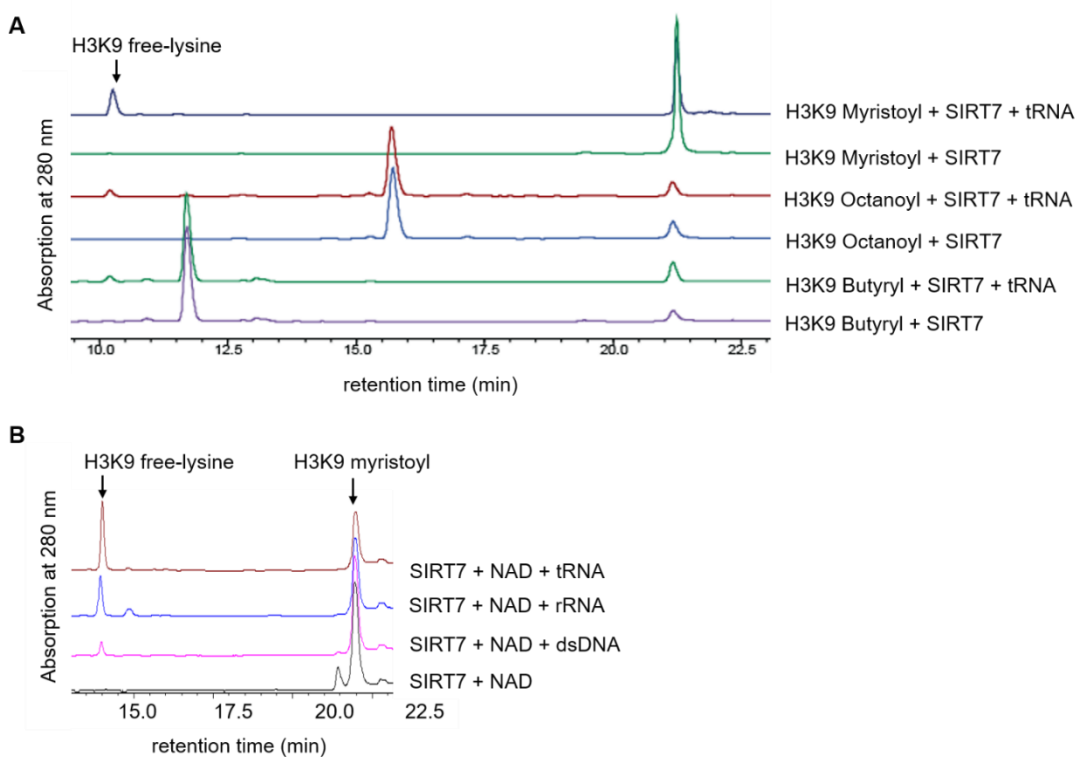


**Figure 3.2** SIRT7 has efficient defatty-acylase activity upon RNA activation. (A) Overlaid HPLC traces showing that SIRT7 can hydrolyze fatty acyl groups with different carbon chain length from lysine residues. (B) HPLC traces showing that SIRT7 demyristoylase activity is dramatically activated by rRNA and tRNA.

**SIRT7 exhibits efficient defatty-acylase activity upon activation by RNA**

It was recently reported that defatty-acylation (removing long chain fatty acyl groups) is an intrinsic activity of several sirtuins[10, 21, 22]. In particular, SIRT6, which is also a class IV sirtuin like SIRT7, can remove long chain fatty acyl groups more efficiently in vitro. Therefore, we investigated whether SIRT7 could also remove long chain fatty acyl groups. We tested the activity of recombinant human SIRT7 on H3K9 peptides with different acyl groups (butyryl, octanoyl, and myristoyl). In the absence of RNA, no deacylation product was detected (except very little that was observed when

using the H3K9 myristoyl peptide) (Figure 3.2). In the presence of tRNA, SIRT7 was able to catalyze the hydrolysis of all three H3K9 acyl peptides. Among the three acyl peptides, the hydrolysis of myristoyl lysine was the most efficient (Figure 3.2A & B), suggesting that SIRT7 has a preference for long chain fatty acyl groups similar to its closest sirtuin member, SIRT6[10].

To quantitatively compare the effects of tRNA activation, we determined the turnover number ($k_{cat}$) and Michaelis constant ($K_m$) of SIRT7 on H3K9 peptides with different acyl groups (Table 3.1). The molar ratio of tRNA to SIRT7 was fixed at 3:1 (Figure 3.3). The $k_{cat}/K_m$ for demyristoylation with tRNA (52 $M^{-1}s^{-1}$) was approximately 50-fold better than that for deacetylation (~1 $M^{-1}s^{-1}$) on H3K9 peptides. tRNA improved the catalytic efficiency of SIRT7 for demyristoylation nearly 50-fold, which was achieved mainly by increasing $k_{cat}$ (30-fold), as well as decreasing $K_m$ slightly (1.5-fold). Similarly, tRNA improved the catalytic efficiency of SIRT7 on H3K18 acyl peptides (Table 3.1).

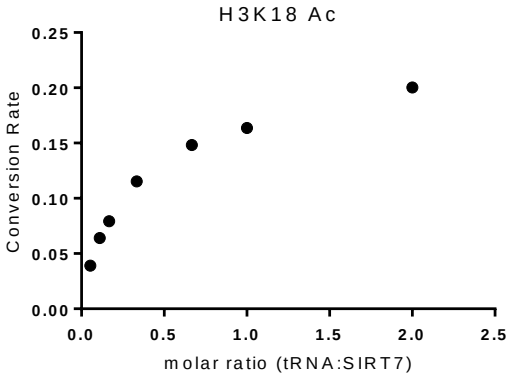


**Figure 3.3** The activity of SIRT7 with different amount of tRNA. The conversation rates for deacetylation of SIRT7 on H3K18 Ac peptide (50 μM) were plotted against the tRNA to SIRT7 molar ratios. SIRT7 was fixed at 3 μM, and the reaction was incubated at 37 ℃ for 45 minutes.

**Table 3.1** Catalytic efficiencies of SIRT7 on H3 acyl peptides with different nucleic acids

| acyl peptide | activator | $k_{cat}$ ($min^{-1}$) | $K_m$ (μM) | $k_{cat}/K_m$ ($M^{-1}s^{-1}$) |
|---|---|---|---|---|
| H3K18 Ac | - | NP | NP | NP |
| | tRNA | 1.2 ± 0.2 | 309 ± 59 | 65 |
| H3K18 Myr | - | NP | NP | NP |
| | tRNA | 0.02 ± 0.002 | <2 | >200 |
| H3K9 Ac | - | NP | NP | NP |
| | dsDNA | 0.05 ± 0.02 | 840 ± 452 | 1.0 |
| | tRNA | ND | ND | ~1.0 |
| H3K9 Myr | - | 0.004 ± 0.001 | 65 ±26 | 1.1 |
| | dsDNA | 0.04 ± 0.005 | 32 ±10 | 21 |
| | tRNA | 0.1 ± 0.01 | 41 ± 7 | 52 |
| H3K9 But | tRNA | ND | ND | ~2.0 |
| H3K9 Oct | tRNA | ND | ND | ~2.0 |

ND: Not determined because V~[S] was linear. Only $k_{cat}/K_m$ value could be obtained.

NP: No product formed (product formation was below HPLC detection limit).

Ac: acetyl; But: butyryl; Oct: octanoyl; Myr: myristoyl.

**SIRT7 associates with RNA in mammalian cells.**

Previous studies have demonstrated that SIRT7 interacts with transcription

factors, such as ELK4 and MYC, and almost exclusively resides in a chromatin-enriched fraction[14, 17]. We believe in this scenario, DNA acts as the activator of SIRT7, which hydrolyzes acetylated H3K18 and suppresses transcription. We have thus far revealed that RNA species (rRNA and tRNA) can serve as effective activators for SIRT7 in vitro. Therefore, we asked whether SIRT7 directly binds RNA in mammalian cells. To address this question, we stably overexpressed Flag-tagged SIRT7 in HEK 293T cells and performed RNA immunoprecipitation (RIP). Empty vector and Flag-tagged SIRT6 were used as negative controls. Co-immunoprecipitated RNA was labeled with [$^{32}$P]pCp at the 3'-end and further resolved on the denaturing gel. As shown in Figure 3.4A, Flag-SIRT7 was able to pull down several major RNA species, which were resistant to Dnase treatment but were completely degraded by Rnase. In contrast, very little RNA was pulled down by Flag-SIRT6.

To dissect which domain(s) of SIRT7 interacts with RNA, we expressed Flag-tagged SIRT7 truncation mutants (ΔN 56-400, ΔC 1-364, and core domain 56-364, Figure 3.4B) and conducted CLIP (UV-crosslinking and immunoprecipitation of RNA) experiments and further labeled the 3'-end of immunoprecipitated RNA with [$^{32}$P]pCp (Figure 3.4C). Interestingly, SIRT7 core domain (56-364) was incapable of pulling down any RNA species while both ΔN and ΔC were still able to pull down RNA. Thus, both the N- and C-termini of SIRT7 contribute to its interaction with endogenous RNA.

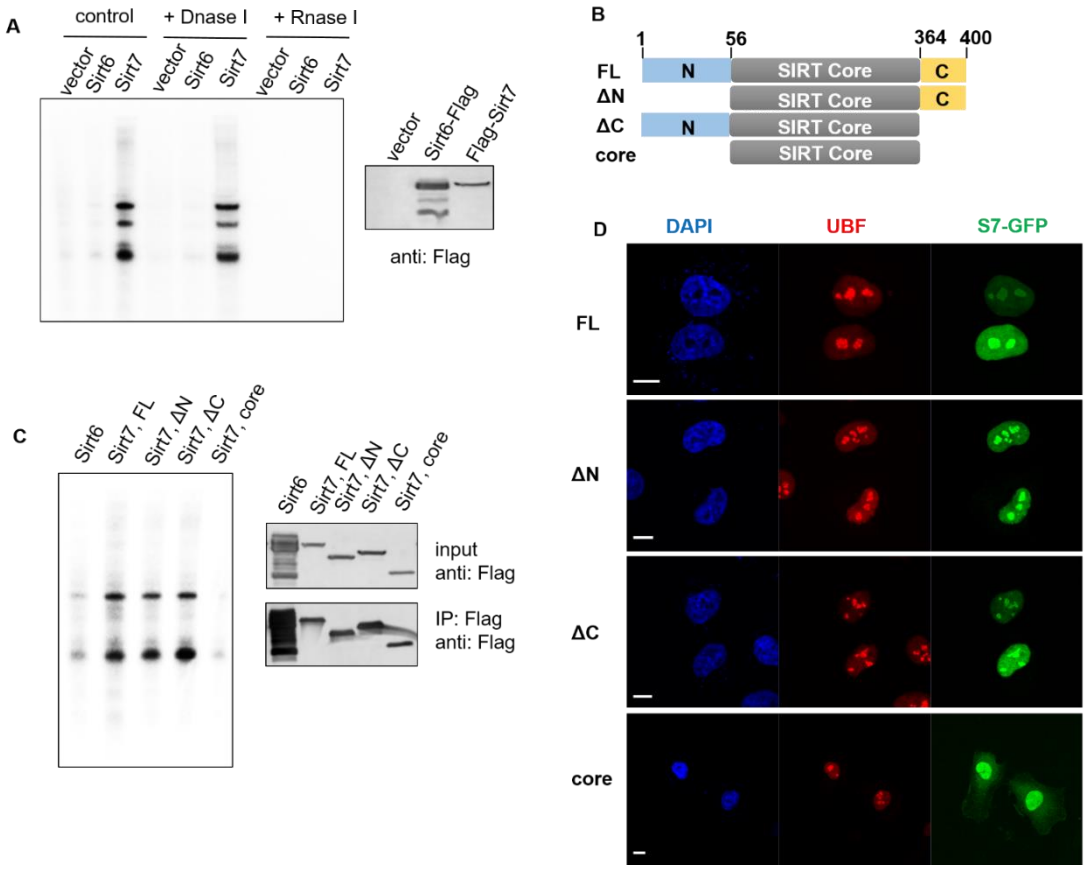


**Figure 3.4** SIRT7 associates with RNA in mammalian cells. (A) SIRT7 pulled down endogenous RNA species. SIRT6 was used as a negative control. (B) Scheme showing SIRT7 full-length (FL: 1-400), N-terminal deletion (ΔN: 56-400), C-terminal deletion (ΔC: 1-364), and core domain (56-364). (C) SIRT7 core domain did not bind endogenous RNA. (D) SIRT7 core domain was no longer localized in nucleoli and dispersed into nucleoplasm and cytoplasm. Scale bar: 10 μm.

We next investigated whether association with RNA correlated with SIRT7 subcellular localization. We transiently overexpressed GFP-tagged SIRT7 truncation proteins and examined their localization in Hela cells. FL, ΔN, ΔC are all localized in the nucleus with enrichment in nucleoli as indicated by co-localization with UBF. In contrast, the core domain of SIRT7 did not show nucleoli-enriched localization and

some SIRT7 molecules were also localized in the cytosol (Figure 3.4D). These results support that SIRT7 interacts with RNA in cells and this interaction may be important for its proper localization.

**SIRT7 mainly interacts with rRNA in vivo.**

In order to characterize the repertoire of RNAs that are associated with SIRT7 in vivo, we sequenced the RNAs co-immunoprecipitated with Flag-tagged SIRT7 using RIP-seq (RNA immunoprecipitation sequencing). As summarized in Figure 3.5, in the cytosol, 99% of the RNA binding partners of SIRT7 turned out to be rRNA and similarly in the nucleus, 97% of the RNAs associated with SIRT7 were rRNAs, consistent with the reported roles of SIRT7 involved in pre-rRNA transcription and processing[11, 20]. We further mapped all the rRNA reads to human pre-rRNA sequences (Figure 3.6). The majority of SIRT7-interacting rRNA reads corresponded to the transcribed regions of mature rRNA (18S, 5.8S and 28S rRNA), constant with our RIP-$^{32}$P-labeling results (Figure 3.4 & Figure 3.8). Noticeably, we also identified 5S rRNA in the RIP-seq result (Figure 3.7). The 5S rRNA is transcribed by Pol III. Our result is in agreement with a previous SIRT7 interactome study, which demonstrates that SIRT7 modulates Pol III function by interacting directly with components of the Pol III transcription complex[19].

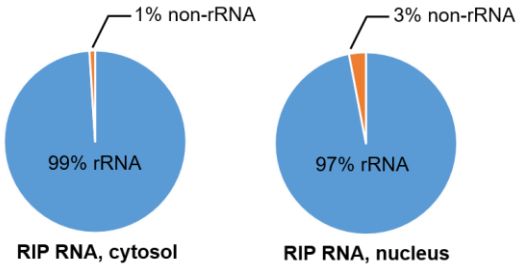

**Figure 3.5** SIRT7 mainly interacts with rRNA in vivo. Pie-charts showing that rRNAs are the predominant binding partners of SIRT7 in both cytosol and nucleus.

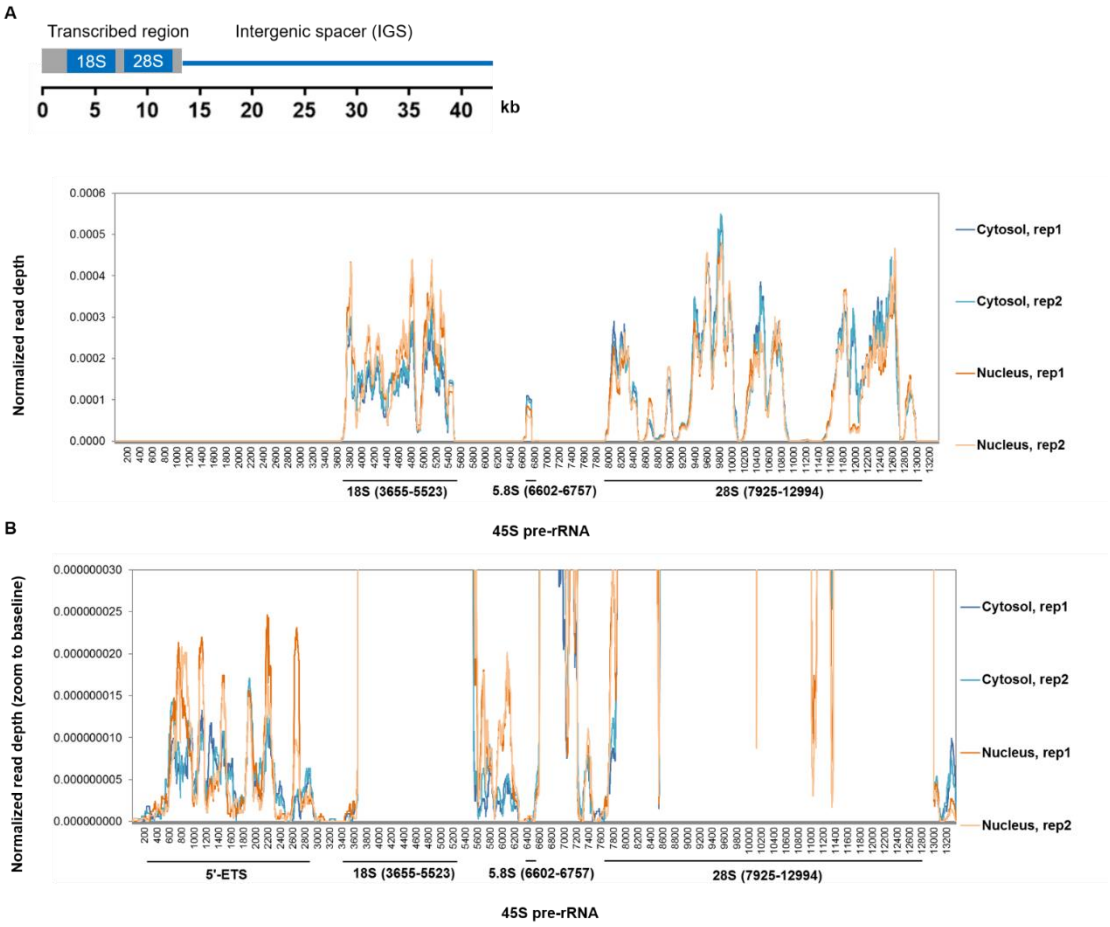


**Figure 3.6** (A) SIRT7-RIP RNA reads mapped to a custom annotation file of one human rDNA repeat encoding 45S pre-rRNA. The regions transcribing 18S, 5.8S and 28S rRNA are indicated. (B) Some SIRT7 -RIP RNA reads were mapped to 5'-ETS (external transcribed spacer) region of the 45S pre-rRNA.

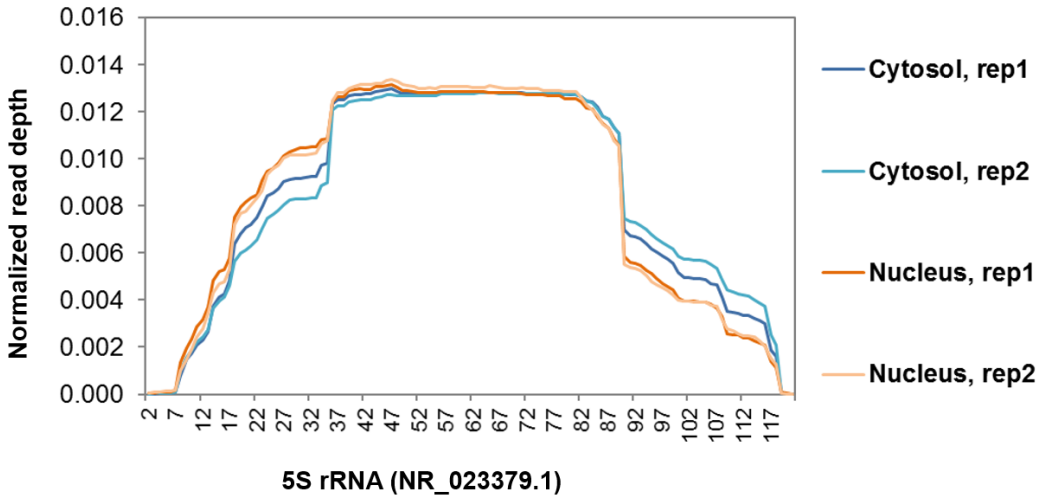


**Figure 3.7** SIRT7-RIP RNA reads mapped to a custom annotation file of one human 5S rDNA repeat.

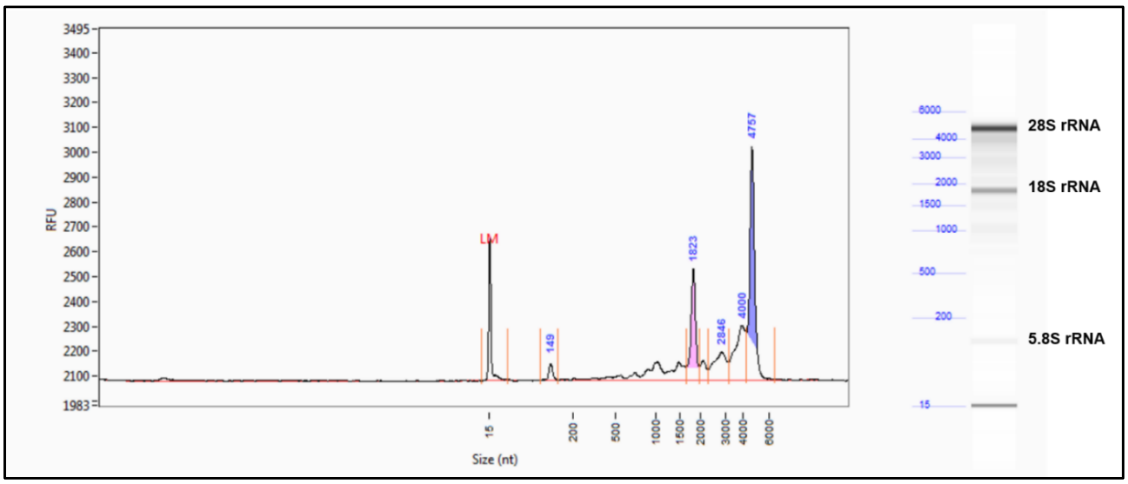


**Figure 3.8** Bioanalyzer result showing the size distribution of RNA co-immunoprecipitated with Flag-SIRT7.

**SIRT7 interacts with different messenger RNA under metabolic stress.**

SIRT7 has been reported to be involved in a variety of stress response processes such as ER stress[17], glucose deprivation[13] and hypotonic stress[20]. We hence investigated whether SIRT7-asscoiated RNA species altered upon stress exposure. We treated HEK

293T cells stably overexpressing Flag-tagged SIRT7 with tunicamycin (ER stress inducer) or glucose starvation (metabolic stress). RNA that bound with SIRT7 were immunoprecipitated and further labeled with [$^{32}$P]pCp at 3'-end. As shown in Figure 3.9A, the most abundant SIRT7-interacting RNA remained mostly unchanged under stress. However, the pattern of RNA species that SIRT7 associated with less abundantly did alter significantly as marked by red stars.

For the 3% non-rRNA binding partners of SIRT7, we further removed rRNA and sequenced non-rRNA species under both normal and no glucose conditions. The results indicated that 82% of the non-rRNA pool was mRNA while 11% was non-coding RNA (ncRNA). Under no glucose condition, 84% of the non-rRNA repertoire was mRNA while 9% was ncRNA (Figure 3.9B). We also calculated the coefficient of determination ($R^2$) values between biological replicates. As summarized in Table 3.2, the $R^2$ values between all the biological replicates are greater than 0.98, suggesting a tight correlation between duplicated samples.

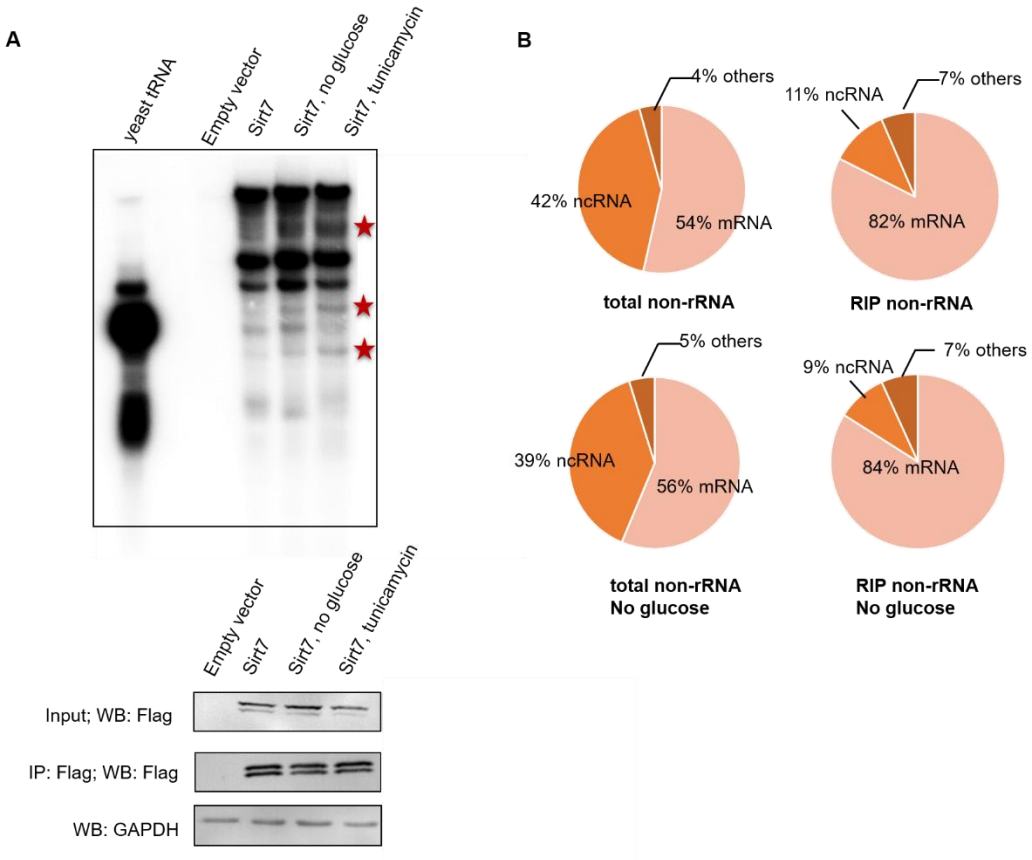


**Figure 3.9** SIRT7 interacts with messenger RNA in vivo. (A) SIRT7 pulled down different RNA species (marked by red star) in the presence of stress including ER stress (tunicamycin) and glucose starvation. (B) Pie-charts showing the composition of mRNA binding partners of SIRT7 using RIP-seq.

**Table 3.2** Summary of coefficients of determination ($R^2$) between biological replicates

| Stress | - | - | + | + | - | - | + | + |
|---|---|---|---|---|---|---|---|---|
| RIP | - | - | - | - | + | + | + | + |
| $R^2$ | N-tot-1 | N-tot-2 | NoG-tot-1 | NoG-tot-2 | N-RIP-1 | N-RIP-2 | NoG-RIP-1 | NoG-RIP-2 |
| N-tot-1 | 1 | **0.981563** | | | | | | |
| N-tot-2 | **0.981563** | 1 | | | | | | |
| NoG-tot-1 | | | 1 | **0.983398** | | | | |
| NoG-tot-2 | | | **0.983398** | 1 | | | | |
| N-RIP-1 | | | | | 1 | **0.98494** | | |
| N-RIP-2 | | | | | **0.98494** | 1 | | |
| NoG-RIP-1 | | | | | | | 1 | **0.983442** |
| NoG-RIP-2 | | | | | | | **0.983442** | 1 |

RIP: RNA immunoprecipitation; N-tot: normal total input; NoG-tot: no glucose total input; N-RIP: normal Flag-SIRT7 RIP; NoG-RIP: no glucose Flag-SIRT7 RIP.

We further compared mRNA species bound with SIRT7 under normal and stress conditions. As shown in Figure 3.10A, the number of distinct mRNA species associated with SIRT7 with glucose deprivation was only 1/3 of that under normal condition. The majority (87 out of 108) of mRNA targets of SIRT7 without glucose was in common with mRNA bound with SIRT7 normally. Gene Ontology analysis of SIRT7-bound mRNA suggested that the main biological processes are comprised of translation (ribosome protein mRNA cluster) and chromatin assembly (histone mRNA cluster), and the top KEGG pathway was ribosome (Figure 3.10B). To search for genes of which enrichment fold increased or unchanged in SIRT7-RIP in the presence of metabolic stress, we plotted FPKM (no glucose/normal)$_{RIP}$ against FPKM (no glucose/normal)$_{input}$ (FPKM: Fragments Per Kilobase of transcript per Million mapped reads). As shown in

Figure 3.10C, several genes in responsive to stress such as GRP78 (HSPA5), nucleolin (NCL) and PARP1 were inclined to interact with SIRT7 when cells were depleted of glucose.

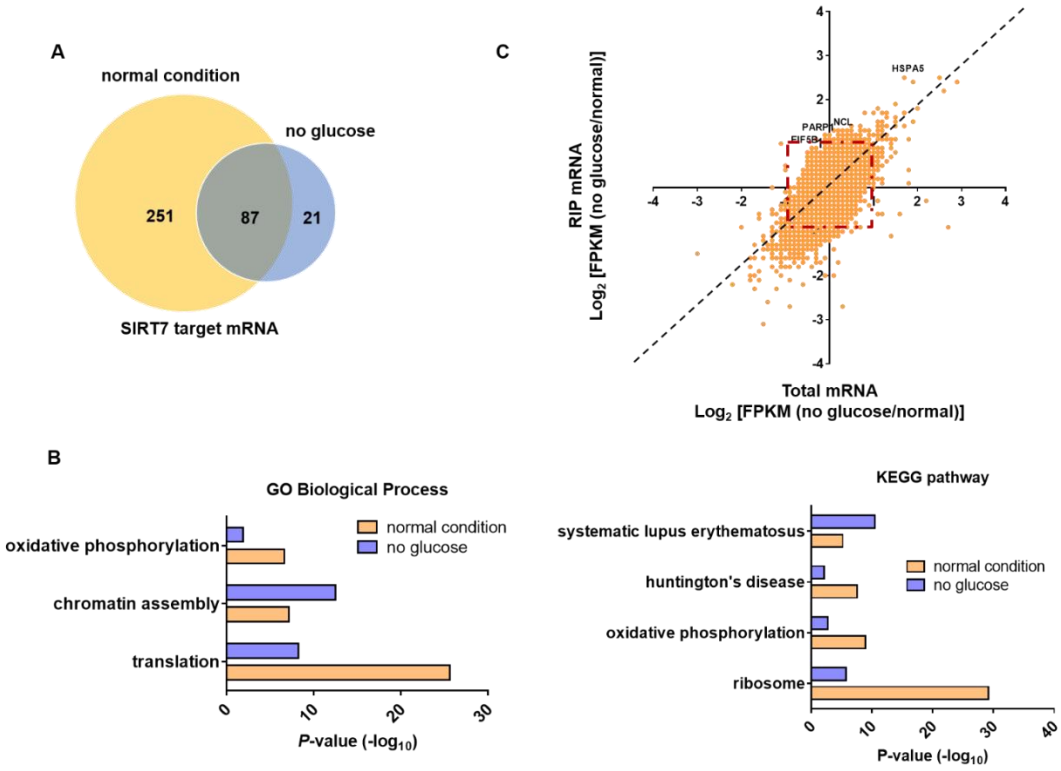


**Figure 3.10** SIRT7 associates with different mRNA under normal and stress conditions. (A) Comparison of mRNA bound with SIRT7 between normal and glucose deprivation conditions. (B) Gene Ontology (GO) categories of SIRT7 RIP-seq mRNA peaks. The most representative clusters are shown based on P value ($-\log_{10}$). (C) Scatter plots showing genes that are more enriched in SIRT7-RIP (no glucose) than in SIRT7-RIP (normal). All the genes plotted have passed the significance test using DEseq analysis.

The interaction between SIRT7 and identified mRNA was validated by reverse transcription-quantitative polymerase chain reaction (RT-qPCR) using gene-specific primers. As summarized in Figure 3.11, Class I genes represented by histone mRNA

preferred to bind with SIRT7 under normal condition, whereas Class II genes were prone to interact with SIRT7 in the presence of stress. Interestingly, a significant portion of Class II genes are known to be involved in the stress response.

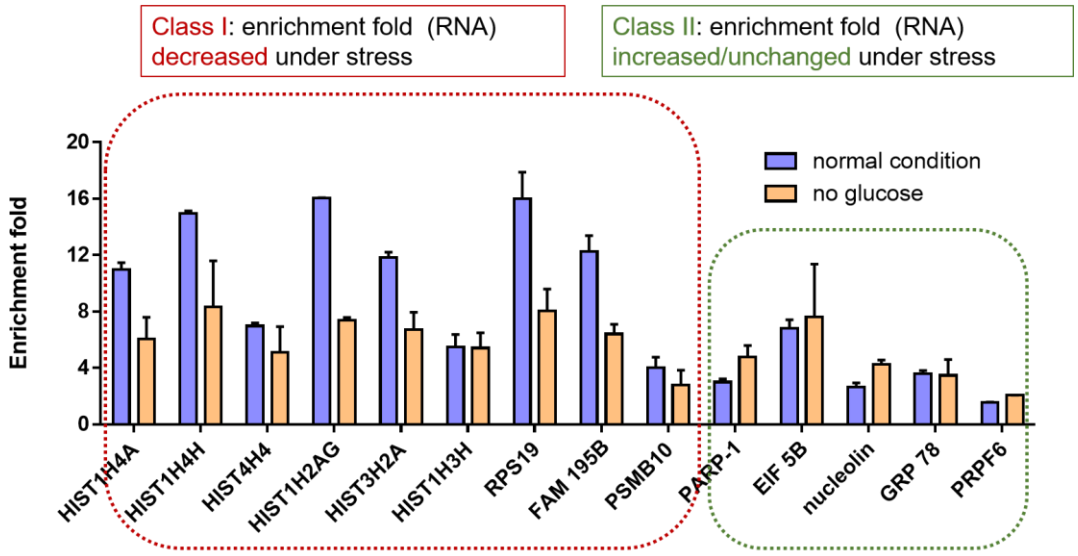


**Figure 3.11** Validation of representative SIRT7 mRNA targets under both normal and glucose deprivation conditions. Enrichment fold was calculated by comparing relative RNA level in SIRT7-RNA co-immunoprecipitation versus SIRT7-RNA input. Relative RNA level was quantified by gene-specific RT-qPCR using actin as the internal control. Error bars shown are mean±s.d., n=6 (two biological replicates×three technical replicates).

**SIRT7 can bind to and be activated by rRNA in vitro.**

To confirm that SIRT7 directly binds to rRNA, we in vitro transcribed 5S and 5.8S rRNAs, and determined the binding affinities of SIRT7 for 5S and 5.8S rRNA using a fluorescence polarization (FP) assay. In vitro transcribed 5S and 5.8S rRNA were gel-purified and subsequently labeled with fluorescein 5-thiosemicarbazide (FTSC) at the 3' end. By fixing the rRNA fluorescent probe at 5 nM, we titrated SIRT7 protein

concentration from 25 nM to 5000 nM. As plotted in Figure 3.12A & 3.12B, the dissociation constants ($K_d$) of SIRT7 were determined to be 81 nM for 5S rRNA and 2.4 μM for 5.8S rRNA.

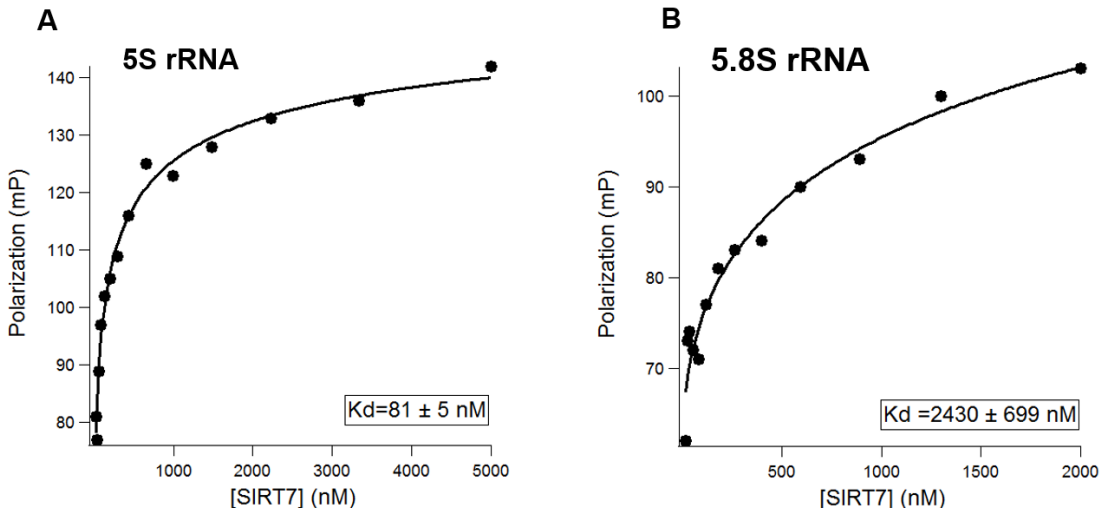


**Figure 3.12** Fluorescence Polarization (FP) assay to determine binding affinity of SIRT7 for rRNA. (A) The dissociation constant ($K_d$) of SIRT7 for 5S rRNA. (B) The $K_d$ of SIRT7 for 5.8S rRNA. Human full-length 5S and 5.8S rRNA were in vitro transcribed.

We then measured the catalytic efficiencies of SIRT7 on H3K18 Ac and H3K9 myristoyl peptides in the presence of 5S or 5.8S rRNA (Table 3.3). With H3K18 Ac as the substrate, the catalytic efficiencies of SIRT7 with 5S and 5.8S rRNA were 5-6-fold lower than those with tRNA (12.5 and 10.7 $M^{-1}s^{-1}$ versus 65 $M^{-1}s^{-1}$). In contrast, with H3K9 myristoyl as the substrate, the catalytic efficiencies of SIRT7 with 5S and 5.8S rRNA were 2-3-fold better than those with tRNA (155 and 98 $M^{-1}s^{-1}$ versus 52 $M^{-1}s^{-1}$). Thus, 5S rRNA and 5.8S rRNA are competent activators for the defatty-acylase activity

of SIRT7 in vitro. The fact that 5S rRNA served as a better activator of SIRT7 than 5.8S rRNA is consistent with the higher binding affinity of 5S rRNA for SIRT7.

**Table 3.3** Catalytic efficiencies of SIRT7 on H3 acyl peptides with rRNA

| Acyl peptides | Activator | $k_{cat}$ ($min^{-1}$) | $K_m$ (μM) | $k_{cat}/K_m$ ($M^{-1}s^{-1}$) |
|---|---|---|---|---|
| H3K18 Ac | - | NP | NP | NP |
| | 5.8S rRNA | 0.3 ± 0.02 | 532 ± 55 | 10.7 |
| | 5S rRNA | 0.3 ± 0.05 | 440 ± 122 | 12.5 |
| H3K9 Myr | - | 0.004 ± 0.001 | 65 ±26 | 1.1 |
| | 5.8S rRNA | 0.03 ± 0.009 | 5.7 ± 0.6 | 98 |
| | 5S rRNA | 0.05 ± 0.004 | 5.1 ± 1.5 | 155 |

NP: No product formed (product formation was below HPLC detection limit).
Ac: acetyl; Myr: myristoyl.

**Both amino (N-) and carboxyl (C-) termini of SIRT7 are important for its activities.**

Sirtuin proteins consist of a conserved central catalytic core, flanked by highly variable N- and C-terminal extensions[23, 24]. We have shown that both N- and C-terminal extensions of SIRT7 are important for its full activation by dsDNA in vitro[18]. Therefore, we tested whether the N- and C-terminal extensions of SIRT7 were also important for its activation by RNA. We purified a set of recombinant SIRT7 proteins from E. coli: full-length (FL, 1-400), N-terminal deletion (ΔN, 56-400), C-terminal deletion (ΔC, 1-364), and core domain (56-364). Using H3K18 Ac peptide as the substrate and tRNA as the in vitro activator, we measured the activities of the four SIRT7 constructs. SIRT7 ΔC and the core domain, which lack the C-terminal domain,

exhibited no detectable enzymatic activity within the detection limit of the HPLC-based assay (Table 3.4), suggesting that the C-terminus is essential for SIRT7's deacetylase activity. SIRT7 ΔN still showed some activity in the presence of tRNA, but the turnover number $k_{cat}$ (0.002 $s^{-1}$) was only 1/10 of FL SIRT7 ($k_{cat}$=0.02 $s^{-1}$). Thus, the N-terminus of SIRT7 is also important for the deacetylase activity.

We also measured the activities of the different SIRT7 constructs on the H3K9 myristoyl peptide (Table 3.4). Deletion of either N- or C-terminal of SIRT7 decreased the demyristoylase activity of SIRT7, and the core domain had only about 5% of the activity of full length, again suggesting that both the N- and C-termini of SIRT7 are important for SIRT7's catalytic activities.

**Table 3.4** Catalytic efficiencies of SIRT7 truncates on H3K18 Ac and H3K9 Myr peptides

| SIRT7 | Acyl Peptide | activator | $k_{cat}$ ($min^{-1}$) | $K_m$ (μM) | $k_{cat}/K_m$ ($M^{-1}s^{-1}$) | relative catalytic efficiency to FL |
|---|---|---|---|---|---|---|
| FL | H3K18 Ac | - | NP | NP | NP | NA |
| | H3K18 Ac | tRNA | 1.2 ± 0.2 | 309 ± 59 | 65 | 1 |
| | H3K9 Myr | - | 0.004 ± 0.001 | 65 ±26 | 1.1 | 1 |
| | H3K9 Myr | tRNA | 0.1 ± 0.01 | 41 ± 7 | 52 | 1 |
| ΔN | H3K18 Ac | - | NP | NP | NP | NA |
| | H3K18 Ac | tRNA | 0.1 ± 0.003 | 294 ± 15 | 6.8 | 0.10 |
| | H3K9 Myr | - | 0.002 ± 0.0002 | 90 ± 16 | 0.4 | 0.36 |
| | H3K9 Myr | tRNA | 0.02 ± 0.002 | 18 ± 4.2 | 23 | 0.44 |
| ΔC | H3K18 Ac | - | NP | NP | NP | NA |
| | H3K18 Ac | tRNA | NP | NP | NP | NA |
| | H3K9 Myr | - | 0.003 ± 0.0003 | 18 ± 4.7 | 2.9 | 2.6 |
| | H3K9 Myr | tRNA | 0.04 ± 0.006 | 25 ± 8.6 | 27 | 0.52 |
| core | H3K18 Ac | - | NP | NP | NP | NA |
| | H3K18 Ac | tRNA | NP | NP | NP | NA |
| | H3K9 Myr | - | 0.001 ± 0.0001 | 89 ± 22 | 0.1 | 0.09 |
| | H3K9 Myr | tRNA | 0.005 ± 0.0003 | 39 ± 4.5 | 2.1 | 0.04 |

NP: No product formed (product formation was below HPLC detection limit).
NA: Not available.
FL: 1-400; ΔN: 56-400; ΔC: 1-364; core: 56-364.

**Mutagenesis revealed residues of SIRT7 important for RNA-binding and activity.**

To further identify key residues at the N- and C-termini of SIRT7 that contribute crucially to SIRT7's interaction with RNA, we first utilized a bioinformatics tool, Bind N (http://bioinfo.ggc.org/bindn/), and identified nine clusters of amino acids located at the N- and C- termini that might be important for binding to nucleic acids. Each cluster contains at least one basic amino acid (Lys or Arg, highlighted in pink in Figure 3.13A) and is conserved among different species (except for M9, in which one Thr residue is replaced with Ala in some species). We then mutated all the residues in each cluster to alanine to generate mutants M1-M9 (Figure 3.13A).

We measured the dissociation constants ($K_d$) between 5S rRNA and the different SIRT7 mutants using the FP assay (Table 3.5). All the mutants had increased $K_d$ values. In particular, the $K_d$ values of M2, M3, M4, M5, M6, M8 and M9 for 5S were 20~80-fold higher than that of WT SIRT7. Thus, these clusters are important for binding to 5S RNA.

Using the H3K18 Ac and H3K9 Myr peptides, we screened the activities of these mutants with and without 5S rRNA. With H3K18Ac as the substrate, since we could not determine the basal activity of SIRT7 without RNA, we only compared the substrate conversion rates of SIRT7 WT and the mutants in the presence of 5S rRNA. With H3K9 Myr as the substrate, we determined the substrate conversion rates with and without 5S RNA. Among the nine mutants, M9 (392KRTKRKK398 mutated to 392AAAAAAA398) showed no detectable deacetylase activity and very little demyristoylase activity, while M1, M3, M4, and M7 exhibited significantly reduced deacetylase and demyristoylase activities in the presence of 5S rRNA (Figure 3.13B-C

& Table 3.5). In contrast, M2, M5, M6, and M8 largely retained the enzymatic activities in the presence of 5S rRNA.

Considering the fact that mutants with high $K_d$ values might not fully bind with RNA in the assay condition (Figure 3.13B-C), we calculated the fraction of SIRT7 bound to 5S rRNA (Table 3.5). For two of the mutants, M3 and M4, the decreased activities (~40% of WT) can be explained by the decreased "active fraction" bound with 5S rRNA (50%-60%). In contrast, for M1 and M7 (~90% bound to 5S rRNA under assay conditions), the decreased enzymatic activities (20%-30% of WT) could not be fully explained by decreased binding to 5S rRNA. One possible explanation is that the M1 and M7 mutants may impede SIRT7's conformational change (which is important for activities) induced by RNA binding. Similarly, the M9 mutant, with almost no detectable deacetylase and demyristoylase activities in the presence of 5S rRNA, was defective in binding to 5S rRNA (85 fold lower than WT) and also impeded RNA-induced conformational alteration. In contrast, the M5 and M6 mutants, after correcting for the fractions bound to 5S rRNA, had higher activities than WT. Altogether, these results reveal a delicate relationship between the binding of SIRT7 to RNA and the activation by RNA.

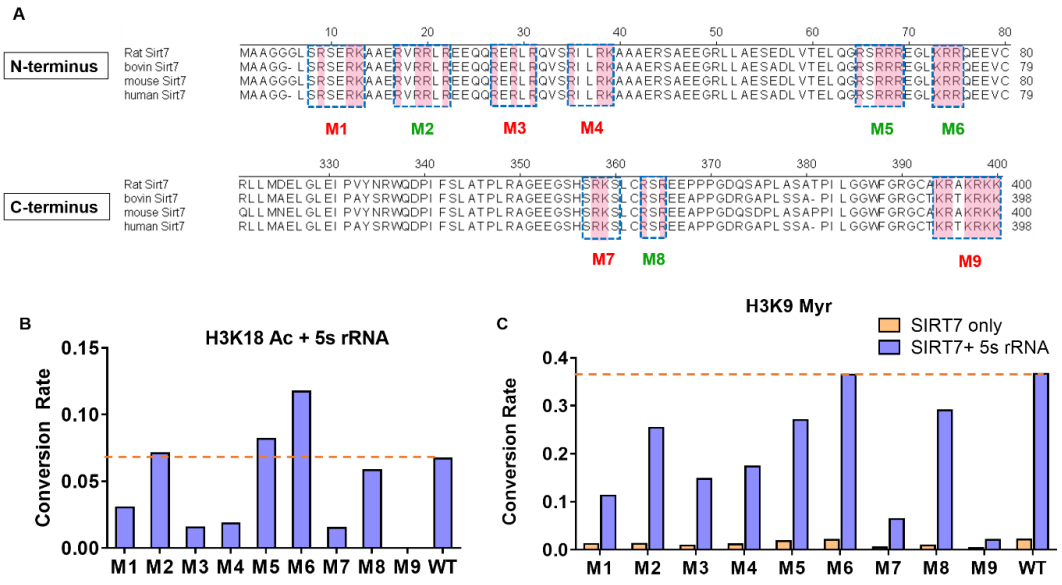


**Figure 3.13** Mutagenesis to identify key residues of SIRT7 involved in binding to RNA. (A) Schematics showing the residues mutated to alanines in the nine SIRT7 mutants. Basic amino acids are highlighted in pink. Red mutants: mutants with significantly decreased enzymatic activity (less than 50% of WT activity); Green mutants: mutants with more than 10-fold decrease in binding affinity but relatively unchanged enzymatic activity; (B) Conversation rates of SIRT7 mutants on H3K18 acetyl (Ac) peptide in the presence of 5S rRNA. SIRT7 (2 μM) was incubated with 100 μM of H3K18 acetyl peptide at 37 °C for 45 minutes with 6 μM of 5S rRNA. (C) Conversation rates of SIRT7 mutants on H3K9 myristoyl (Myr) peptide with 5S rRNA. SIRT7 (2 μM) was incubated with 20 μM of H3K9 myristoyl peptide at 37 °C for 45 minutes with 6 μM of 5S rRNA.

**Table 3.5** Summary of SIRT7 WT and mutants' activities and RNA-binding affinities in the presence of 5S rRNA

| SIRT7 | $K_d$ (nM) | Relative Deacetylation (H3K18 Ac) | Relative Demyristoylation (H3K9 Myr) | Fraction of SIRT7 bound with 5SRNA in the assay ** |
|---|---|---|---|---|
| WT | 81 ± 5 | 1.00 | 1.00 | 0.98 |
| M1* | 520 ± 130 | 0.45 | 0.31 | 0.89 |
| M2 | 1600 ± 250 | 1.06 | 0.69 | 0.74 |
| M3* | 3000 ± 570 | 0.23 | 0.40 | 0.62 |
| M4* | 4200 ± 600 | 0.28 | 0.47 | 0.54 |
| M5 | 3800 ± 230 | 1.22 | 0.74 | 0.56 |
| M6 | 4000 ± 1500 | 1.74 | 1.00 | 0.55 |
| M7* | 540 ± 40 | 0.23 | 0.17 | 0.89 |
| M8 | 1600 ± 50 | 0.87 | 0.79 | 0.74 |
| M9* | 6800 ± 1000 | 0.00 | 0.06 | 0.43 |

* Mutants with flawed catalytic activities (less than 50% of WT SIRT7) in the presence of 5S rRNA. Conversion Rate of WT SIRT7 was set at 1.00, all the mutants' conversion rates were normalized using that of WT SIRT7.

** SIRT7 (2 μM) was incubated with 6 μM of 5S rRNA. The fraction of SIRT7 bound with 5S rRNA was calculated assumpting that one molecule of SIRT7 associates with one molecule of 5S rRNA.

In summary, we have identified RNA as an even more potent activator of SIRT7 and SIRT7 can efficiently remove long chain fatty acyl groups in vitro. SIRT7 plays important roles in the maintenance of oncogenic transformation[14], non-alcoholic fatty liver formation[15-17], ribosome biogenesis, and protein synthesis[19]. Despite the reported functions, the enzymatic activity and physiological substrates of SIRT7 are largely

underexplored. SIRT7 has been shown to associate with chromatin to deacetylate histone H3[14] or transcription factors to regulate transcription[17]. However, no reports have established the connection between SIRT7's physiological functions and its interaction with RNA molecules. Here we have demonstrated that SIRT7 interacts predominantly with mature regions of RNA polymerase I-transcribed 45S pre-rRNA (28S, 18S, and 5.8S) and RNA polymerase III-transcribed 5S rRNA. We have further shown that SIRT7 can be effectively activated by in vitro transcribed human 5S and 5.8S rRNA. Recent studies have revealed a multifaceted role of SIRT7 in regulating the transcription and processing of pre-rRNA[20]. Our finding that a variety of RNA species can dramatically enhance the catalytic efficiency of SIRT7 explains how SIRT7 could function as an efficient deacylase in vivo despite previous report that no appreciable amount of product could be formed in vitro in the absence of nucleic acids in the assay. Our findings suggest that SIRT7 is only activated at the right locations where corresponding DNA or RNA molecules are bound to SIRT7.

Both the N- and C- termini are important for SIRT7's activity. Subsequent systematic mutagenesis studies revealed that the polybasic sequences (residue 392-398, KRTKRKK) at the very end of SIRT7's C-terminal region contributed crucially to its binding and activation by RNA. Interestingly, this stretch of polybasic amino acids (residue 392-398, KRTKRKK) has also been previously characterized as a nucleolar localization signal[25]. Furthermore, SIRT7 nucleoli localization has been linked to its interaction with newly synthesized pre-rRNA[26]. Thus, this polybasic sequence seems to play a central role in controlling SIRT7's interaction with RNA, its dynamic subcellular localization, and its catalytic activity.

The regulation of SIRT7 activity by DNA and RNA may be important for further investigation of its role in various stress responses. For example, under normal conditions, SIRT7 may predominantly bind to rRNA and regulate ribosome biogenesis. Under certain stress conditions where rRNA production is inhibited, more SIRT7 may be released from rRNA to bind to other nucleic acids (e. g. DNA or mRNA. Note that certain mRNAs were pulled down by SIRT7) and be activated to work on other substrate proteins, which serves to regulate transcription (when SIRT7 binds to DNA) or translation (when SIRT7 binds to mRNA) in response to stress stimuli. In this way, SIRT7 may act to sense the stress and coordinate changes in ribosomal biogenesis, transcription, and translation. This model needs to be tested in future studies.

Upon RNA activation, SIRT7 shows robust defatty-acylase activity that is more efficient than its deacetylase activity. Thus, similar to SIRT6 which has physiologically relevant deacetylase and defatty-acylase activities, SIRT7 is also likely to be multifunctional. Although we currently do not know the physiological substrates for the defatty-acylase activity of SIRT7, we believe this activity is likely physiologically relevant. Protein lysine fatty acylation was first reported over two decades ago, but to date, only a few proteins are reported to have this modification, and the only known biological function is the regulation of TNFα secretion[10]. However, given that five of the seven human sirtuins possess defatty-acylase activities in vivo or in vitro[21, 22], we believe protein lysine fatty acylation is more abundant and important than currently appreciated. Future studies to identify the substrate proteins of SIRT7's defatty-acylation activity will broaden our understanding of protein lysine fatty acylation and the biological function of SIRT7.

The finding that DNA[18] and RNA can significantly activate SIRT7 also opens up opportunities to develop small molecule modulators of SIRT7. Sirtuin inhibitors have been reported to be potential therapeutic candidates for several human diseases.[27, 28] SIRT7 inhibitors in particular could be useful for treating cancer.[14] However, no effective SIRT7 inhibitors have been reported due to the lack of efficient activity assays. With the more efficient activities of SIRT7 in the presence of DNA or RNA, it is now possible to use the activity assay to develop SIRT7 inhibitors.

## Materials and Methods

**SIRT7 purification**. The coding sequences (CDS) of full length human SIRT7 (1-400), ΔN (56-400), ΔC (1-364), and the core domain (56-364) were inserted into the pET28a vector. Nine full length SIRT7 mutants in pET28a vector were constructed using two-step PCR mutagenesis and all the sequences were confirmed by DNA sequencing. Purification procedures of both SIRT7 WT and mutants are the same as previously described[18].

**Synthesis of acyl peptides**. Acyl peptides representing residues 4-13 and 12-24 of Histone H3 ($NH_2$-KQTARKSTGGWW-COOH and $NH_2$-GGKAPRKQLATKAWW-COOH) were synthesized as previously described[18].

Acyl modifications (acetyl, butyryl, octanoyl, myristoyl) on lysine residues were introduced using Fmoc-Lys(acyl)-OH. The purified free-lysine and acetyl H3K9 and H3K18 peptides were dissolved in water, whereas butyryl, octanoyl and myristoyl H3K9 peptides were dissolved in DMSO. The concentrations of peptides were

determined using the 280 nm absorption and the extinctions coefficient of the two Trp residues attached at the C-termini of the peptides.

**Activity assays and kinetics measurement for SIRT7.** The activity of SIRT7 was detected using an HPLC based method. The reactions contained 50 mM Tris, pH 8.0, 150 mM NaCl, 1 mM DTT, 2 mM $NAD^+$, 50 μM peptides, SUPERase-In$^{TM}$ Rnase inhibitor (Thermo), and 2 μM SIRT7. Different nucleic acids were added as the in vitro activators: Salmon sperm DNA (10 mg/mL) Sigma (cat # D1626), ribosomal RNA from bioPLUS (cat # 11020001), and yeast tRNA from Thermo (cat# AM-7119). Mass ratio of RNA/DNA to SIRT7 was maintained at 3:1 in the assays shown in Figure 1A, 1B and 1E. For all the other experiments, molar ratio of RNA (tRNA, 5S rRNA and 5.8S rRNA) to SIRT7 was fixed at 3:1 unless specified otherwise. Reactions were incubated at 37 °C for 1 h. The reactions were quenched with 1 volume of 10% (v/v) TFA and spun down for 10 min at 18,000 g to remove proteins. The supernatants were then analyzed by HPLC using a reverse phase analytical column (Kinetex XB-C18 100A, 75 mm × 4.60 mm, 2.6 μm, Phenomenex). The product and substrate concentrations were determined using their absorption peak areas at 280 nm from the two Trp residues added at C-termini of the peptide substrates.

For kinetics experiment using acetyl peptides as substrates, the reactions contained 2 mM $NAD^+$, 50 mM Tris, pH 8.0, 150 mM NaCl, 1 mM DTT, 2 μM SIRT7 (full-length) or 8 μM SIRT7 (ΔN, 56-400). Peptide concentrations used for H3K18 Ac and H3K9 Ac were 10, 30, 50, 100, 150, 250 and 500 μM and the reaction time was 45 minutes. The quenched reactions were analyzed by HPLC. The product and substrate concentrations were quantified as described above and converted to initial

rates, which were then plotted against the peptide concentrations and fitted to the Michaelis-Menten equation using the Graphpad Prism 6 program.

For kinetics measurement with other acyl peptides (H3K9 butyryl, octanoyl and myristoyl), the reactions contained 2mM $NAD^+$, 50 mM Tris, pH 8.0, 150 mM NaCl, 1mM DTT, 2 μM SIRT7 (FL) or 5 μM SIRT7 deletion mutants (ΔN 56-400, ΔC 1-364, core 56-364). The peptide concentrations used were 2, 5, 10, 15, 20, 30, 50, 80 μM and the reaction time was 45 minutes. Reactions were quenched with 10% (v/v) TFA in methanol and then analyzed by HPLC. Data analysis was performed as described above.

**Cell culture and viral transfection.** Human 293T and Hela cell lines were acquired from the American Type Culture Collection (ATCC). Cells were cultured in DMEM (Thermo Fisher) supplemented with penicillin-streptomycin (Thermo Fisher) and 10% fetal bovine serum (FBS). Lentivirus transfection was performed as previously described[10]. Briefly, coding sequences (CDS) of SIRT7 (FL, ΔN, ΔC and core) were cloned into pCDH-CMV-MCS-EF1-Puro vector with an N-terminal Flag tag. For lentiviral packaging, 293T cells were co-transfected with pCMV-dR8.2, pMD2.G (obtained from Addgene) and corresponding SIRT7 pCDH plasmid or empty pCDH vector, and the medium supernatant containing the lentiviruses was collected and filtered after 48h. For virus infection, cells were incubated with virus-containing supernatant in the presence of 8 μg/mL polybrene. After 72h, infected cells were selected using 1.5 μg /mL puromycin for one week.

**Fluorescence microscopy.** Coding sequences (CDS) of human SIRT7 (FL, ΔN,

ΔC and core) were inserted into the 5'-end of EGFP cDNA (pEGFP-N1 vector). Hela cells were transfected with EGFP-tagged SIRT7 using Fugene 6 transfection reagent following manufacturer's instruction for 24h. For immunofluorescence, cells were permeabilized with 0.3% triton X-100 in PBS for 10 minutes at room-temperature (RT). After washing three times with PBS, cells were fixed with 4% paraformaldehyde in PBS for 15 minutes at RT. Cells were then blocked in PBS containing 5% BSA and 0.3% triton X-100 for 1h. Primary antibody (UBF, Santa Cruz Biotechnology cat # sc13125) was diluted at 1:50 in PBS containing 1% BSA and 0.3% triton X-100 and incubated with the cells for 1h. After rinsing three times with PBS, fluorophore-conjugated secondary antibody (Goat anti-mouse, Alexa Fluor® 594, Thermo) was diluted at 1:500 and applied for 1h at RT in the dark. Samples were washed three times with PBS and stained with prolong gold anti-fade reagent (Cell signaling technology) with DAPI. Confocal images were taken using a 63x, 1.4 NA objective, on an inverted microscope (Leica), and acquired with ZEN software. Image resizing, cropping, and brightness were uniformly adjusted in Photoshop (Adobe).

**RIP to pull down RNA that binds to SIRT7**. RNA immunoprecipitation (RIP) experiment was conducted following a previous report[29]. Two 15-cm plates of HEK 293T cells stably overexpressing Flag-tagged SIRT7 or Flag-tagged SIRT6 were grown to 80% confluency. For CLIP (crosslinking and immunoprecipitation of in vivo RNA) experiments, 293T cells stably overexpressing Flag-SIRT7 (FL, ΔN, ΔC and core) were UV-irradiated (254 nm, 0.3 J/cm$^2$). Cells were washed twice with ice-cold PBS and collected. Cell pellets were lysed in 1mL WCE buffer (1% NP-40, 30 mM Tris, pH 7.5, 100 mM NaCl, 66 mM KCl, 1 mM $MgCl_2$, 1 mM DTT, 25 μL of 20U/μl

SUPERase-In™ Rnase inhibitor, complete protease inhibitor cocktail) on ice for 20 minutes. Then 2 μL of TURBO Dnase (Thermo) was added to each sample. The mixture was incubated at 37°C for 3 minutes and left on ice for at least 1 minute. Then the mixture was spun at 16,000g in a tabletop centrifuge for 15 min to pellet insoluble cell debris.

For subcellular fractionation, the protocol was adapted as previously described[30]. Briefly, the cell pellet was resuspended in 500 μL Buffer A (20 mM Tris pH 8.0, 10 mM KCl, 1.5 mM $MgCl_2$, 1mM DTT, 5% glycerol, 0.1% NP-40, 25 μL of 20U/μL SUPERase-In™ Rnase inhibitor, complete protease inhibitor cocktail) and incubated on ice for 5 mins. After centrifugation at 1300g for 10 mins at 4 °C, the supernatant was collected as crude cytosol fraction, which was further clarified at 17,000g for 20 mins. The pellet was washed twice with 1mL Buffer A (no NP-40) and then re-suspended in 500 μL Buffer C (20 mM Tris pH 8.0, 5% glycerol, 300 mM NaCl, 1.5 mM $MgCl_2$, 1 mM DTT, 1% NP-40, 25 μL of 20U/μL SUPERase-In™ Rnase inhibitor, complete protease inhibitor cocktail), held on ice for another 20 mins, then incubated with 1 μL Benzonase nuclease (Sigma) at 37 °C for 3 mins. Cell debris was removed by spinning at 17,000 g for 20 mins and the supernatant was collected as the crude nuclear fraction.

The supernatant (total cell lysate or fractionated cytosolic and nuclear lysates) was then incubated with anti-Flag M2 affinity gel (50 μL for two 15-cm plates of HEK 293T cells, pre-washed twice with PBS and four times with WCE buffer before incubation) for 2h at 4℃ with gentle shaking. Beads were washed with 1 mL of WCE buffer six times, changing to new tubes for the final wash. For the CLIP experiment,

beads were washed four times with 1mL high-salt buffer (50 mM Tris-HCl, pH 7.4; 1 M NaCl; 1 mM EDTA; 1% NP-40; 0.1% SDS; 0.5% sodium deoxycholate). The second wash was rotated at 4 ºC for at least 1 min. Then the beads were washed twice with 1 mL of WCE buffer before proteinase K digestion.

Proteinase K solution (4 µg/µL) in PK buffer (100 mM Tris pH 7.5, 10 mM EDTA, 50 mM NaCl) was pre-incubated at 37 ℃ for 20 minutes to inactivate any RNase. After washing, anti-Flag beads were re-suspended in 200 µLproteinase K solution and incubated at 37 ℃ for 20 minutes with gentle shaking. Another 200 µL of PK buffer (no proteinase K) with 2% SDS was added to the beads suspension and further incubated at 37 ℃ for another 20 minutes to completely digest proteins.

RNA was extracted using phenol-chloroform extraction followed by ethanol precipitation. Typically, 400 µL of sample was mixed with 400 µL of acid-phenol:chloroform:isoamyl alcohol (125:24:1, v/v/v, pH 4.5, Thermo) and vortex vigorously. Samples were spun at 16,000 g for 15 minutes at 4 ℃. Upper aqueous layer was transferred to a new tube, mixed with 400 µL of chloroform, and vortexed vigorously. After spinning at 16,000g for 15 minutes, the aqueous layer was transferred and mixed with 40 µL of 3M NaOAC (pH 5.30), 1 mL of pure ethanol, and 2 µL of Rnase-free glycogen (20 mg/mL, Thermo cat # 10814010). RNA was precipitated at -20 ℃ for 2h. The mixture was spun at 16,000g for 30 min at 4℃. Supernatant was removed and RNA pellet was washed with 70% ethanol twice. After air drying the RNA pellet for 5 minutes at RT, RNA pellet was dissolved in 20-40 µL of DEPC (Diethylpyrocarbonate)-treated $H_2O$ and stored at -80 ℃.

**Total RNA isolation**. Total input RNA was purified using TRI reagent (Sigma) according to manufacturer's instruction. For each isolation, 50 µL of total cell lysate was incubated with 500 µL of TRI reagent and vortexed briefly to mix. Then 100 µL (1/5 volume of TRI reagent) of chloroform was added to the sample, vortexed, and incubated at room temperature for 5 minutes. Samples were spun at 16,000 g for 15 minutes at 4 ℃. The upper aqueous layer was transferred to a new tube and 250 µL of (1/2 volume of TRI reagent) isopropanol, 25 µL of NaOAC (pH 5.30) and 1 µL of RNase-free glycogen were added to the sample and incubated at -20 ℃ for 2 hours. The samples were spun at 16,000 g for 30 minutes at 4℃. The RNA pellet was washed twice with 70% ethanol and re-solubilized in DEPC-$H_2O$.

**RNA 3'-end labeling using [$^{32}$P] pCp.** RNA (2-5 µg) were 3'-end labeled with T4 RNA ligase 1 (NEB) and homemade 5'-$\alpha^{32}$P 5'-3' cytidine bis-phosphate overnight at 4℃ in 1x RNA ligase buffer (50 mM Tris, pH 7.5, 10 mM $MgCl_2$, 1 mM DTT, 1 mM ATP, 10% v/v DMSO). Unincorporated radioactive materials were removed using NucAway™ Spin Columns (Ambion), and one half of the labeling reaction was resolved on a 12% denaturing polyacrylamide gel containing 7M urea. The gel was sealed with plastic wrap and imaged on a PhosphoImager immediately.

**RIP-seq and data analysis.** The RIP-seq experiment was conducted using two biological replicates for each sample. For the total repertoire of SIRT7 RIP-RNA, we sequenced both cytosolic and nuclear RNAs that were associated with Flag-SIRT7 respectively. In order to deep sequence the non-rRNA repertoire, rRNA was subtracted from both pre-RIP input RNA and RNA co-immunoprecipitated with Flag-SIRT7

using the RiboZero Magnetic Gold Human/Mouse/Rat Kit (Illumina). All RNA samples were treated with Dnase I in solution to completely remove genomic DNA. RNA samples were quantified with a Qubit 2.0 (RNA HS kit; Thermo) and were then analyzed on the BioAnalyzer High Sensitivity DNA chip (Agilent) to determine RNA integrity before library construction.

Stranded RNA-seq libraries were generated with the NEB Next Ultra RNA library Prep kit (NEB) using 25-100ng RNA. All samples were sequenced on an Illumina NextSeq500 to generate single-end 75-bp reads. Following removal of rRNA-matching reads with bowtie2, the deep sequencing data was mapped to the Human genome (UCSC hg19) by Tophat version 2.0. Cufflinks v2.2.1 was used to generate FPKM (Fragments Per Kilobase of Exon Per Million fragments mapped) values and statistical analysis of differential gene expression for annotated genes. Enrichment fold was calculated as $\log_2$ ($FPKM_{IP}/FPKM_{input}$) against SIRT7 target genes with sufficient expression level (FPKM>5). For analysis of rRNA sequences in non-rRNA-subtracted libraries, depth of coverage counts was generated with samtools pileup and normalized to total reads per pre-rRNA in order to compare distribution of read depth over assembled rRNA transcript to indicate relative binding preference. Gene ontology (GO) annotations were performed using DAVID v6.7.

**Reverse transcription and RT-qPCR.** RNA templates were in solution treated with Dnase I to remove any contaminant genomic DNA, and then were reversely transcribed to cDNA using a primer mixture consisting of oligo dT and random hexamers by Superscript III First-strand synthesis kit (Thermo). Real-time quantitative PCR (RT-qPCR) was performed to access the relative abundance of mRNA using iTaq

Universal SYBR Green Supermix (Biorad) according to manufacturer's instruction with 200-500 ng total cDNA as the template. β-Actin was used as an internal control for the following reasons: (1) β-actin mRNA was not bound by SIRT7 from RIP sequencing data; (2) β-actin expression is not affected by SIRT7. The primers used for RT-PCR are listed as below:

| Gene | NCBI Gene ID | Forward | Reverse |
|---|---|---|---|
| beta actin | 60 | CATGTACGTTGCTATCCAGGC | CTCCTTAATGTCACGCACGAT |
| HIST1H4A | 8359 | AAGGGTTTGGGTAAGGGGG | TAGATCAGACCAGAGATCCGC |
| HIST1H4H | 8365 | GAGGAGCTAAGCGTCATCGC | ACACCTTCAGAACACCACGAG |
| HIST4H4 | 121504 | TGCTGCGGGACAATATCCAAG | AACCGCCGAAACCATAAAGGG |
| HIST1H2AG | 8969 | GCTAAGGCCAAGACTCGCTC | GACCCGCTCGGCATAGTTG |
| HIST3H2A | 92815 | GGTCGTGGTAAGCAGGGTG | CGCTCCGAATAGTTGCCCTT |
| HIST1H3A | 8350 | ACTGCTCGGAAGTCTACTGGT | GCGCTGGAAAGGTAGTTTACGA |
| RPS19 | 6223 | AAGCTGAAAGTCCCCGAATGG | AGTTCTCATCGTAGGGAGCAAG |
| FAM 195B | 348262 | AACGTCCGCTTCATTTACGAA | GGTTAGGGACCTTCTCCACATAC |
| PSMB10 | 5699 | TCCTTCGAGAACTGCCAAAGA | ATCGTTAGTGGCTCGCGTATC |
| PARP-1 | 142 | CGGAGTCTTCGGATAAGCTCT | TTTCCATCAAACATGGGCGAC |
| EIF5B | 9669 | AGGGCTTATGACAAAGCAAAACG | CCCAAGTACGCAGATAATAGGGG |
| NCL | 4691 | GGTGGTCGTTTCCCCAACAAA | GCCAGGTGTGGTAACTGCT |
| GRP78 | 3309 | CATCACGCCGTCCTATGTCG | CGTCAAAGACCGTGTTCTCG |
| PRPF6 | 24148 | CACCACGCGGTCAGACATT | TCCCCAACGGTTCTCTTGC |

**T7 in vitro transcription.** Full-length mature human 5S and 5.8S rRNAs were made by in vitro transcription using HiScribe T7 high yield RNA synthesis kit (NEB) according to manufacturer's instruction. Briefly, 50 ng of linear dsDNA was used as the template (IDT), and mixed with 2 μL 10X T7 reaction buffer, rNTP mix (final concentration of each rNTP was 10 mM), 2 μL T7 RNA polymerase mix and DEPC water up to 20 μL. Transcription reaction was proceeded at 37 °C overnight in the presence of 0.5 μL SUPERase-In$^{TM}$ Rnase inhibitor (20 U/μL, Thermo). Then 2 μL Dnase I was added to the reaction mixture to remove template DNA. RNA transcripts were purified using canonical phenol-chloroform extraction followed by ethanol

precipitation. Final RNA pellets were re-solubilized using DEPC-$H_2O$ and stored at -80°C.

**Fluorescence polarization (FP).** FP assay was performed as previously described[31]. In vitro transcribed 5S and 5.8S rRNAs were PAGE purified and eluted into 10 mM Tris pH 7.5 buffer. Purified RNAs were then 3'-end labeled with fluorescein 5-thiosemicarbazide (Thermo Fisher) as previously described[31]. The purified 5S rRNA and 5.8S rRNA were diluted to 6.33 nM (1.3X) using EMSA buffer (20 mM Tris pH 8.0, 100 mM NaCl, 5 mM $MgCl_2$, 1mM DTT, 2.5% glycerol, 0.01% triton X-100) with 0.5 µL SUPERase In™ Rnase inhibitor. The mixtures were heated to 65°C for 5 minutes and then placed at room temperature to anneal for ~20 minutes. Binding reactions were prepared with labeled RNA (final 5nM) and varying concentrations of recombinant SIRT7 or its mutants (SIRT7 WT: from 0 to 5000 nM, SIRT7 mutants: from 0 to 15,000 nM) in EMSA buffer to a final volume of 50 µL in black flat-bottom 96-well half-area microplate (Corning). All solutions were prepared using DEPC-$H_2O$ to prevent RNA degradation. Reactions were equilibrated for 2 hours at room temperature in the dark before taking FP measurements on a Synergy H1 Microplate Reader (BioTek) with the appropriate filter for fluorescein (Excitation: 485/20, Emission: 528/20). Data was fit to a Hill equation using Igorpro software (Wavemetrics), which includes the Levenberg-Marquadt algorithm and statistical analysis tools.

**References**


1. Imai, S., Armstrong, C. M., Kaeberlein, M., and Guarente, L. (2000) Transcriptional silencing and longevity protein Sir2 is an NAD-dependent histone deacetylase, Nature 403, 795-800.
2. Imai, S., and Guarente, L. (2010) Ten years of NAD-dependent SIR2 family deacetylases: implications for metabolic diseases, Trends Pharmacol Sci 31, 212-220.
3. Tanner, K. G., Landry, J., Sternglanz, R., and Denu, J. M. (2000) Silent information regulator 2 family of NAD- dependent histone/protein deacetylases generates a unique product, 1-O-acetyl-ADP-ribose, Proc Natl Acad Sci U S A 97, 14178-14182.
4. Frye, R. A. (2000) Phylogenetic classification of prokaryotic and eukaryotic Sir2-like proteins, Biochem Biophys Res Commun 273, 793-798.
5. Haigis, M. C., and Sinclair, D. A. (2010) Mammalian sirtuins: biological insights and disease relevance, Annu Rev Pathol 5, 253-295.
6. Houtkooper, R. H., Pirinen, E., and Auwerx, J. (2012) Sirtuins as regulators of metabolism and healthspan, Nat Rev Mol Cell Biol 13, 225-238.
7. Michishita, E., Park, J. Y., Burneskis, J. M., Barrett, J. C., and Horikawa, I. (2005) Evolutionarily conserved and nonconserved cellular localizations and functions of human SIRT proteins, Mol Biol Cell 16, 4623-4635.
8. Tan, M., Peng, C., Anderson, K. A., Chhoy, P., Xie, Z., Dai, L., Park, J., Chen, Y., Huang, H., Zhang, Y., Ro, J., Wagner, G. R., Green, M. F., Madsen, A. S., Schmiesing, J., Peterson, B. S., Xu, G., Ilkayeva, O. R., Muehlbauer, M. J., Braulke, T., Muhlhausen, C., Backos, D. S., Olsen, C. A., McGuire, P. J., Pletcher, S. D., Lombard, D. B., Hirschey, M. D., and Zhao, Y. (2014) Lysine glutarylation is a protein posttranslational modification regulated by SIRT5, Cell Metab 19, 605-617.
9. Du, J., Zhou, Y., Su, X., Yu, J. J., Khan, S., Jiang, H., Kim, J., Woo, J., Kim, J. H., Choi, B. H., He, B., Chen, W., Zhang, S., Cerione, R. A., Auwerx, J., Hao,

Q., and Lin, H. (2011) Sirt5 is a NAD-dependent protein lysine demalonylase and desuccinylase, Science 334, 806-809.

10. Jiang, H., Khan, S., Wang, Y., Charron, G., He, B., Sebastian, C., Du, J., Kim, R., Ge, E., Mostoslavsky, R., Hang, H. C., Hao, Q., and Lin, H. (2013) SIRT6 regulates TNF-alpha secretion through hydrolysis of long-chain fatty acyl lysine, Nature 496, 110-113.
11. Ford, E., Voit, R., Liszt, G., Magin, C., Grummt, I., and Guarente, L. (2006) Mammalian Sir2 homolog SIRT7 is an activator of RNA polymerase I transcription, Genes Dev 20, 1075-1080.
12. Tsai, Y. C., Greco, T. M., Boonmee, A., Miteva, Y., and Cristea, I. M. (2012) Functional proteomics establishes the interaction of SIRT7 with chromatin remodeling complexes and expands its role in regulation of RNA polymerase I transcription, Mol Cell Proteomics 11, M111 015156.
13. Chen, S., Seiler, J., Santiago-Reichelt, M., Felbel, K., Grummt, I., and Voit, R. (2013) Repression of RNA polymerase I upon stress is caused by inhibition of RNA-dependent deacetylation of PAF53 by SIRT7, Mol Cell 52, 303-313.
14. Barber, M. F., Michishita-Kioi, E., Xi, Y., Tasselli, L., Kioi, M., Moqtaderi, Z., Tennen, R. I., Paredes, S., Young, N. L., Chen, K., Struhl, K., Garcia, B. A., Gozani, O., Li, W., and Chua, K. F. (2012) SIRT7 links H3K18 deacetylation to maintenance of oncogenic transformation, Nature 487, 114-118.
15. Ryu, D., Jo, Y. S., Lo Sasso, G., Stein, S., Zhang, H., Perino, A., Lee, J. U., Zeviani, M., Romand, R., Hottiger, M. O., Schoonjans, K., and Auwerx, J. (2014) A SIRT7-dependent acetylation switch of GABPbeta1 controls mitochondrial function, Cell Metab 20, 856-869.
16. Yoshizawa, T., Karim, M. F., Sato, Y., Senokuchi, T., Miyata, K., Fukuda, T., Go, C., Tasaki, M., Uchimura, K., Kadomatsu, T., Tian, Z., Smolka, C., Sawa, T., Takeya, M., Tomizawa, K., Ando, Y., Araki, E., Akaike, T., Braun, T., Oike, Y., Bober, E., and Yamagata, K. (2014) SIRT7 controls hepatic lipid metabolism by regulating the ubiquitin-proteasome pathway, Cell Metab 19, 712-721.

17. Shin, J., He, M., Liu, Y., Paredes, S., Villanova, L., Brown, K., Qiu, X., Nabavi, N., Mohrin, M., Wojnoonski, K., Li, P., Cheng, H. L., Murphy, A. J., Valenzuela, D. M., Luo, H., Kapahi, P., Krauss, R., Mostoslavsky, R., Yancopoulos, G. D., Alt, F. W., Chua, K. F., and Chen, D. (2013) SIRT7 represses Myc activity to suppress ER stress and prevent fatty liver disease, Cell Rep 5, 654-665.
18. Tong, Z., Wang, Y., Zhang, X., Kim, D. D., Sadhukhan, S., Hao, Q., and Lin, H. (2016) SIRT7 Is Activated by DNA and Deacetylates Histone H3 in the Chromatin Context, ACS Chem Biol 11, 742-747.
19. Tsai, Y. C., Greco, T. M., and Cristea, I. M. (2014) Sirtuin 7 plays a role in ribosome biogenesis and protein synthesis, Mol Cell Proteomics 13, 73-83.
20. Chen, S., Blank, M. F., Iyer, A., Huang, B., Wang, L., Grummt, I., and Voit, R. (2016) SIRT7-dependent deacetylation of the U3-55k protein controls pre-rRNA processing, Nat Commun 7, 10734.
21. Feldman, J. L., Baeza, J., and Denu, J. M. (2013) Activation of the protein deacetylase SIRT6 by long-chain fatty acids and widespread deacylation by mammalian sirtuins, J Biol Chem 288, 31350-31356.
22. Teng, Y. B., Jing, H., Aramsangtienchai, P., He, B., Khan, S., Hu, J., Lin, H., and Hao, Q. (2015) Efficient demyristoylase activity of SIRT2 revealed by kinetic and structural studies, Sci Rep 5, 8529.
23. Borra, M. T., Langer, M. R., Slama, J. T., and Denu, J. M. (2004) Substrate specificity and kinetic mechanism of the Sir2 family of NAD+-dependent histone/protein deacetylases, Biochemistry 43, 9877-9887.
24. Sauve, A. A., Wolberger, C., Schramm, V. L., and Boeke, J. D. (2006) The biochemistry of sirtuins, Annu Rev Biochem 75, 435-465.
25. Kiran, S., Chatterjee, N., Singh, S., Kaul, S. C., Wadhwa, R., and Ramakrishna, G. (2013) Intracellular distribution of human SIRT7 and mapping of the nuclear/nucleolar localization signal, FEBS J 280, 3451-3466.
26. Chen, S., Seiler, J., Santiago-Reichelt, M., Felbel, K., Grummt, I., and Voit, R. (2013) Repression of RNA polymerase I upon stress is caused by inhibition of RNA-dependent deacetylation of PAF53 by SIRT7, Mol Cell 52, 303-313.

27. Villalba, J. M., and Alcaín, F. J. (2012) Sirtuin activators and inhibitors, BioFactors 38, 349-359.
28. Hu, J., Jing, H., and Lin, H. (2014) Sirtuin inhibitors as anticancer agents, Future Med Chem 6, 945-966.
29. Wang, X., Lu, Z., Gomez, A., Hon, G. C., Yue, Y., Han, D., Fu, Y., Parisien, M., Dai, Q., Jia, G., Ren, B., Pan, T., and He, C. (2014) N6-methyladenosine-dependent regulation of messenger RNA stability, Nature 505, 117-120.
30. Mendez, J., and Stillman, B. (2000) Chromatin association of human origin recognition complex, cdc6, and minichromosome maintenance proteins during the cell cycle: assembly of prereplication complexes in late mitosis, Mol Cell Biol 20, 8602-8612.
31. Pagano, J. M., Kwak, H., Waters, C. T., Sprouse, R. O., White, B. S., Ozer, A., Szeto, K., Shalloway, D., Craighead, H. G., and Lis, J. T. (2014) Defining NELF-E RNA binding in HIV-1 and promoter-proximal pause regions, PLoS Genet 10, e1004090.

# CHAPTER 4

## Explore Physiological Substrates of Defatty-acylase Activity of SIRT7


### Abstract

SIRT7 is a member of the sirtuin family of nicotinamide adenine dinucleotide (NAD)-dependent protein lysine deacylases that regulate multiple important biological processes. Previous studies have demonstrated that upon nucleic acids (RNA/DNA) activation, SIRT7 prefers to hydrolyze long chain fatty acyl groups from lysine residues in vitro using peptide as the substrate. Here I report that the novel defatty-acylase activity of SIRT7 is likely to be physiologically relevant since upon Sirt7 knockdown, global lysine fatty-acylation level slightly increased especially with the treatment of Brefeldin A (BFA, an ER stress inducer). I also showed that SIRT7 could disperse to nucleoplasm, and even cytoplasm in the presence of metabolic stress. Stable isotope labeling by amino acids in cell culture (SILAC) profile of lysine fatty-acylation proteome identified a list of putative physiological substrates of which lysine fatty acylation level was regulated by SIRT7. Future validation of these proteins and optimization of proteomics methodology would greatly facilitate the discovery of physiological substrates of SIRT7's defatty-acylase activity, and thus broaden our understanding of protein lysine fatty acylation and the biological function of SIRT7.

## Introduction

Sirtuins are critical enzymes that govern genome stability, metabolism and aging[1]. Among the seven human sirtuins, SIRT1-3 have robust deacetylase activities, while SIRT4-7 have only weak deacetylase activities in vitro[2-6]. It was recently reported that, SIRT5 and SIRT6, two of the four sirtuins with weak deacetylase activity, preferentially hydrolyze succinyl/malonyl and long-chain fatty acyl lysine, respectively[7, 8]. The novel enzymatic activities of SIRT5 and SIRT6 suggested that SIRT7 may also work on alternative substrates. Our previous studies have demonstrated that human SIRT7, which has weak deacetylase activity in vitro, catalyzes the hydrolysis of lysine fatty acylation much more efficiently in an RNA/DNA-dependent manner. The next important question is whether the defatty-acylase activity of SIRT7is physiologically relevant.

## Results and Discussion

### Sirt7 knockdown slightly increased global lysine fatty-acylation level.

To investigate whether the defatty-acylase activity of SIRT7 is physiologically relevant, I examined whether global lysine fatty-acylation is regulated by SIRT7. I transiently knocked down Sirt7 expression in HEK 293T cells using short hairpin RNA (shRNA) (Figure 4.1B). Control knockdown was carried out using a scrambled shRNA. Both control and Sirt7 knockdown (Sirt7 KD) cells were cultured in the presence of Alk14, an alkyne-tagged fatty acid analogue that can covalently modify fatty-acylated proteins[9]. Cells were collected and separated into cytosolic and nuclear fractions (Figure 4.1B). Then equal amounts of each group of cell lysates were conjugated to BODIPY-

azide (BODIPY-$N_3$) using click chemistry to detect proteins modified by Alk14. Hydroxylamine was used to remove cysteine fatty acylation before resolving samples by gel electrophoresis (Figure 4.1A).

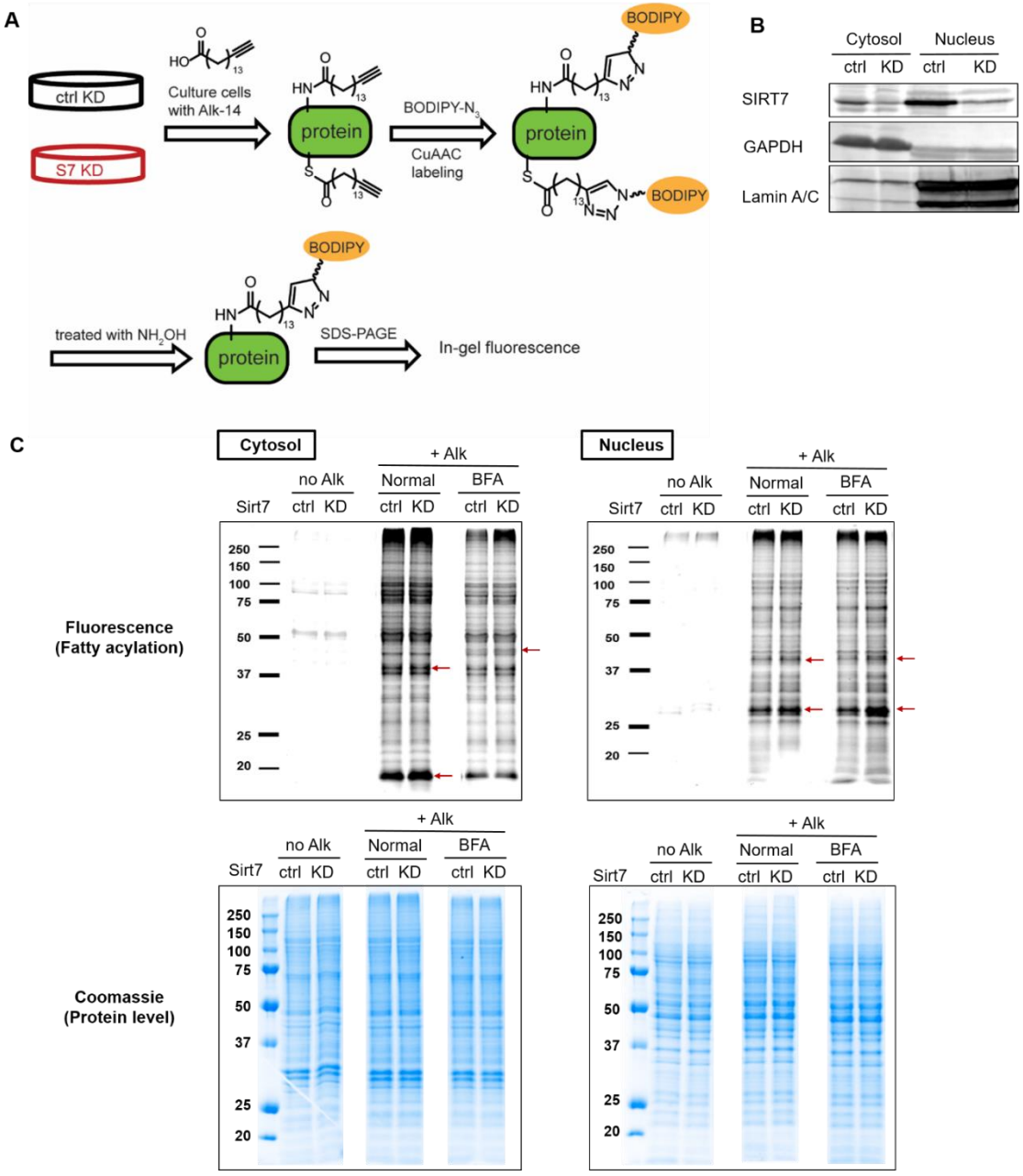


**Figure 4.1** Profiling of lysine fatty-acylation level in Sirt7 control (ctrl) and knockdown (KD) HEK 293T cells. (A) Scheme showing the method of in-gel fluorescence to determine lysine fatty acylation level in Sirt7 ctrl and KD cells. (B) Western blot showing Sirt7 knockdown efficiency. (C) Sirt7 KD increased global lysine fatty acylation level in 293T cells under both normal and stress conditions. Samples were treated with 500 mM $NH_2OH$ at 95 ℃ for 10 minutes to remove cysteine fatty-acylation. Alk: Alkyne-14. BFA: Brefeldin-A.

As shown in Figure 4.1C, both cytosolic and nuclear fractions of Sirt7 KD cells had increased global lysine fatty-acylation level compared with those of control cells. Since SIRT7 has been reported to be upregulated under ER stress[10], I further demonstrated that SIRT7 decreased lysine fatty-acylation level of several proteins upon Brefeldin-A (BFA) treatment (Figure 4.1C). I also observed similar effects using Hela cells (Figure 4.2). The data together suggested that SIRT7 regulates global lysine fatty acylation level. By contrast, the global acetylation level was not affected by Sirt7 (Figure 4.3).

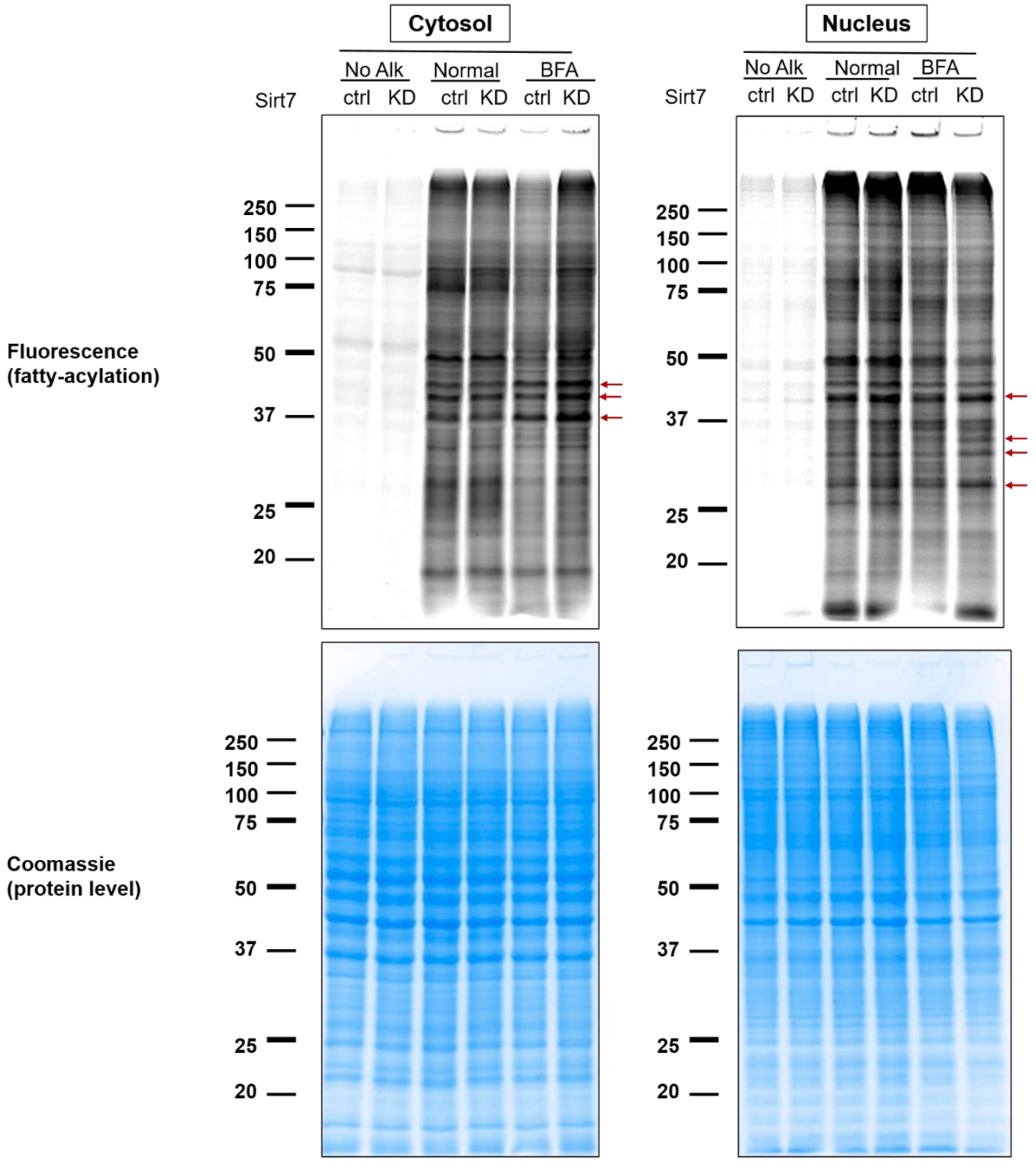


**Figure 4.2** Sirt7 KD increased global lysine fatty acylation level in Hela cells. Samples were treated with 500 mM $NH_2OH$ at 95 ℃ for 10 minutes to remove cysteine fatty-acylation.

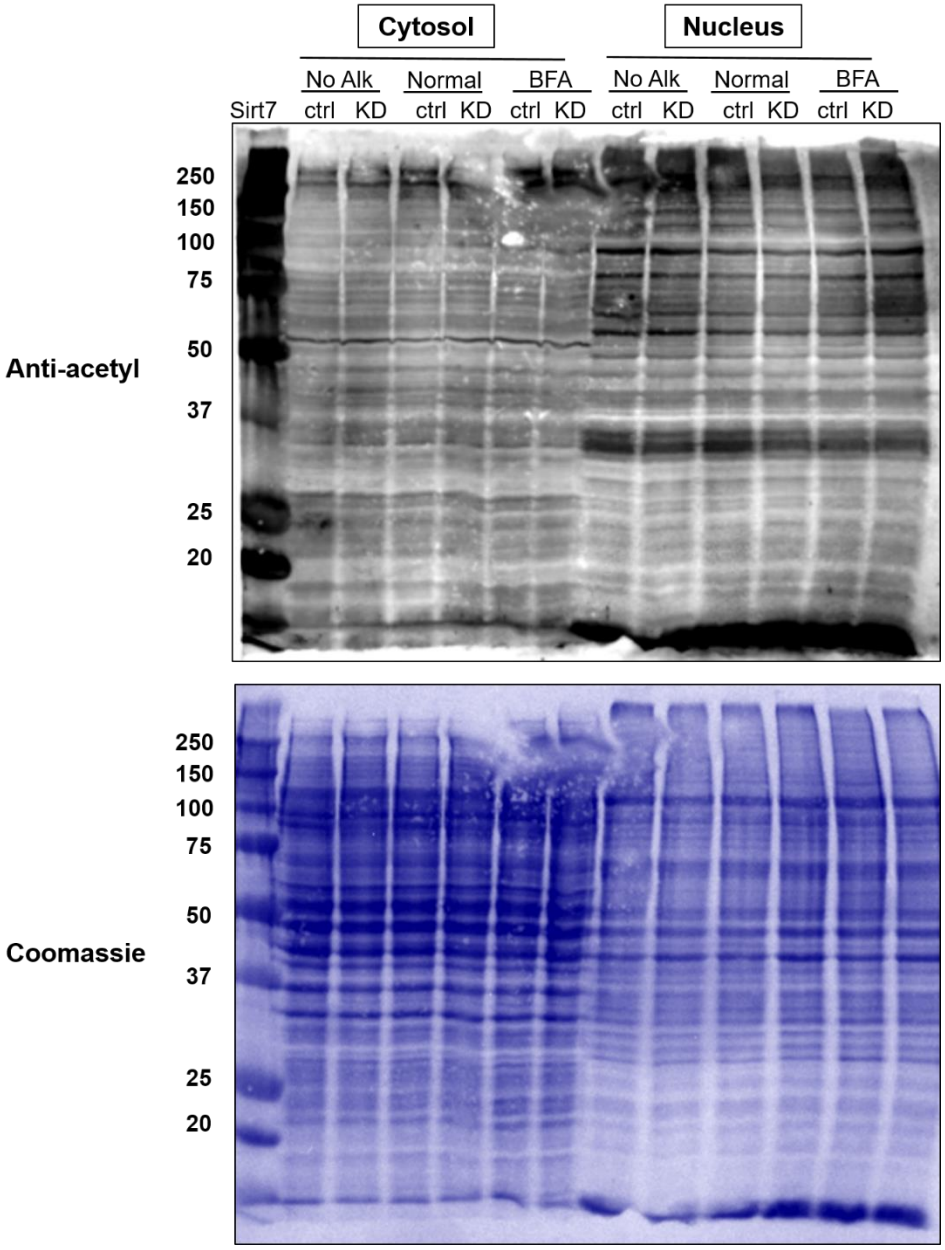


**Figure 4.3** Sirt7 KD does not alter global acetylation level in either cytosol or nucleus in HEK 293T cells.

**SIRT7 dispersed into nucleoplasm and cytoplasm under metabolic stress.**

SIRT7 is reported to be mainly in the nucleus and concentrated in the nucleoli. However, several reports suggest that under certain conditions, such as inhibition of

rRNA transcription, SIRT7 can dissociate from nucleoli and disperse to nucleoplasm.[11, 12]. I wondered whether certain stress conditions could also cause SIRT7 to translocate to the cytoplasm. To test this, I expressed SIRT7-GFP and examined SIRT7 localization in cells under different metabolic stresses. Tunicamycin is an ER stress inducer and SIRT7 was recently suggested to be involved in ER stress response[10]. Without tunicamycin, most SIRT7 is localized in the nucleus and concentrated in a few spots that are consistent with the reported nucleolar localization (Figure 4.4A). However, in the presence of tunicamycin, a significant plasma membrane localization of SIRT7 was observed with a corresponding decrease in nuclear localization. Moreover, glucose deprivation also caused SIRT7 to translocate into the cytoplasm (Figure 4.4B). The change in cellular localization of SIRT7 under stress is also consistent with the changes in the associated RNA species under stress (Figure 3.9A).

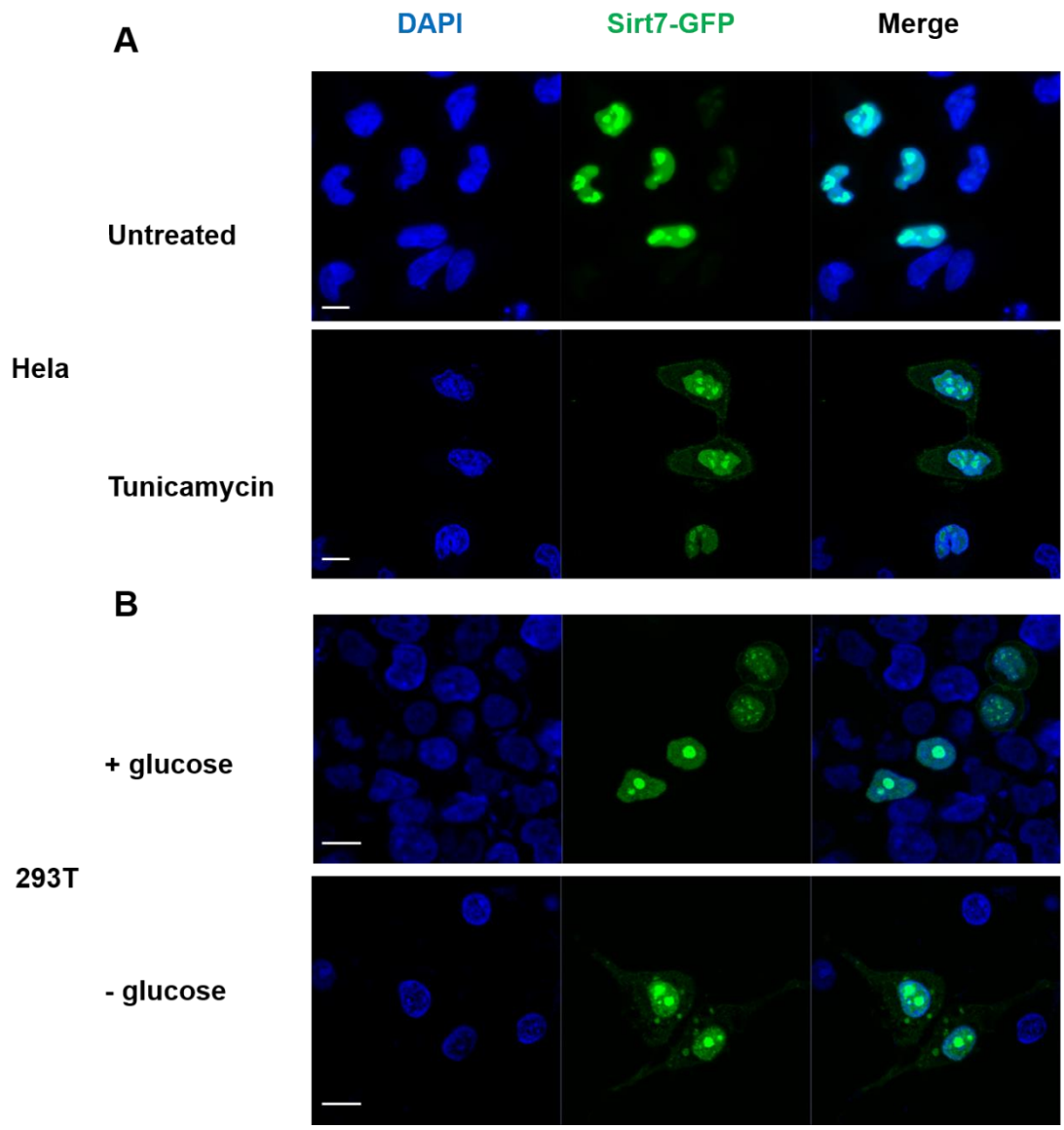


**Figure 4.4** SIRT7-GFP partially translocated to cytoplasm in the presence of metabolic stress. (A) Tunicamycin treatment induced SIRT7-GFP cytoplasmic translocation. (B) Glucose deprivation induced SIRT7-GFP cytoplasmic translocation. Scale bar: 10 μm.

I further examined endogenous SIRT7 localization with metabolic stress using immunofluorescence. As shown in Figure 4.5, under normal condition, SIRT7 protein

was localized in nucleus with some enrichment in the nucleoli. In the addition of tunicamycin, SIRT7 was dispersed into cytoplasm with some co-localization with 1,4-galactosyltransferase (GalT, a marker for the trans-Golgi membranes and network). Moreover, AICAR treatment (mimic of glucose starvation) only triggered endogenous SIRT7 to disperse into nucleoplasm, not into cytoplasm.

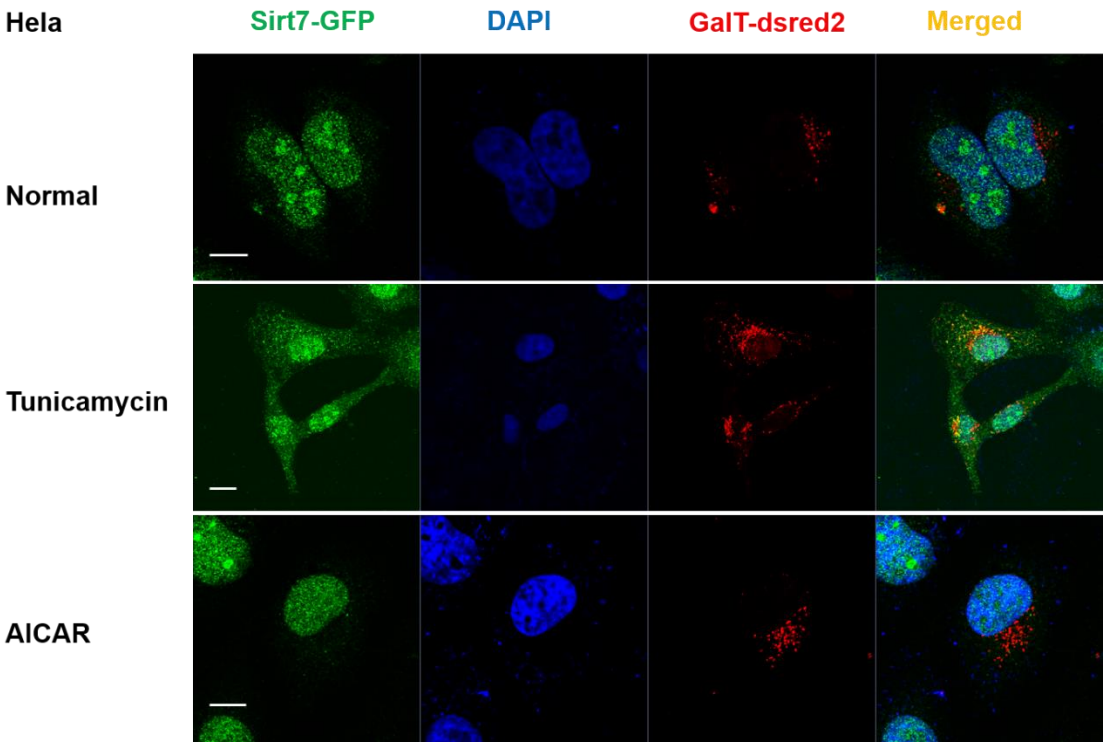


**Figure 4.5** Endogenous SIRT7 dispersed into nucleoplasm and cytoplasm in the presence of metabolic stress. (A) Tunicamycin treatment induced SIRT7 cytoplasmic translocation. Cells were treated with 5 μg/ml tunicamycin for 20h. (B) AICAR treatment (1 mM, 20h) induced SIRT7 to disperse into nucleoplasm. Scale bar: 10 μm.

**SILAC-Profile of Lysine Fatty-acylation Proteome responsive to Sirt7.**

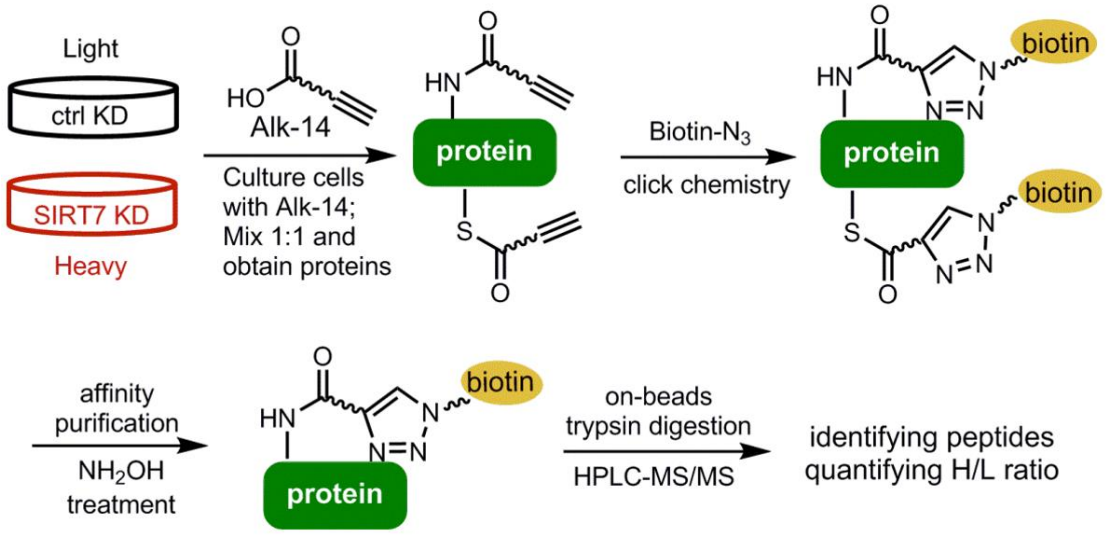


**Figure 4.6** Scheme showing the method of SILAC quantification of lysine fatty acylation in Sirt7 ctrl and KD cells.

To identify potential substrates of SIRT7 with higher lysine fatty acylation levels in Sirt7 KD cells, I used stable isotope labeling of amino acids in cell culture (SILAC) to carry out quantitative analysis[13,14]. As shown in Figure 4.6, control and Sirt7 KD HeLa cells were cultured in light and heavy medium, respectively, for six passages. Cells were then cultured in the presence of Alk14. Total lysates from the two cell lines were mixed at a 1:1 ratio and conjugated to biotin-azide using click chemistry. Proteins immobilized on streptavidin beads were treated with hydroxylamine to remove cysteine fatty acylation, digested with trypsin, and analyzed by HPLC-MS/MS. I identified 395 quantifiable proteins with a false discovery rate (FDR) of less than 1% and protein score higher than 20 (Figure 4.7). In Sirt7 KD cells, 19 proteins exhibited statistically significant increased fatty acylation levels (SILAC heavy/light ratio > 1.3 with $P<0.05$)

(Table 4.1) compared with control.

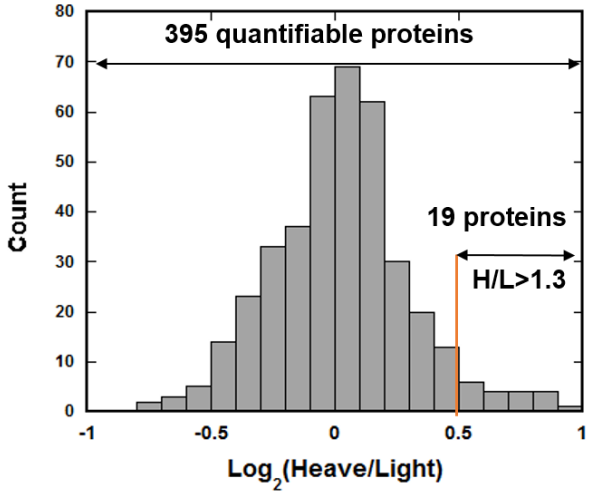


**Figure 4.7** Histogram showing Heavy/Light (H/L) ratio distribution of quantifiable proteins between Sirt7 ctrl and KD cells.

**Table 4.1** Proteins with higher H/L (Sirt7 KD/ctrl) ratio from SILAC

| Protein Description | Gene Name | Heavy/Light |
|---|---|---|
| PREDICTED: heterogeneous nuclear ribonucleoprotein R isoform X2 | HNRNPR | 1.967 |
| very long-chain acyl-CoA synthetase isoform 2 | SLC27A2 | 1.864 |
| protocadherin-7 isoform c precursor | PCDH7 | 1.827 |
| Ras-related protein Ral-A precursor | RalA | 1.793 |
| tumor necrosis factor receptor superfamily member 10D precursor | TNFRSF10D | 1.788 |
| probable phospholipid-transporting ATPase IIA | ATP9A | 1.708 |
| importin-5 | IPO5 | 1.671 |
| PREDICTED: carbamoyl-phosphate synthase [ammonia], mitochondrial isoform X1 | CPS1 | 1.639 |
| PREDICTED: HLA class I histocompatibility antigen, B-15 alpha chain isoform X1 | HLA-B | 1.629 |
| leucine-rich repeat-containing protein 15 isoform a precursor | LRRC15 | 1.605 |
| PREDICTED: CD59 glycoprotein isoform X1 | CD59 | 1.584 |
| N-acetyllactosaminide beta-1,3-N-acetylglucosaminyltransferase | B3GNT1 | 1.582 |
| PREDICTED: delta/notch-like EGF repeat containing isoform X1 | DNER | 1.562 |
| PREDICTED: SUN domain-containing protein 1 isoform X4 | SUN1 | 1.499 |
| PREDICTED: CLPTM1-like isoform X1 | CLPTM1L | 1.496 |
| PREDICTED: bone marrow stromal antigen 2 isoform X1 | BST2 | 1.474 |
| niban-like protein 1 isoform 2 | FAM129B | 1.445 |
| integrin beta-4 isoform 3 precursor | ITGB4 | 1.435 |
| Ras GTPase-activating-like protein IQGAP1 | IQGAP1 | 1.422 |
| HLA class I histocompatibility antigen, Cw-1 alpha chain precursor | HLA-C | 1.373 |

Up to date, a total of four proteins (H3K18[15], PAF53[16], GABPβ1[17], and U3-55k[18]) have been reported as the substrates of SIRT7 deacetylase activity. Compared with the broad collection of substrate proteins of other sirtuins, it suggests that our understanding of SIRT7 is still very limited which on the other hand means opportunities to be explored. We have previously reported that nucleic acids (dsDNA and RNA) are able to significantly activate SIRT7's deacetylase activity. Moreover, upon activation, SIRT7 exhibited more efficient long-chain defatty-acylase activity compared with its decetylase activity in vitro. Therefore, it would be very intriguing to identify substrate proteins of SIRT7's long-chain defatty-acylase activity.

Lysine fatty acylation is only known to occur on a few proteins, including TNFα, a SIRT6 target. Our global fatty acylation labeling result indicates that some proteins are potentially modified by lysine fatty acylation and regulated by SIRT7. Unlike other abundant protein post-translational modifications such as acetylation and phosphorylation which are relatively small and hydrophilic groups (acetyl and phosphate respectively), there are two main limited factors for characterization of long-chain fatty-acylation modification: 1) lack of specific antibody for detection and enrichment; 2) challenging detection by mass spectrometry.

In order to characterize the identity, modified lysine residue(s), and even the exact chemical structure of the modification group (e.g. carbon chain length and degree of unsaturation), our group developed different methods (described below) to overcome the above difficulties principally utilizing mass spectrometry.

1) SILAC proteomics study to identify potential proteins of which lysine fatty-acylation is regulated by SIRT7.

As illustrated in this chapter (Figure 4.6 &4.7, Table 4.1), I have utilized SILAC quantitative proteomics coupled with "click chemistry" to introduce a biotin affinity tag on fatty-acylated proteins for further enrichment and mass spectrometry analysis. A putative list of SIRT7's substrates was generated, and future biochemical validation is required to confirm the proteomics results.

Potential pitfalls: A high proportion of false positive hits was observed due to the following reasons: a) higher H/L (Sirt7 KD/ctrl) ratio could arise from higher protein expression level due to Sirt7 knockdown. This could be eliminated by performing a SILAC-proteomics analysis of total cellular proteins from both Sirt7 KD and ctrl cells; b) Since the majority of protein fatty-acylation is constituted by N-terminal glycine myristoylation, it is possible that proteins with higher H/L (Sirt7 KD/ctrl) ratio somehow exhibited higher level of N-terminal myristoylation rather than lysine fatty-acylation in Sirt7 KD cells. c) Unspecific protein interaction could also result in false positive hits.

2) For specific protein target, we also established a method to identify modified residue(s) directly by mass spectrometry.

Flag-tagged protein was overexpressed in desired cell lines (e.g. stable Sirt7 KD HEK293T cell to accumulate lysine fatty-acylation), labeled with Alk-14 and further immuneprecipitated by anti-Flag M2 affinity resin followed with 3XFlag peptide elution to acquire a decent quantity of soluble target protein. "Click chemistry" using a cleavable biotin-$N_3$ followed with streptavidin beads enrichment allowed efficient enrichment of the desired pool of lysine fatty-acylated protein (with hydroxylamine treatment). After cleaving the modified protein from streptavidin beads, the sample was

digested with trypsin (or other mass spec-grade protease) and submitted for mass spec analysis.

Potential pitfalls: a) fatty-acylated peptides are extremely hydrophobic, which could easily result in sample loss during pipetting and storage using normal tips and Eppendorf tubes. Therefore, glass tips and tubes are recommended for the peptide handling in the later stage. b) Considering the low percentage of target protein employing lysine modification, it is important to start with large mass of soluble overexpressed Flag-tagged protein so as to reach the detection limit of mass spec. Moreover, the methodology for mass spec identification also need to be carefully examined and optimized.

**Materials and Methods**

**Cell culture and viral transfection.** Human 293T and Hela cell lines were acquired from the American Type Culture Collection (ATCC). Cells were cultured in DMEM (Thermo Fisher) supplemented with penicillin-streptomycin (Thermo Fisher) and 10% fetal bovine serum (FBS). To generate transient Sirt7 knockdown cell lines, the pLKO.1-puro lentiviral shRNAs constructs toward luciferase and Sirt7 were purchased from Sigma-Aldrich. Luciferase shRNA (SHC007 and Sirt7 shRNA1 (TRCN0000359663) were used. Lentivirus particles were generated as described above. HEK 293T or Hela cells were infected with lentivirus in the presence of 8 μg/ml polybrene for 6 h, and then incubated with fresh DMEM medium supplemented with 10% FBS for another 48 h before subsequent global labeling experiments. To generate stable Sirt7 knockdown cell line, 293T cells were co-transfected with pCMV-dR8.2,

pMD2.G (obtained from Addgene) and Sirt7 shRNA1 or luciferase shRNA, and the medium supernatant containing the lentiviruses was collected and filtered after 48h. For transfection, Hela cells were incubated with virus-containing supernatant in the presence of 8 μg/ml polybrene. After 72h, infected cells were selected using 1.5 μg /ml puromycin for one week.

**Global fluorescent labeling of fatty-acylated proteins in Sirt7 ctrl and KD cells.** Prior to harvest, Cells were cultured in the presence of 50 μM Alk-14 probe for 6h in DMEM medium supplemented with 10% FBS. To induce ER stress, Sirt7 ctrl and KD cells were incubated with 5 μg/ml Brefeldin-A (BFA) for 6h in the presence of 50 μM Alk-14.

Subcellular fractionation was adapted as previously described[19]. Briefly, the cell pellet was resuspended in Buffer A (20 mM Tris pH 8.0, 10 mM KCl, 1.5 mM $MgCl_2$, 1mM DTT, 5% glycerol, 0.1% NP-40) with protease inhibitor cocktail (Sigma) freshly added and incubated on ice for 5 min. After centrifugation at at 1300g for 10 mins at 4 $^oC$, the supernatant was collected as crude cytosol fraction, which was further clarified at 17,000g for 20 mins. The pellet was re-suspended in Buffer C (20 mM Tris pH 8.0, 5% glycerol, 500 mM NaCl, 1.5 mM $MgCl_2$, 0.5 mM EDTA, 1 mM DTT, 1% NP-40) with fresh EDTA-free protease inhibitor, held on ice for another 20 mins, then incubated with 1μl Benzonase nuclease (Sigma) at 37 $^oC$ for 3 mins to release chromatin-associated proteins. Cell debris was removed by spinning at 17,000 g for 20 mins and the supernatant was collected as the crude nuclear fraction. Equal amounts of total protein (~100 μg) from the nuclear and cytoplasmic fractions were dispensed into 1.5 ml Eppendorf tube respectively. BODIPY-$N_3$ (5 mM stock in DMF) was added

to the reaction to a final concentration of 100 μM, followed by the addition of Tris[(1-benzyl-1H-1,2,3-triazol-4-yl)methyl]amine (TBTA, 100 mM stock in DMF, final concentration 500 μM), $CuSO_4$ (100 mM stock in water, final concentration 500 μM), and TCEP (40 mM stock in water, final concentration 1 mM). TCEP (40 mM) and $CuSO_4$ stock (100 mM) solutions were prepared fresh. The click chemistry reactions were allowed to proceed at room temperature for 30 minutes. The proteins were then precipitated with methanol/chloroform/water (4:1.5:3 volume ratio with the reaction volume set as 1) and the protein pellets were washed twice with 1ml of ice-cold methanol. After drying the protein pellet in the air for 10~15 mins, 20 μl of 4% SDS buffer (4% (w/v) sodium dodecyl sulfate (SDS), 150 mM NaCl, 50 mM triethanolamine pH 7.4) was added to completely dissolve the protein pellet. Loading dye with 100 mM reducing reagent DTT was added and the samples were heated at 95 ℃ for 15 min. To remove cysteine fatty acylation, 500 mM $NH_2OH$ (final concentration) was added and the samples were heated at 95 ℃ for 10 min. Finally, protein samples were resolved on 12% SDS-PAGE and visualized by Typhoon 9400 Variable Mode Imager (GE Healthcare Life Sciences) with setting of Blue (488 nm)/520BP40 PMT 600 V (normal sensitivity), and analyzed by ImageQuant TL v2005.

**Fluorescence microscopy.** Coding sequences (CDS) of human SIRT7 was inserted into the 5'-end of EGFP cDNA (pEGFP-N1 vector). Cells were transfected with EGFP-tagged Sirt7 using Fugene 6 transfection reagent following manufacturer's instruction for 24h. For immunofluorescence, cells were permeabilized with 0.3% triton X-100 in PBS for 10 minutes at room-temperature (RT). After washing three times with PBS, cells were fixed with 4% paraformaldehyde in PBS for 15 minutes at

RT. Cells were then blocked in PBS containing 5% BSA and 0.3% triton X-100 for 1h. Primary antibody (SIRT7, Santa Cruz Biotechnology cat # sc365344) was diluted at 1:50 in PBS containing 1% BSA and 0.3% triton X-100 and incubated with the cells for 1h. After rinsing three times with PBS, fluorophore-conjugated secondary antibody (Goat anti-mouse, Alexa Fluor® 594, Thermo) was diluted at 1:500 and applied for 1h at RT in the dark. Samples were washed three times with PBS and stained with prolong gold anti-fade reagent (Cell signaling technology) with DAPI. Confocal images were taken using a 63x, 1.4 NA objective, on an inverted microscope (Leica), and acquired with ZEN software. Image resizing, cropping, and brightness were uniformly adjusted in Photoshop (Adobe).

**SIRT7 target identification by SILAC and Alk14 labeling**. The Sirt7 knockdown HeLa cells and the control knockdown cells were grown in heavy DMEM media ($^{13}C_6$, $^{15}N_2$-Lys and $^{13}C_6$, $^{15}N_4$-Arg; Thermo, catalog # 89983) and light DMEM media with 10% SILAC-dialyzed FBS, respectively, for at least five passages. The fatty acid analogue (Alk14) was added into the media and incubated for 6 hrs before cell harvesting. To selectively enrich the fatty-acylated proteins, the Alk14-labelled lysates were conjugated to biotin-azide via a click chemistry reaction and the affinity purification was performed using streptavidin beads following the method that was described by Yount et al[14]. Principally, the cells were lysed in 4% SDS buffer (4% (w/v) SDS, 150 mM NaCl, 50 mM triethanolamine, pH 7.4) with EDTA-free protease cocktail inhibitors (Sigma) and the protein concentration was determined by bicinchoninic acid (BCA) assay (Pierce, catalog # 23225). Lysates (8 mg total protein) from control and knockdown cells were combined in 1:1 ratio and the volume was

brought up to 4.77 ml with 4% SDS buffer (4% (w/v) SDS, 150 mM NaCl, 50 mM triethanolamine, pH 7.4) with EDTA-free protease cocktail inhibitors. The biotin-azide was conjugated to Alk14-labelled proteins via addition of click chemistry master mix: 100 µl of 5 mM biotin-azide, 30 µl of 100 mM TBTA dissolved in DMF, 50 µl of 100 mM $CuSO_4$ and 50 µl of 100 mM TCEP. The reaction proceeded at room temperature for 1.5 hrs. The proteins were then precipitated with methanol/chloroform and the protein pellets were washed twice with 50 ml of ice-cold methanol. The protein pellets were resuspended in 1 ml of 4% SDS buffer (4% (w/v) SDS, 150 mM NaCl, 50 mM triethanolamine, pH 7.4) and were adjusted to 1% SDS with 3 ml of 1% Brij97 buffer (1% (w/v) Brij97, 150 mM NaCl, 50 mM triethanolamine, pH 7.40). The proteins were incubated with streptavidin beads for 1 hr at room temperature. Unbound proteins were removed and the beads were washed once with 10 ml of PBS/0.2% SDS and three times with 10 ml of PBS buffer. Then Hydroxylamine solution (0.5M, pH 7.40) was added to the beads and incubated at room temperature for 1 hr with gentle rotation in order to remove acyl modifications on cysteine residues.

The beads were washed three times with 10 ml of 20 mM Tris pH 7.4 with 500 mM KCl and then three times with 10 ml of 20 mM Tris pH 7.4. After washing, 500 µl of 8M urea in PBS, 25 µl of 200 mM TCEP were added to the beads and the mixture was gently rotated at room temperature for 30 min. Afterwards, 25 µl of 400 mM iodoacetamide was added and the mixture was further incubated for 30 min at room temperature. The supernatant was removed and the beads were washed twice with 1 ml of 2 M urea in PBS before incubating with 2 µg of trypsin in 500 µl PBS containing 2M urea and 1 mM $CaCl_2$ at 37 $^oC$ for 8 hrs with gentle rotation. The supernatant containing

tryptic peptides was collected and diluted with water to 1 ml and adjusted to pH 2-3 with 10% TFA. The peptide solution was purified using Sep-Pak Vac C18 cartridge[20]. The eluted sample was lyophilized and submitted for nano LC-MS/MS analysis.

**Nano LC-MS/MS analysis.** The tryptic digest samples were reconstituted in 2% acetonitrile with 0.5% formic acid and were injected about 1 µg each time for nanoLC-ESI-MS/MS analysis, which was carried out on a LTQ-Orbitrap Elite mass spectrometer (Thermo-Fisher Scientific, San Jose, CA) equipped with a"Plug and Play" nano ion source device (CorSolutions LLC, Ithaca, NY). The Orbitrap was interfaced with a nano HPLC carried out by Dionex UltiMate3000 MDLC system (Thermo Dionex, Sunnyvale, CA). The SILAC samples (2-4µL) were injected onto a Acclaim PepMap nano Viper C18 trap column (5 µm, 100 µm × 2 cm, Thermo Dionex) at a flow rate of 20 µL/min for on-line desalting and then separated on a homemade C18 RP nano column (5 µm, 75 µm x 50 cm, Magic C18, Bruker) which was installed in the "Plug and Play" device with a 10-µm spray emitter (New Objective, Woburn, MA). The peptides were then eluted in a 120 min gradient of 5% to 38% acetonitrile in 0.1% formic acid at a flow rate of 300 nL/min. The Orbitrap Elite was operated in positive ion mode with nano spray voltage set at 1.6 kV and source temperature at 275 °C. Internal calibration was performed with the background ion signal at m/z 445.120025 as the lock mass. The instrument was performed at data-dependent acquisition (DDA) mode by one precursor ions MS survey scan from m/z 300 to 1800 at resolution 60,000 using FT mass analyzer followed by up to 10 MS/MS scans at resolution 15,000 on the top 10 most intensive peaks with multiple charged ions above an ion intensity threshold of 10000 in FT survey scan mode. Dynamic exclusion parameters were set at repeat

count 1 with a 20 s repeat duration, exclusion list size of 500, 30 s exclusion duration, and ±10 ppm exclusion mass width. Collision induced dissociation (CID) parameters were set at the following values: isolation width 2.0 m/z, normalized collision energy 35 %, activation Q 0.25, and activation time 0.1 ms. All data are acquired under Xcalibur 2.2 operation software (Thermo-Fisher Scientific).

The mass spectrometry raw data files were imported into Proteome Discoverer v1.4. Subsequently, CID peak lists were searched against reference human sequence database. The following search settings were used: Carbamidomethylation on cysteines as static modification; $^{13}C_8$-Lysine, $^{13}C_{10}$-Arginine, deamidation on Asparagine and Glutamine, oxidation on methionine and acetylation at N terminus as variable modifications; 1 missed cleavage allowed; precursor mass tolerance of 10 ppm and 0.5 Da on the fragment masses. For both identification and quantitation, only spectra with medium confidence or higher were accepted, based on the algorithms of Proteome Discoverer. The event detector and precursor ion quantifier algorithms of Proteome Discoverer were used for quantitation, using a 2 ppm mass variability and a 0.2 min retention time tolerance on precursor ion pairs. The peptide ratios were calculated using the same number of isotopes. Protein ratios were based on the median peptide ratio. Proteins were grouped by Proteome Discoverer.

**References**

1. Houtkooper, R. H., Pirinen, E., and Auwerx, J. (2012) Sirtuins as regulators of metabolism and healthspan, Nat. Rev Mol Cell Biol 13, 225-238.

2. Michishita, E., Park, J. Y., Burneskis, J. M., Barrett, J. C., and Horikawa, I. (2005) Evolutionarily conserved and nonconserved cellular localizations and functions of human SIRT proteins, Mol. Biol. Cell 16, 4623-4635.

3. Liszt, G., Ford, E., Kurtev, M., and Guarente, L. (2005) Mouse Sir2 homolog SIRT6 is a nuclear ADP-ribosyltransferase, J. Biol. Chem. 280, 21313-21320.

4. Michishita, E., McCord, R. A., Berber, E., Kioi, M., Padilla-Nash, H., Damian, M., Cheung, P., Kusumoto, R., Kawahara, T. L. A., Barrett, J. C., Chang, H. Y., Bohr, V. A., Ried, T., Gozani, O., and Chua, K. F. (2008) SIRT6 is a histone H3 lysine 9 deacetylase that modulates telomeric chromatin, Nature 452, 492-496.

5. Haigis, M. C., Mostoslavsky, R., Haigis, K. M., Fahie, K., Christodoulou, D. C., Murphy, A. J., Valenzuela, D. M., Yancopoulos, G. D., Karow, M., Blander, G., Wolberger, C., Prolla, T. A., Weindruch, R., Alt, F. W., and Guarente, L. (2006) SIRT4 Inhibits glutamate dehydrogenase and opposes the effects of calorie restriction in pancreatic b Cells, Cell 126, 941-954.

6. Barber, M. F., Michishita-Kioi, E., Xi, Y., Tasselli, L., Kioi, M., Moqtaderi, Z., Tennen, R. I., Paredes, S., Young, N. L., Chen, K., Struhl, K., Garcia, B. A., Gozani, O., Li, W., and Chua, K. F. (2012) SIRT7 links H3K18 deacetylation to maintenance of oncogenic transformation, Nature 487, 114-118.

7. Jiang, H., Khan, S., Wang, Y., Charron, G., He, B., Sebastian, C., Du, J., Kim, R., Ge, E., Mostoslavsky, R., Hang, H. C., Hao, Q., and Lin, H. (2013) SIRT6 regulates TNF-a secretion through hydrolysis of long-chain fatty acyl lysine, Nature 496, 110-113.

8. Du, J., Zhou, Y., Su, X., Yu, J., Khan, S., Jiang, H., Kim, J., Woo, J., Kim, J. H., Choi, B. H., He, B., Chen, W., Zhang, S., Cerione, R. A., Auwerx, J., Hao, Q., and Lin, H. (2011) Sirt5 is an NAD-dependent protein lysine demalonylase and desuccinylase, Science 334, 806-809.

9. Jiang, H., Khan, S., Wang, Y., Charron, G., He, B., Sebastian, C., Du, J., Kim, R., Ge, E., Mostoslavsky, R., Hang, H. C., Hao, Q., and Lin, H. (2013) SIRT6 regulates TNF-alpha secretion through hydrolysis of long-chain fatty acyl lysine, Nature 496, 110-113.

10. Shin, J., He, M., Liu, Y., Paredes, S., Villanova, L., Brown, K., Qiu, X., Nabavi, N., Mohrin, M., Wojnoonski, K., Li, P., Cheng, H. L., Murphy, A. J., Valenzuela, D. M., Luo, H., Kapahi, P., Krauss, R., Mostoslavsky, R., Yancopoulos, G. D., Alt, F. W., Chua, K. F., and Chen, D. (2013) SIRT7 represses Myc activity to suppress ER stress and prevent fatty liver disease, Cell. Rep 5, 654-665.

11. Ford, E., Voit, R., Liszt, G., Magin, C., Grummt, I., and Guarente, L. (2006) Mammalian Sir2 homolog SIRT7 is an activator of RNA polymerase I transcription, Genes Dev. 20, 1075-1080.

12. Ryu, D., Jo, Y. S., Lo Sasso, G., Stein, S., Zhang, H., Perino, A., Lee, J. U., Zeviani, M., Romand, R., Hottiger, M. O., Schoonjans, K., and Auwerx, J. (2014) A SIRT7-dependent acetylation switch of GABPbeta1 controls mitochondrial function, Cell Metab.

13. Ong, S. E., Blagoev, B., Kratchmarova, I., Kristensen, D. B., Steen, H., Pandey, A., and Mann, M. (2002) Stable isotope labeling by amino acids in cell culture,

SILAC, as a simple and accurate approach to expression proteomics, Mol. Cell. Proteomics 1, 376-386.

14. Yount, J. S., Zhang, M. M., and Hang, H. C. (2011) Visualization and identification of fatty acylated proteins using chemical reporters, Curr. Protoc. Chem. Biol. 3, 65-79.

15. Barber, M. F., Michishita-Kioi, E., Xi, Y., Tasselli, L., Kioi, M., Moqtaderi, Z., Tennen, R. I., Paredes, S., Young, N. L., Chen, K., Struhl, K., Garcia, B. A., Gozani, O., Li, W., and Chua, K. F. (2012) SIRT7 links H3K18 deacetylation to maintenance of oncogenic transformation, Nature 487, 114-118.

16. Chen, S., Seiler, J., Santiago-Reichelt, M., Felbel, K., Grummt, I., and Voit, R. (2013) Repression of RNA polymerase I upon stress is caused by inhibition of RNA-dependent deacetylation of PAF53 by SIRT7, Mol. Cell 52, 303-313.

17. Ryu, D., Jo, Y. S., Lo Sasso, G., Stein, S., Zhang, H., Perino, A., Lee, J. U., Zeviani, M., Romand, R., Hottiger, M. O., Schoonjans, K., and Auwerx, J. (2014) A SIRT7-dependent acetylation switch of GABPbeta1 controls mitochondrial function, Cell. Metab 20, 856-869.

18. Chen, S., Blank, M. F., Iyer, A., Huang, B., Wang, L., Grummt, I., and Voit, R. (2016) SIRT7-dependent deacetylation of the U3-55k protein controls pre-rRNA processing, Nat. Commun 7, 10734.

19. Mendez, J., and Stillman, B. (2000) Chromatin association of human origin recognition complex, cdc6, and minichromosome maintenance proteins during the cell cycle: assembly of prereplication complexes in late mitosis, Mol. Cell. Biol. 20, 8602-8612.

20. Jiang, H., and Lin, H. (2012) Labeling substrate proteins of poly(ADP-ribose) polymerases with clickable NAD analog, Curr. Protoc. Chem. Biol. 4, 19-34.

# APPENDIX A: PERMISSION FOR FULL PAPER REPRODUCTION

Chapter 2: Reprinted with permission from Tong, Z et al. (2016) ACS Chem Biol 11, 742-747.



**PERMISSION/LICENSE IS GRANTED FOR YOUR ORDER AT NO CHARGE**

This type of permission/license, instead of the standard Terms & Conditions, is sent to you because no fee is being charged for your order. Please note the following:

- Permission is granted for your request in both print and electronic formats, and translations.
- If figures and/or tables were requested, they may be adapted or used in part.
- Please print this page for your records and send a copy of it to your publisher/graduate school.
- Appropriate credit for the requested material should be given as follows: "Reprinted (adapted) with permission from (COMPLETE REFERENCE CITATION). Copyright (YEAR) American Chemical Society." Insert appropriate information in place of the capitalized words.

One-time permission is granted only for the use specified in your request. No additional uses are granted (such as derivative works or other editions). For any other uses, please submit a new request.